

Requirements for leukocyte transendothelial migration via the transmembrane chemokines CX3CL1 and CXCL16

Von der Fakultät für Mathematik, Informatik und Naturwissenschaften der RWTH
Aachen University zur Erlangung des akademischen Grades eines Doktors der
Naturwissenschaften genehmigte Dissertation

vorgelegt von
M. Eng.
Nicole Schwarz

aus Strausberg

Berichter: Herr Privatdozent
Dr. rer. nat. Andreas Ludwig

Herr Universitätsprofessor
Dipl. Ing. Dr. Werner Baumgartner

Tag der mündlichen Prüfung: 16. März 2010

**Diese Dissertation ist auf den Internetseiten der Hochschulbibliothek online
verfügbar.**

Meinen Eltern für die Unterstützung.

Es ist besser, ein paar Fragen zu stellen, als alle Antworten schon zu kennen.

James Thurber

Table of contents

1. Abstract.....	5
2. Introduction	7
2.1 Current model of leukocyte extravasation	7
2.2 Chemokines	10
2.3 Chemokine receptors	12
2.4 CX3CL1 and its receptor CX3CR1	14
2.5 CXCL16 and its receptor CXCR6	21
2.6 ADAMs	23
3. Aim of this thesis	25
4. Materials and Methods	26
4.1 Materials	26
4.2 Methods	31
5. Results	48
5.1 CX3CR1-CX3CL1 interaction	48
5.2 Model system for CX3CR1-CX3CL1 function	55
5.3 Molecular analysis of CX3CR1-CX3CL1 function	62
5.4 Involvement of ADAMs in CX3CR1-CX3CL1 function	74
5.5 CXCR6-CXCL16 function	80
6. Discussion	88
7. Literature.....	103
8. List of figures.....	115
9. List of tables	117
10. Abbreviations	118
11. Vectors	123
11.1 hCX3CR1 in pcDNA3.1+.....	123
11.2 hCX3CR1 R127N in pcDNA3.1+	124
11.3 hCX3CR1 N289A in pcDNA3.1+	125

Table of contents

11.3 hCX3CR1 Y293A in pcDNA3.1+	126
11.4 hCX3CR1 S319X in pcDNA3.1+.....	127
11.5 hCXCR6 in pcDNA3.1+.....	128
11.6 hCXCR6 R127N in pcDNA3.1+	129
11.7 hCXCR6 F128Y in pcDNA3.1+.....	130
12. Curriculum Vitae.....	131
13. Publications	132
14. Declaration	134
15. Acknowledgements	135

1 Abstract

The chemokines CX3CL1 and CXCL16 and their receptors CX3CR1 and CXCR6 are described in vascular inflammation and inflammatory cell recruitment. CX3CL1 and CXCL16 are transmembrane surface proteins on endothelial cells inducing firm adhesion of leukocytes via the interaction with their receptors. After shedding from the cell surface by the metalloproteinases ADAM10 and ADAM17, they act as soluble chemoattractants for CX3CR1- and CXCR6-expressing leukocytes, respectively.

Here, it was demonstrated that expression of transmembrane CX3CL1 on endothelial cells promotes leukocyte transendothelial migration, and details of the underlying mechanisms using mutated CX3CR1 variants were elucidated. The DRY motif required for Gi-protein-coupling was mutated to DNY, which abolished the intracellular calcium release in response to CX3CL1, but did neither affect CX3CL1 binding nor uptake. Truncation of the C-terminus reduced ligand uptake, but not ligand binding and calcium responses. Both variants effectively mediated firm cell adhesion, but not chemotaxis towards soluble CX3CL1. Furthermore, they failed to induce transmigration, but mediated retention of leukocytes on the CX3CL1-expressing cell layer. Pharmacologic and transcriptional inhibition of ADAM10 led to reduced shedding of transmembrane CX3CL1, which was associated with an almost complete suppression of transmigration in response to transmembrane CX3CL1. These results indicate a multistep process of leukocyte recruitment by transmembrane CX3CL1 involving adhesion, signaling, initiation of transmigration, and finally proteolytic release of the transmigrating leukocytes.

In contrast, transmembrane CXCL16 did not promote adhesion of CXCR6-expressing cells, while soluble CXCL16 mediated chemotaxis. CXCR6 bears a DRF instead of the DRY motif. Since this mutation is implicated in the constitutive activity of other receptors, the DRF of CXCR6 was changed into DRY and DNF. Reconstitution of the DRY motif did not affect ligand binding and resulted in a slight decrease in calcium

signaling, whereas the mutation into DNF abolished calcium signaling. Both mutated receptors still failed to induce adhesion to CXCL16-expressing cells. Signaling seemed to depend on the arginine residue but not on the tyrosine/phenylalanine residue in DRY/F. These results indicate that CXCL16 predominantly functions as a soluble chemokine. Furthermore, cell recruitment by transmembrane chemokines differs. While CX3CL1 induces signaling-independent adhesion and signaling-dependent transmigration, CXCL16 does not induce adhesion, but chemotaxis.

2 Introduction

Inflammation is a fundamental defense reaction caused by tissue damage or injury. Its primary purpose is the protection of the organism by removing or neutralizing injurious agents and repairing the surrounding tissue. The inflammatory response involves three major stages: first, dilation of the blood vessel leading to an increase of blood flow; second, structural changes in the microvascular system; and third, localized recruitment of various leukocyte subsets to sites of inflammation. The current model of leukocyte extravasation from the vasculature into inflamed tissue comprises several steps governed by diverse molecules such as cytokines, adhesion molecules and chemokines acting as either soluble mediators, membrane-expressed ligands or signal transducing receptors.

2.1 Current model of leukocyte extravasation

Leukocyte extravasation is a multistep process that consists of at least five major stages, and is halted when any one of them is suppressed (see Figure 1). On recognition of pathogens, resident cells like macrophages or dendritic cells undergo activation and release pro-inflammatory cytokines like IL-1, TNF α and chemokines. Endothelial cells of blood vessels near the site of infection start to express cellular adhesion molecules, such as selectins, as a result of activation by these cytokines.

The selectins (P, E, and L) are type 1 transmembrane glycoproteins that bind to modified sialyl Lewis X (sLex) present in their ligands in a Ca²⁺-dependent fashion. L-selectin is expressed by most leukocytes, whereas the E and P forms are expressed on endothelial cells that were activated by proinflammatory stimuli. Binding of endothelial E- and P-selectins to their corresponding ligands on the leukocytes slows down the velocity of leukocytes in the bloodstream, leading to a rolling movement of the cells on the vascular wall (reviewed in: [Barreiro et al., 2004]).

As leukocytes start tethering to the vascular endothelium and their rolling velocity

slows, integrins are activated upon encountering immobilized chemokines and integrin ligands exposed on the apical endothelial surface [Campbell et al., 1998]. This activation step enables the arrest of leukocytes and their subsequent firm adhesion to the endothelium under physiological flow conditions.

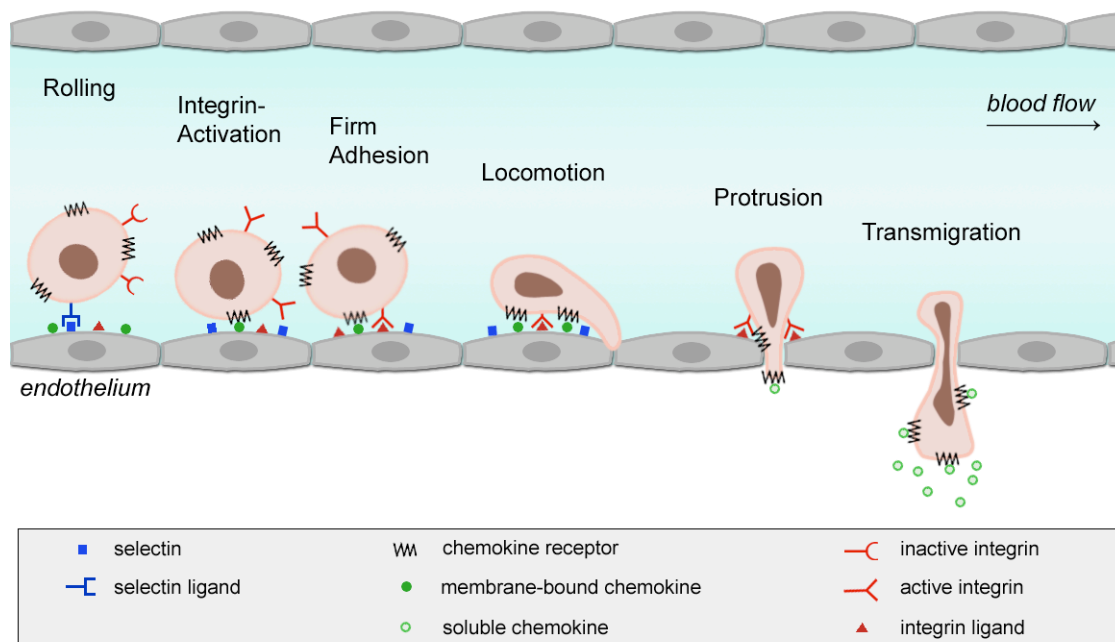


Figure 1: Multiple steps are necessary for leukocyte extravasation. Leukocytes recognize and bind selectins that are expressed by cytokine-activated endothelial cells leading to a rolling movement. Subsequently, integrins become activated and undergo a conformational change. In the next step integrins, adhesion molecules and chemokine receptors bind to their respective ligands on the endothelial cell surface, leading to firm adhesion. Then, leukocytes crawl on the cell surface in search of an appropriate site for transmigration. After protrusion between two adjacent endothelial cells transmigration towards an increasing chemokine-gradient occurs. Figure modified after: [Man et al., 2007].

Integrins comprise a family of 24 heterodimeric receptors, each of which is composed of an α -subunit and a β -subunit. These molecules dynamically alter their adhesive properties through conformational changes [Beglova et al., 2002; Nishida et al., 2006]. The most relevant integrins for leukocyte adhesion to the endothelium are members of

the $\beta 2$ subfamily, particularly LFA-1 ($\alpha L\beta 2$), as well as VLA-4 ($\alpha 4\beta 1$).

Most of the ligands are transmembrane proteins that belong to the immunoglobulin superfamily, such as endothelial intercellular adhesion molecule-1 (ICAM-1, ligand to LFA-1) and vascular cell adhesion molecule-1 (VCAM-1, ligand to VLA-4) [Gahmberg et al., 1990].

Chemoattractants stimulate the directional leukocyte migration called chemotaxis. Chemokines are small chemotactic polypeptides that induce leukocyte migration towards increasing concentration gradients of chemokines. However, soluble chemokine gradients are unlikely to exist at the luminal endothelial surface, since they could be easily washed away. Therefore, it has been proposed that chemokines could act as bound form to exert proadhesive and migratory effects on leukocytes in the lumen of blood vessels. There are several chemokines that are known to be immobilized on the endothelial cell surface by binding to glycosaminoglycans, like IL-8 and RANTES [Rot et al., 1992; Tanaka et al., 1993]. Additionally, there exist two special chemokines termed CX3CL1 and CXCL16 that are produced as membrane-anchored molecules by the endothelium, and can be shed to a soluble form by metalloproteinases of the ADAM (a disintegrin and metalloprotease) family [Bazan et al., 1997; Garton et al., 2001; Hundhausen et al., 2003]. CX3CL1 and CXCL16 likely play a role as transmembrane adhesion molecules as well as soluble chemoattractants.

Subsequent to firm adhesion, leukocytes transmigrate through the endothelium without irreversibly impairing its integrity. Two routes exist that the cells can use: they can either move between the endothelial cells (paracellular) or they can migrate through an endothelial cell (transcellular). It is still unclear to which extent each of the ways is involved in transmigration. For paracellular transmigration, leukocytes encounter tight junctions and adherence junctions and engage other transmembrane receptors, including junctional molecules such as platelet/endothelial cell adhesion molecule-1 (PECAM-1), members of the junctional adhesion molecule (JAM) family, and CD99, which contribute to sequential steps of the transmigration process [Muller et al., 1993; Martin-Padura et

al., 1998; Schenkel et al., 2002].

Transmigration requires a morphological change of leukocytes. They become polarized with at least two regions that can be identified: the cell front and the cellular uropod [del Pozo et al., 1995]. This allows the cell to coordinate the intracellular forces that are needed for directed cell crawling [Geiger and Bershadsky, 2002]. Once the leukocyte has encountered an appropriate site for transmigration, it extends pseudopods between two adjacent cells. During the transmigration process, chemokine receptors polarize on the leading edge, resulting in a functional specialization of this cell domain in signal transduction [Nieto et al., 1997]. Since transmigration is mediated by intracellular phosphorylation signals through chemokine receptors, this re-organization may act as a sensor mechanism for chemokine-guided cell trafficking [Bokoch, 1995].

2.2 Chemokines

The superfamily of chemokines consists of at least 42 small chemotactic cytokines. They share structural characteristics such as the size (8-10 kDa) and the presence of conserved cysteine residues in the N-terminal region forming their 3-dimensional shape. Chemokines are classified into four groups according to the number and position of these cysteine residues. CXC-chemokines are characterized by the presence of one amino acid between the first two cysteines, whereas in CC-chemokines the first two cysteines are adjacent to each other. The C-chemokine family only contains two of the four conserved cysteine residues, and in the CX3C-chemokine family, with its only member CX3CL1, three amino acids separate the first two cysteines (see Figure 2).

Chemokines consist of an elongated N-terminus that includes the first cysteine. Following the first two cysteines, the structure forms a so-called N-loop consisting of approximately ten residues that is succeeded by a sequence of α -helices and two antiparallel β -sheets interrupted by loops. The so-called 30- and 50-loops contain the third and fourth cysteine residue. Due to disulfide bonds between the first and the third

and between the second and the fourth cysteine the molecule is stabilized. The sequence identities between different chemokines vary from less than 20% to over 90%.

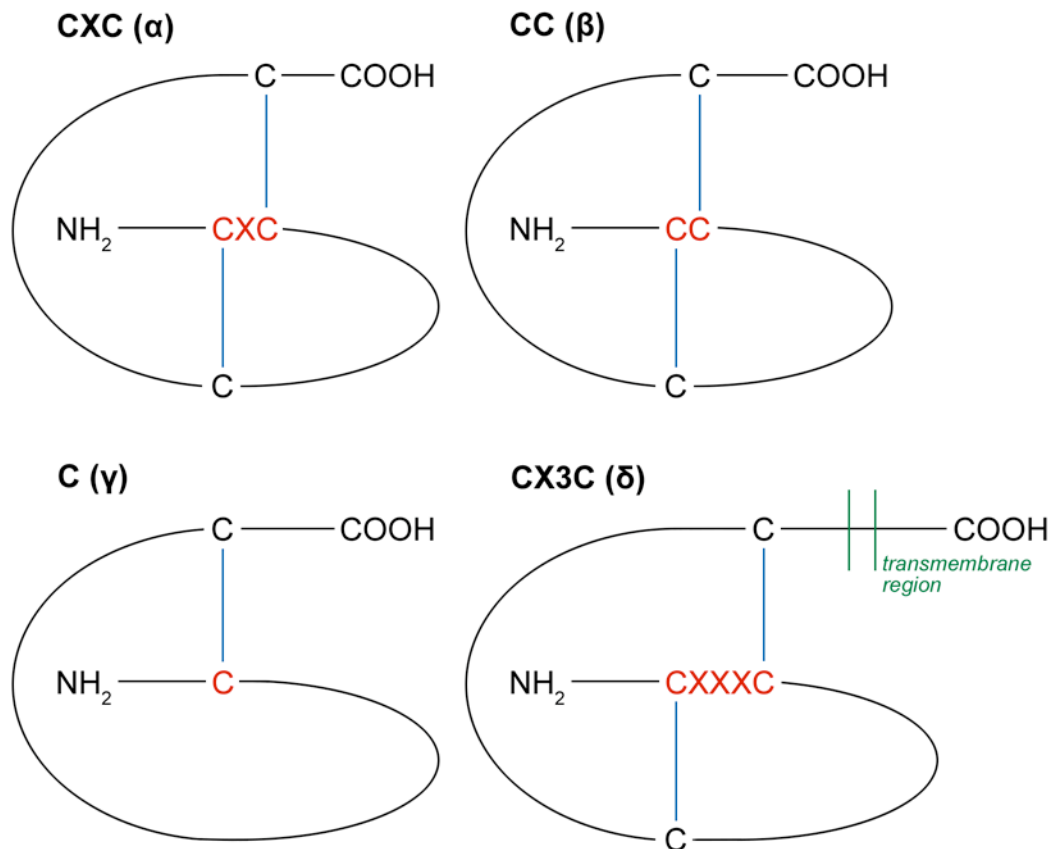


Figure 2: Chemokines are divided into four groups based on their first two cystein residues. Chemokines are subdivided into four groups based on the positioning of the first two conserved cysteine residues. In CXC α chemokine family, one amino acid is located between the first two chemokines; in CC β chemokine family, the first two cysteines are adjacent to each other; in CX3C δ chemokine family, there are three interfering amino acids; in C γ chemokine family, only two of the conserved cysteine residues are present. Figure modified after: [Rostene et al., 2007].

The three-dimensional structure of each monomer is virtually identical, but the quaternary structure of chemokines differs for each subfamily. Structural studies reveal

several regions of chemokines to be involved in receptor binding and function, with the N-terminal region playing an important role [Onuffer and Horuk, 2002; Allen et al., 2007].

Some chemokines are considered pro-inflammatory and can be induced during an immune response to promote cells of the immune system to a site of infection, while others are considered homeostatic and are involved in controlling the migration of cells during normal processes of tissue maintenance or development.

2.3 Chemokine receptors

Chemokines exert their biological effects by interacting with G-protein-linked 7-transmembrane-spanning receptors, called chemokine receptors that are selectively found on the surfaces of their target cells. These chemokine receptors are part of a much bigger superfamily of G-protein-coupled receptors that include receptors for hormones, neurotransmitters, paracrine substances, inflammatory mediators, certain proteases, taste and odorant molecules, and even photons and calcium ions.

G-protein-coupled receptors are associated with a heterotrimeric G-protein (guanine nucleotide-binding protein) consisting of three subunits (α , β and γ). On conformational changes by ligand-binding, the receptor can act as guanine nucleotide exchange factor and activate the G-protein by exchanging its bound GDP to GTP. The α -subunit with the bound GTP then dissociates from the β - and γ -subunits and further affects intracellular signaling depending on the α -subunit type.

There are two general signal transduction pathways involved in G-protein-coupled receptors: cAMP signal pathway and phosphatidylinositol signal pathway. $G_{\alpha i}$, or inhibitory regulative G-protein, associated signaling leads to an inhibition of adenylate cyclase that catalyzes the formation of cAMP from ATP. In phosphatidylinositol signaling, phosphatidylinositol 4,5-bisphosphate (PIP₂) is cleaved into the second messengers inositol 1,4,5-trisphosphate (IP₃) and diacylglycerol (DAG) by

phospholipase C. IP₃ then activates Ca²⁺-release channels in endoplasmatic reticulum membranes, where it can bind to calmodulin or can be used to activate protein kinase C together with DAG. Protein kinase C, in turn, catalyzes the phosphorylation of several cellular proteins, resulting in altered protein activity.

GPCRs become desensitized after prolonged exposition to their ligands. G-protein receptor kinases can phosphorylate the intracellular part of active receptors, leading to the binding of β -arrestin that either prevents the receptor from binding to its ligand or, as in the most cases, promotes the removal of the receptor from the membrane via clathrin-mediated endocytosis, called internalization. When the receptor is dephosphorylated in the acidic microenvironment, it can be re-expressed at the cell surface [Krueger et al., 1997; Laporte et al., 1999]

G-protein-coupled receptors are grouped into six classes according to their sequence homology and functional similarity, with the largest group being class A or rhodopsin-like GPCRs. Chemokine receptors belong to the group of class A GPCR. To date 19 distinct chemokine receptors have been described in mammals, and they are thought to predominantly couple to the G α i -subunit.

Chemokine receptors are further subdivided into different families that correspond to the 4 distinct subfamilies of chemokines they bind (CXC chemokine receptors, CC chemokine receptors, CX₃C chemokine receptors and XC chemokine receptors). Each of the chemokine receptors binds only a single class of chemokines, although they can bind several members of the same class with high affinity. Furthermore, several chemokines can bind and activate a number of chemokine receptors.

2.3.1 Structural characteristics

Chemokine receptors measure approximately 350 amino acids in length. A short extracellular N-terminus is acidic overall and may be sulfated on tyrosine residues and contains N-linked glycosylation sites. Seven α -helical transmembrane domains - with

three intracellular and three extracellular connecting loops composed of hydrophilic amino acids - are oriented perpendicularly to the plasma membrane. A disulfide bond links highly conserved cysteines in extracellular loops 1 and 2. G-proteins are coupled through the C-terminus segment and possibly through the third intracellular loop [Murdoch and Finn, 2000].

Throughout the GPCR super-family, several highly conserved motifs have been identified. The aspartate-arginine-tyrosine (DRY) sequence in the second intracellular loop is required for activation of Gi-proteins, whereas the NPX2-3Y motif located in the seventh transmembrane region of most GPCRs contributes to ligand binding, activation and internalization of the receptor [Slice et al., 1994; Arora et al., 1995]. Additionally, GPCRs typically carry several serine residues within the intracellular C-terminal region, which can become phosphorylated by G-protein-coupled receptor kinases and mediate interaction with β -arrestins and desensitization of the receptor towards its ligand [Kim and Caron, 2008]. Table 1 shows the conserved motifs mentioned above and their functional relevance as shown for other GPCRs in which the motifs were altered.

2.4 CX3CL1 and its receptor CX3CR1

2.4.1 Fractalkine

CX3CL1 (fractalkine) is expressed as a cell surface protein on dendritic, epithelial, neuronal and most prominently on endothelial cells [Bazan et al., 1997]. CX3CL1 (like CXCL16) is a unique member of the chemokine family as it occurs in a membrane-tethered and a soluble form. It is expressed as type I transmembrane protein (N-terminus extracellular), and its ectodomain can be proteolytically cleaved from the cell surface. This process is known as shedding. ADAM10 is implicated in constitutive shedding of fractalkine [Hundhausen et al., 2003], whereas ADAM17 mediates PMA-induced shedding [Garton et al., 2001].

Table 1: Conserved motifs in GPCR class A. Conserved motifs in the G-protein-coupled receptor class A were mutated in a variety of receptors. The table shows the consequence of altering motifs.

Motif	Receptor	Consequence	Reference
DRY	rhodopsin	impaired stimulation of transducin	[Acharya and Karnik, 1996]
	gonadotropin-releasing hormone receptor	impaired internalization and IP3 response	[Arora et al., 1997]
	CXCR4	loss of activity	[Berchiche et al., 2007]
	oxytocin receptor	constitutive activity	[Fanelli et al., 1999]
	CCR5	loss of activity	[Gosling et al., 1997]
	CCR5	loss of G-protein activation	[Lagane et al., 2005]
	mCX3CR1	impaired signaling and chemotaxis	[Haskell et al., 1999]
	dopamine D2 and D3 receptors	impaired signaling	[Kim et al., 2008]
	alpha 1B adrenergic receptor	no G-protein coupling, constitutive desensitization	[Wilbanks et al., 2002]
	angiotensin II type 1A receptor	no G-protein coupling, constitutive desensitization	[Wilbanks et al., 2002]
	vasopressin receptor	non-signaling, constitutive desensitization	[Barak et al., 2001]
	V2 vasopressin receptor	no G-protein stimulation	[Rosenthal et al., 1993]
	NPX2-3Y	M1/M2 muscarinic receptor	decrease in signaling
alpha1B-adrenergic receptor		loss of receptor-mediated response	[Scheer et al., 2000]
histamine H2 receptor		loss of basal activity	[Alewijjnse et al., 2000]
beta-1-adrenergic receptor		impaired internalization and binding	[Barak et al., 1995]
angiotensin II receptor		impaired binding and signal transduction	[Hunyady et al., 1995]
truncation	gastrin-releasing hormone receptor	no impairments	[Slice et al., 1994]
	IL8Rbeta	migration impairment	[Ben-Baruch et al., 1995]
	CCR5	sustained calcium response	[Kraft et al., 2001]

The membrane-tethered form consists of a chemokine domain anchored to the plasma membrane through an extended mucin-like stalk, a transmembrane helix and an intracellular domain. Analysis of the C-terminal cleavage fragments, which remain in the cell membrane, reveals multiple cleavage sites used by ADAM10 [Hundhausen et al., 2007].

Compared to other chemokines, CX3CL1 has at least three unique structural features that may mediate its function as an adhesion molecule. It is a transmembrane molecule with a cytoplasmic tail that may participate in signal transduction, it has a mucin domain, and it has a three-dimensional structure that is slightly different from other chemokines [Mizoue et al., 1999]. The fractalkine mucin domain is a 26 nm long stalk that functions in extending the chemokine domain away from the cell surface and is functionally similar to the stalk regions of the selectin family of molecules. It does not contribute to fractalkine binding affinity and efficacy for stimulating calcium mobilization in CX3CR1-expressing cells [Harrison et al., 2001].

2.4.2 CX3CR1

CX3CL1 binds to a single receptor (CX3CR1, also known as V28) that is expressed on several leukocyte subsets including monocytes, NK cells, T cell populations, dendritic cells and microglia [Imai et al., 1997; Combadiere et al., 1998; Dichmann et al., 2001]. CX3CR1 belongs, as all chemokine receptors, to the group of G-protein-coupled heptahelical receptors and couples to Gi/o [Wong, 2003].

The CX3CR1 gene is multi-exonic with the ORF residing entirely in a single exon, like most chemokine receptors. There are three functionally independent promoter regions that direct CX3CR1 transcription, giving rise to three different transcripts that may be expressed selectively in different cell populations [Garin et al., 2002]. Four naturally occurring receptor variants (T57A, V122I, V249I and T280M) are described in humans [Faure et al., 2000]. While M280 is never found in the absence of I249, the

converse is not true [McDermott et al., 2003]. The I249 allele has been associated with reduced fractalkine binding affinity as well as with reduced risk for acute coronary events and improved endothelium-dependent vasodilation [McDermott et al., 2001; Moatti et al., 2001].

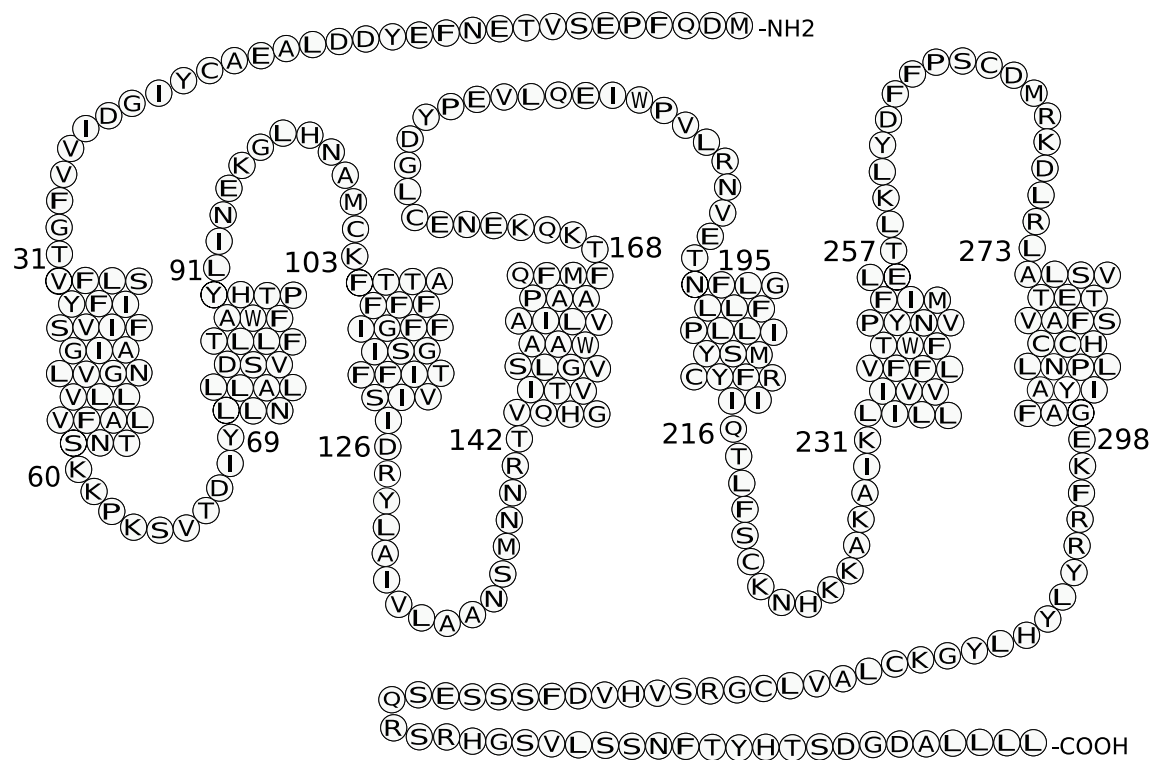


Figure 3: Schematic view of CX3CR1. CX3CR1 is a seven-transmembrane G-protein-coupled receptor belonging to the family of chemokine receptors. Targeted mutation of selected acidic amino acid residues demonstrated that the binding activity of CX3CR1 is critically dependent on the two negatively charged residues Asp25 and Glu254 located on the N-terminal domain and third extracellular loop, respectively. Furthermore, the initial interaction triggers the engagement of Glu13, Asp16, and Asp266, which are necessary for CX3CR1 activation [Chen et al., 2006]. The numbers specify the positions of the various amino acid residues in the protein. The transmembrane domains are illustrated by the cylindrical arrangements of the amino acids.

2.4.3 Consequences of CX3CR1-CX3CL1 interaction

Transmembrane as well as soluble CX3CL1 binds to CX3CR1. However, both CX3CL1 variants mediate different steps of the recruitment process and employ distinct mechanisms. Transmembrane CX3CL1 serves as an adhesion molecule, mediating enhanced leukocyte adhesion to endothelial cells under flow conditions. This activity is largely independent of CX3CR1-mediated Gi-protein activation and predominantly a result of the physical interaction of the transmembrane chemokine with its receptor [Fong et al., 1998]. By contrast, soluble CX3CL1 acts as a chemoattractant inducing directional cell migration via CX3CR1 signaling and activation of Gi -proteins [Imai et al., 1997].

Fractalkine expression is upregulated after stimulation with IL-1 β , LPS, IFN γ and TNF α , and it can induce its own expression, which is both mediated via the NF- κ B pathway [Garcia et al., 2000]. Treatment with CX3CL1 increases endothelial cell proliferation in a dose- and time-dependent manner [Lee et al., 2006], and the molecule may serve as survival factor for microglial cells and monocytes [Boehme et al., 2000; Landsman et al., 2009].

Receptor activation by soluble fractalkine induces activation of Akt and p53, ERK and eNOS phosphorylation in a time- and dose-dependent manner, and nuclear translocation of NF- κ B. It does not induce SAPK/JNK and p38 phosphorylation. Furthermore, stimulation with CX3CL1 induces a calcium flux response in CX3CR1 expressing cells in a concentration-dependent manner. The G-protein-coupled receptor inhibitor pertussis toxin (PTX) efficiently blocks fractalkine-induced phosphorylation of ERK, Akt and eNOS, suggesting that the receptor is linked to Gi-proteins [Lee et al., 2006].

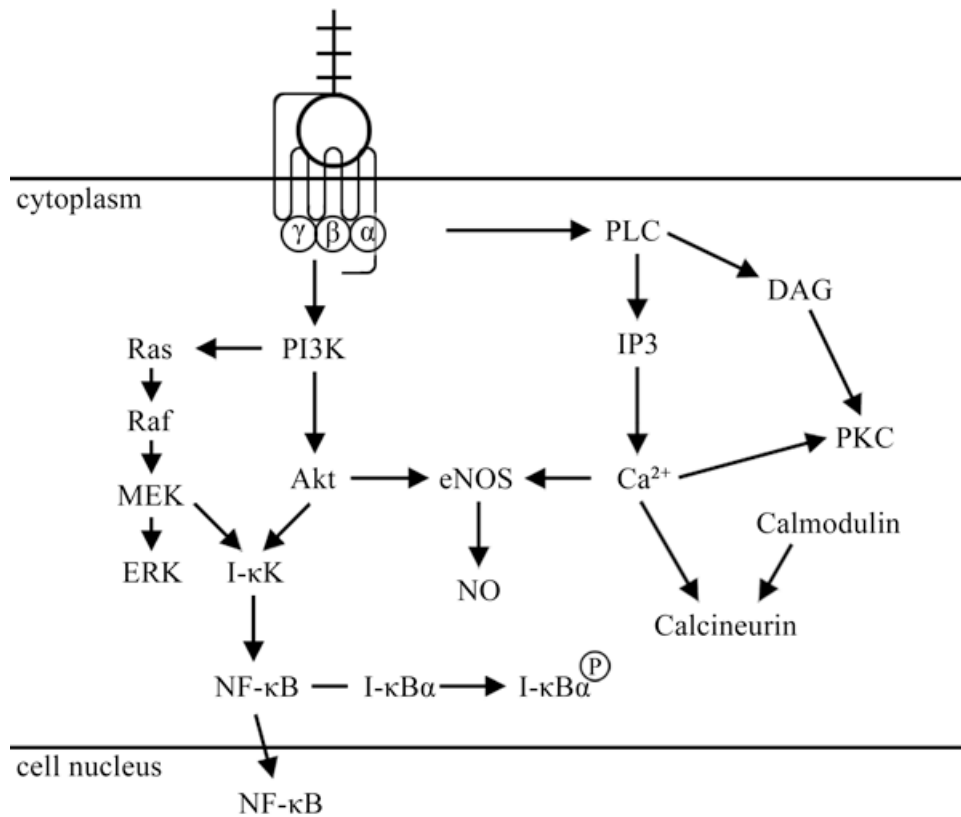


Figure 4: Schematic view of CX3CR1 signaling. On binding of CX3CL1 to its receptor CX3CR1, G-protein subunit α uncouples, and PI3-kinase (PI3K) and Phospholipase C (PLC) become activated. PLC activation leads to diacylglycerol (DAG) and inositol 1,4,5-trisphosphate (IP3) formation, which stimulate calcium release from the endoplasmic reticulum and subsequent activation of calcineurin, protein kinase C (PKC) and endothelial nitric oxide synthase (eNOS). PI3K activation leads to activation of mitogen-activated protein kinase (MAP kinase) pathway and Akt and subsequent translocation of NF- κ B to the nucleus.

2.4.4 CX3CL1 and CX3CR1 in clinical disease

Accumulating evidence suggests that CX3CL1-CX3CR1 interaction contributes to the development and the progression of many inflammatory diseases, some of which are described in more detail in the following.

Fractalkine is suggested to be involved in atherosclerosis and cardiovascular patho-

physiology. In some human advanced atherosclerotic lesions, high levels of fractalkine mRNA expression have been observed [Greaves et al., 2001]. Apolipoprotein E-deficient (apoE^{-/-}) mice show upregulated CX3CL1 expression, whereas apoE^{-/-} mice crossing with CX3CR1^{-/-} mice resulted in a decreased atherosclerotic lesion formation [Combadière et al., 2003; Lesnik et al., 2003]. Gene polymorphisms V249I and T280M of human CX3CR1 have been reported to be a genetic risk factor for coronary artery disease, whereas CX3CR1-V249I/T280M heterozygosity is associated with a reduced risk of acute coronary events [McDermott et al., 2001; Moatti et al., 2001].

Additionally, fractalkine has been reported to play a role in human renal diseases (glomerulonephritis, renal tumours, and renal transplants) and in kidney disease in animal models. The expression of fractalkine and the presence of CX3CR1-expressing cells have been demonstrated in patients with various types of nephropathies [Furuichi et al., 2001; Cockwell et al., 2002]. Anti-CX3CR1 antibody treatment blocked leukocyte infiltration into the glomeruli and improved renal function, suggesting a role for fractalkine and CX3CR1-expressing cells in the pathogenesis of human glomerulonephritis [Feng et al., 1999].

Furthermore, an increased expression of fractalkine has been detected in lymph nodes and brain tissue from patients with HIV. The increased expression of CX3CL1 is associated with a protection of neurons from two HIV-1 neurotoxins, but induces the depletion of CX3CR1-positive T-helper cells by contact with dendritic cells [Tong et al., 2000; Foussat et al., 2001]. Since HIV-infected patients homozygous for CX3CR1-I249M280 progress to AIDS more rapidly than do those with other haplotypes, it has been concluded that the specific polymorphism, CX3CR1-I249M280, is a genetic risk factor in HIV infection [Faure et al., 2000].

It still remains unclear whether these diseases are mediated by either the transmembrane, the soluble or both variants of CX3CL1. The investigation of each variant is complicated by the fact that transmembrane CX3CL1 is converted into soluble CX3CL1 by limited proteolysis. This process is called shedding and involves several cell

surface enzymes called sheddases. A class of sheddases implicated in the shedding process of CX3CL1 is the ADAM (a disintegrin and metalloproteinase) family with its members ADAM10 (kuzbanian) and ADAM17 (TACE for TNF α converting enzyme).

2.5 CXCL16 and its receptor CXCR6

2.5.1 CXCL16

CXCL16 is a CXC α chemokine, but shares characteristics of CC chemokines (strong homology to MIP-1 β , long loop between Cys2 and Cys3 like CTAK and TECK, and 6 Cys-residues like 6-C-Kine), and shows structural similarities to CX3CL1 like a transmembrane region and a chemokine domain suspended by a mucin-like stalk [Wilbanks et al., 2001]. Initially, CXCL16 was described as scavenger receptor for oxidized low density lipoprotein (ox-LDL), phosphatidylserine, dextran sulphate and bacteria under the name of SR-PSOX (scavenger receptor that binds phosphatidylserine and oxidized lipoprotein) [Shimaoka et al., 2000]. SR-PSOX specifically binds, internalizes and degrades ox-LDL leading to foam cell transformation implicated in the process of atherogenesis [Ross, 1993].

CXCL16 is predominantly expressed by antigen-presenting cells, including subsets of CD19⁺ B cells, CD14⁺ monocytes/macrophages, dendritic cells, aortic smooth muscle cells and by cells in the splenic red pulp [Matloubian et al., 2000; Wilbanks et al., 2001; Chandrasekar et al., 2004]. Like fractalkine, CXCL16 can be shed by ADAM10 to form a soluble chemokine that induces chemotaxis of activated T-cells and bone marrow plasma cells via its receptor CXCR6 [Matloubian et al., 2000; Nakayama et al., 2003; Abel et al., 2004].

2.5.2 CXCR6

CXCR6 (also called Bonzo), like all chemokine receptors a G-protein-coupled heptahelical receptor, is the only known receptor for CXCL16. It is expressed on CD4⁺ T-helper 1, CD8⁺ T-cytotoxic and T-regulatory 1 subsets of T-cells, smooth muscle cells, dendritic cells, B-cells, macrophages, and subsets of natural killer cells [Matloubian et al., 2000; Sharron et al., 2000; Kim et al., 2001; Wilbanks et al., 2001; Hofnagel et al., 2002; Sato et al., 2005]. CXCR6 was firstly described as a fusion co-factor for HIV-1/SIV [Deng et al., 1997], and the polymorphism CXCR6-3E/K is implicated in a prolonged survival time from *Pneumocystis carinii* pneumonia in HIV-positive individuals. In contrast, patients with the polymorphism showed impaired viral suppression after initiation of Highly Active Anti-Retroviral Therapy (HAART) [Passam et al., 2007].

Instead of the conserved DRY-motif that is common for G-protein-coupled receptors, CXCR6 has a DRF-motif. This alteration was already described for the arthropod 5-HT_{2βPan} receptor and was implicated in its constitutive activity [Clark et al., 2004]. The conserved NPX2-3Y motif is unaltered.

2.5.3 Consequences of CXCL16-CXCR6 interaction

CXCL16 mediates adhesion, chemotaxis and calcium signaling in CXCR6-expressing cells [Wilbanks et al., 2001]. As described for CX3CL1, both variants - soluble and transmembrane - might mediate different steps in the process of cell extravasation. CXCL16 is a potent activator of NF-κB, but fails to regulate its own expression, indicating that CXCL16, unlike CX3CL1, is not a NF-κB-responsive chemokine. Both IL-1 and TNFα fail to influence CXCL16 expression in human aortic smooth muscle cells and umbilical vein endothelial cells [Hofnagel et al., 2002].

CXCR6 signals via PI3K, Akt, IκK and IκB phosphorylation. Binding of CXCL16

mediates NF- κ B activation via Akt/PKB, leading to increased proliferation of human aortic smooth muscle cells. Therefore, treatment with CXCL16 does not induce cell death, but promotes cell survival and proliferation. Additionally, CXCL16 binding leads to Bad (Bcl-2-Antagonist of Cell Death)-phosphorylation, indicating its role as anti-apoptotic chemokine. This suggests that chemokines not only play a role in extravasation processes, but also in cell survival and angiogenesis [Chandrasekar et al., 2004].

2.6 ADAMs

ADAMs are type I transmembrane proteins and belong to the metzincin superfamily of zinc-dependent proteases. They generally consist of about 750-800 amino acids. The N-terminal extracellular pro-domain is followed by a highly conserved metalloprotease domain. The active site for the proteolytic cleavage contains HEXGHNLGXXHD and contains a catalytically essential zinc-ion, which is chelated by the three conserved histidin-residues. A conserved methionine residue beneath the active site metal, as part of a "Met-turn", loops the polypeptide chain beneath the catalytic zinc ion, forming a hydrophobic floor to the Zn²⁺ ion binding site [Stocker and Bode, 1995]. The disintegrin-domain might be a ligand for integrins and is succeeded by a cysteine-rich potential cell fusion region. The C-terminal cytoplasmic domain does not share significant sequence similarities. Some of them contain putative consensus sequences for binding to sarcoma (Src) and Src-related SH3 domains [Wolfsberg and White, 1996].

Although a single sheddase may shed a variety of substances, multiple sheddases can cleave the same substrate resulting in different consequences. More than 40 type-1 cell surface proteins are known substrates for ADAMs (reviewed in: [Pruessmeyer and Ludwig, 2008]). CX3CL1 can be cleaved from the cell surface by two distinct enzyme activities. ADAM10 is implicated in the constitutive shedding of CX3CL1 of unstimulated cells, whereas cleavage by ADAM17 is inducible by phorbol esters such as phorbol 12-myristate 13-acetate (PMA) [Garton et al., 2001; Hundhausen et al., 2003].

ADAM10 and ADAM17 are upregulated in activated endothelium and play a role in ectodomain shedding of adhesion molecules during leukocyte recruitment [Boulday et al., 2001]. Since CX3CL1 acts as an adhesion molecule that is upregulated in activated endothelium, it can be cleaved by ADAM10 or 17 to form an additional soluble chemoattractant to recruit more inflammatory cells as well as to allow abrogation of firm adhesion in order to let transmigration take place.

3 Aim of this thesis

This thesis aimed to characterize the role of CX3CL1 in distinct steps of leukocyte recruitment and to elucidate the mechanism of CX3CL1-mediated cell recruitment. Primary cells (PBMC) were investigated for adhesion and chemotaxis in response to soluble and transmembrane CX3CL1 expression on endothelial cells. Then, a model system of cell lines for adhesion and chemotaxis/transmigration induced by CX3CL1 was established and confirmed to show the same behavior as primary cells.

In order to determine which structural characteristics are important, mutated receptor variants altering the DRY motif in the second intracellular loop, the NPX2-3Y motif in the seventh transmembrane domain, and deleting all C-terminal serine residues by truncation were generated. The effect of mutating these highly conserved regions was studied in functional assays like binding, ligand uptake, signaling, adhesion, transmigration, and pseudopod formation.

Since the activity of ADAM10 and 17 is supposed to be required in efficient leukocyte extravasation, it was examined whether the metalloproteases ADAM10 and 17 are required in CX3CL1-mediated function using pharmacological inhibitors to the proteases and shRNA silencing.

CXCL16 is the only other chemokine that is expressed as transmembrane as well as soluble form. This raised the question whether the findings concerning CX3CR1 are similar for CXCR6. Therefore, the CXCL16-CXCR6 interaction was examined in functional assays like adhesion and chemotaxis. Furthermore, the unusual DRF motif of CXCR6 was altered and the functional consequence of the receptor variants was studied.

4 Materials and Methods

4.1 Materials

4.1.1 Cell Culture

Media, supplements and reagents used for cell culture were purchased from PAA (Pasching, Austria) if not stated otherwise. Cells were cultured on cell culture plasticware from Sarstedt (Nuembrecht, Germany).

4.1.2 Primer

All primers were ordered from Eurofins MWG Operon (Ebersberg, Germany). They were diluted to a final concentration of 100 pmol/μl.

Primer	Sequence
hCX3CR1 sense	5'- gaattcaccatggatcagttccctgaatcagt -3'
hCX3CR1 antisense	5'- ctcgagtcagagaaggagcaatgcatctccatca -3'
hCX3CR1 S319X antisense	5'- cggatgaagaatatgcttccaaaaagccgta -3'
hCX3CR1 R127N sense	5'- tcacgacattgataactacctggccatcgtcct -3'
hCX3CR1 R127N antisense	5'- cggatgatgaagaatatgcttccaaaaagccgta -3'
hCX3CR1 N289A sense	5'- cctggctcctctcatctatgcattt -3'
hCX3CR1 N289A and Y293A antisense	5'- caacaatggctaaatgaaccgtct -3'
hCX3CR1 Y293A sense	5'- cctgaatcctctcatcgtcgtcattt -3'
hCXCR6 sense	5'- gaattcaccatggcagagcatt-3'
hCXCR6 antisense	5'-ctcgagctataactggaacat-3'
hCXCR6 R127N sense	5'-cactgtggatcgttacattgta-3'

hCXCR6 R127N antisense	5'-atgcaggtgaggatgagcat-3'
hCXCR6 F128Y sense	5'-atgcaggtgaggatgagcat-3'
hCXCR6 F128Y antisense	5'-atgcaggtgaggatgagcat-3'

4.1.3 Plasmids

Name	Backbone	Restriction sites used
hCX3CR1	pcDNA3.1+	<i>EcoRI XhoI</i>
hCX3CR1-R127N	pcDNA3.1+	<i>EcoRI XhoI</i>
hCX3CR1-N289A	pcDNA3.1+	<i>EcoRI XhoI</i>
hCX3CR1-Y293A	pcDNA3.1+	<i>EcoRI XhoI</i>
hCX3CR1-S319X	pcDNA3.1+	<i>EcoRI XhoI</i>
hCXCR6	pcDNA3.1+	<i>EcoRI XhoI</i>
hCXCR6-R127N	pcDNA3.1+	<i>EcoRI XhoI</i>
hCXCR6-F128Y	pcDNA3.1+	<i>EcoRI XhoI</i>

4.1.4 Antibodies

Antibody	Species	Company	Final Conc.	Application
hCX3CR1-PE	rat IgG2bκ	MBL, Japan	1 μg/ml	FACS
isotype control-PE	rat IgG2bκ	Abcam	1 μg/ml	FACS
hCX3CL1	mouse IgG1	R&D Systems	10 μg/ml	FACS, inhibition
hCX3CL1	mouse	R&D Systems	4 μg/ml	ELISA
hCX3CL1-biotin	mouse	R&D Systems	0.3 μg/ml	ELISA
ICAM-1	mouse IgG1	R&D Systems	10 μg/ml	inhibition
VCAM-1	mouse IgG1	R&D Systems	10 μg/ml	inhibition

isotype control	mouse IgG1	R&D Systems	10 µg/ml	FACS, inhibition
hCXCR6-PE	mouse IgG2b	R&D Systems	5 µg/ml	FACS
isotype control-PE	mouse IgG2b	R&D Systems	5 µg/ml	FACS
6xHis-tag	mouse IgG2b	Abcam	4 µg/ml	FACS
mouse-PE	goat	Jackson Immuno	2.5 µg/ml	FACS
humanFc-PE	goat	Jackson Immuno	5 µg/ml	FACS

4.1.5 Chemicals

All chemicals were ordered from either Sigma-Aldrich (St.Louis, MO) or Roth (Karlsruhe, Germany), if not specified otherwise. All enzymes for cloning were purchased from Fermentas (St.Leon-Rot, Germany), if not specified otherwise.

Name	Company
AlexaFluor647-labeled CX3CL1-CD	Almac, Craigavon, UK
AMAXA nucleofactor	Lonza, Cologne, Germany
Calcein-AM	Biotium Inc., Hayward, CA
Collagen G	Biochrom AG, Berlin, Germany
Collagenase II	Sigma-Aldrich, St.Louis, MO
CXCL16-CD	Peptotech, Hamburg, Germany
CXCL16-6xHis	R&D Systems, Wiesbaden, Germany
CX3CL1-CD	Peptotech, Hamburg, Germany
Endothelial cell growth medium	Promocell, Heidelberg, Germany
Fluo-3-AM	Molecular Probes, Karlsruhe, Germany
Gel loading dye	Fermentas, St.Leon-Rot, Germany
G418	Calbiochem, Hamburg, Germany
HBSS	Gibco, Karlsruhe, Germany

HEPES	Gibco, Karlsruhe, Germany
IFN γ	Peprotech, Hamburg, Germany
Lipofectamine	Invitrogen, Karlsruhe, Germany
NucleoSpin extract II kit	Macherey-Nagel, Dueren, Germany
Pancoll	Pan Biotech, Aidenbach, Germany
pcDNA3.1+	Invitrogen, Karlsruhe, Germany
Pertussis toxin	Calbiochem, Hamburg, Germany
Plasmid DNA purification kit	Macherey-Nagel, Dueren, Germany
Strep-POD	Roche, Grenzach, Germany
TNF α	Peprotech, Hamburg, Germany
TOPO TA cloning kit	Invitrogen, Karlsruhe, Germany

4.1.6 Devices and Materials

Device/Material	Company
AMAXA Nucleofactor	Lonza, Cologne, Germany
Avanti J-25	Beckman Coulter, Palo Alto, CA
Boyden chamber	Neuroprobe, Gaithersburg, MD
Cary Eclipse reader	Varian, Palo Alto, CA
Centrifuge 5415R	Eppendorf, Hamburg, Germany
Centrifuge 5810R	Eppendorf, Hamburg, Germany
EasyCyte Mini	Millipore, Billerica, MA
FACSCalibur	BD Biosciences, San Jose, CA
FACSCanto	BD Biosciences, San Jose, CA
Fluorescence plate reader Tecan Genios	Tecan, Maennedorf, Switzerland

Glass bottom dishes	MatTek, Ashland, MA
Hemocytometer	Brand, Wertheim, Germany
Leica DM-IL microscope	Leica, Wetzlar, Germany
Leica DM-IRB microscope	Leica, Wetzlar, Germany
LSM 7 Duo microscope	Zeiss, Goettingen, Germany
MaxiSorp ELISA plate	Nunc, Langenselbold, Germany
μ -slide VI	ibidi, Munich, Germany
NanoDrop ND-1000	PEQLAB, Erlangen, Germany
Polycarbonate membrane	Neuroprobe, Gaithersburg, MD
Syringe pump	Landgraf, Langenhagen, Germany
TProfessional basic thermocycler	Biometra, Goettingen, Germany
Transwell filters	Costar Corning, Schiphol-Rijk, Netherlands

4.1.7 Inhibitors

The substance GW280264X is a metalloprotease inhibitor based on hydroxamat (Figure 5). It was synthesized at GlaxoSmithKline (Stevenage, UK) and stored at 4°C in a 10 mM stock in DMSO. GW280264 inhibits the proteolytic activity of ADAM17, and to a smaller degree of ADAM10 [Ludwig et al., 2005].

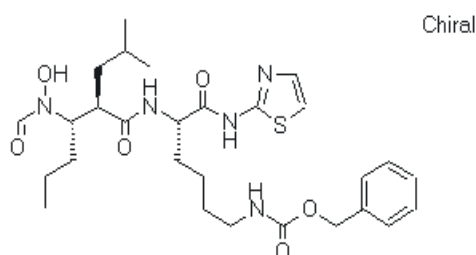


Figure 5: Structure of GW280264X. The metalloprotease inhibitor is based on hydroxamat and inhibits ADAM17 as well as ADAM10. The half maximal inhibitory concentration (IC₅₀) is 8.0 nM for ADAM17 and 11.5 nM for ADAM10.

Dynasore (3-Hydroxynaphthalene-2-carboxylic acid (3,4-dihydroxybenzylidene) hydra-zide) was obtained from Tocris (Bristol, UK) and stored at -20°C at 100 mM in DMSO. The working concentration was 100 μM . It is a small molecule GTPase inhibitor that targets dynamin-1 and dynamin-2. Dynasore blocks dynamin-dependent endocytosis, and scission of endocytic vesicle. It is cell-permable and blocks in a reversible and noncompetitive manner [Macia et al., 2006].

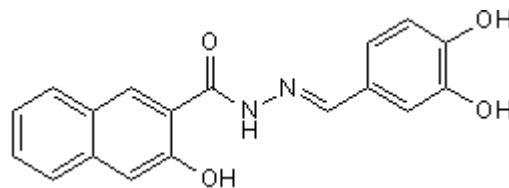


Figure 6: Structure of Dynasore. The small molecule GTPase inhibitor Dynasore blocks dynamin-1 and dynamin-2. The half maximal inhibitory concentration (IC₅₀) is approximately 15 μM .

4.2 Methods

4.2.1 Cell culture

4.2.1.1 Maintenance of cells

The human embryonic kidney cell line HEK293 (ATCC: CRL-1573) was grown in DMEM medium supplemented with 1% penicillin and streptomycin and 10% FCS. The human epithelial cell line ECV304 (ATCC: CRL-1998) was grown in M199 medium supplemented with 1% penicillin and streptomycin and 10% FCS. The murine pre-B-cell cell line L1.2 (Massachusetts Association of Technology Transfer, Tufts University, Boston, MA) was grown in RPMI1640 medium supplemented with gentamycin, 10% FCS, 1% HEPES, 1% pyruvate and β -mercaptoethanol. The primary human umbilical

vein endothelial cells were grown in Endothelial Cell Growth Medium including Supplement.

Cells were subcultured using trypsin-EDTA. To this purpose, cells were washed with PBS and incubated with Trypsin-EDTA for 5 minutes at 37°C. Then, cells were resuspended in PBS, centrifuged at 300×g, and seeded at 1:5 to 1:20.

Cells were counted and viability of cells was tested using Trypan blue. 10 µl of cell suspension was mixed with 10 µl 0.4% Trypan blue and given onto a hemacytometer. Trypan blue exclusively stains dead cells blue. These cells were excluded in counting.

For freezing cells, confluent grown cells were washed with PBS and incubated with Trypsin-EDTA for 5 minutes at 37°C. Subsequently, cells were washed with PBS, centrifuged at 300×g at room temperature, and resuspended in 3 ml pre-cooled medium with 20% FCS and 10% DMSO. 1 ml of cell suspension at a time was given into a cryotube. Cells were then transferred on ice at -20°C over night, at -80°C for 3 days, and at liquid nitrogen for final storage.

4.2.1.2 Transient transfection

Different strategies were used to transiently transfect cells. HEK293 cells were transfected with lipofectamine, while L1.2 cells were transfected using the AMAXA system.

Lipofectamine. Cells were seeded in 6-well-plates and grown to 70% - 80% confluency. Following complexes were prepared for transfection per well of a 6-well-plate:

1.5 µg DNA

3 µl Lipofectamine

100 µl serum-free medium

During the incubation of the reaction setup for 20 minutes at room temperature, cells were washed and medium was exchanged. 100 μl of the complex solution were added to each well drop by drop. Cells were incubated at 37°C in a CO₂ incubator for 48 hours.

AMAXA Nucleofactor. 2×10^6 cells were taken out of the flask, centrifuged at $300 \times g$ for 5 minutes at room temperature and medium was removed. The cell pellet was resuspended with the following solution:

5 μg DNA

18.1 μl Nucleofactor supplement

81.8 μl Nucleofactor solution

The cell/DNA suspension was then transferred into cuvettes, inserted into the Nucleofactor device, and program P16 was applied. Immediately after the program was finished, pre-warmed medium was added to the cuvettes, and the cells were gently transferred into T25 flasks. Cells were incubated at 37°C in a CO₂ incubator for 48 hours.

4.2.1.3 Stable transfection

48 hours after transfection cells were selected for receptor expression using 1 mg/ml G418 because only transfected cells are resistant to G418. For HEK293 cells medium was changed every 3 days, and fresh G418 was added. L1.2 cells were tested for viability every 3 days, and fresh G418 was added every 5 days. The remaining viable cells were cultured to confluency, seeded on 10 cm² plates and partly frozen when confluent. Single clones were established using the limited dilution method. Cells were counted and diluted to 1 cell/100 μl medium containing G418. 100 μl of cell suspension was added per well of a 96-well-plate. After 5 days, 50 μl medium containing 3x G418 was added to the wells. Formation of single cell patches was controlled by microscopy. After reaching confluency, cells were gently transferred to 6-well-plates and T25 flasks. The receptor expression level was checked using flow cytometry analysis. Clones of the different

receptor variants with similar expression levels were chosen for further experiments.

4.2.1.4 Isolation of HUVEC

Primary human umbilical vein endothelial cells were freshly prepared from human umbilical veins. For this purpose, 10 - 15 cm of umbilical vein were flushed with PBS to avoid contamination with blood cells. Afterwards, the vein was filled with collagenase type II solution (40 µg/ml in PBS) and incubated for 15 minutes at 37°C. Cells were then flushed out of the vein with 50 ml PBS and centrifuged at 300xg at room temperature. Cells were resuspended in supplemented HUVEC growth medium and grown on collagen G-coated cell culture dishes (coating: 15 minutes with 40 µg/ml collagen G in PBS). HUVEC were subcultured before reaching confluency for a maximum of 4 passages.

4.2.1.5 Isolation of PBMCs

Human peripheral blood mononuclear cells (PBMC) were isolated from citrated (0.38%) venous blood of healthy volunteers by 1:1 dilution in PBS and subsequent density gradient centrifugation on a Ficoll Hypaque layer (25 ml blood-PBS mixture on 25 ml Ficoll Hypaque) for 40 minutes at RT without brake. PBMC that accumulated in the middle layer were carefully taken off and, after 2-fold washing with PBS, PBMC were used for functional assays as described below.

4.2.2 Cloning

4.2.2.1 hCX3CR1 and its variants in pcDNA3.1

Human CX3CR1 cDNA was previously amplified by Matthias Voss from human

PBMC using the primers indicated in section 4.1.2 and cloned into pcDNA3.1+ using *XhoI* and *EcoRI* as restriction sites generating hCX3CR1-pcDNA3.1+. Based on this plasmid, the truncation variant of hCX3CR1 that lacks all intracellular serine-residues was generated by using an antisense primer with inserted stop codon at serine residue 319 and subsequent restriction site for *XhoI*. cDNA was amplified, and the product was purified using gelelectrophoresis and a gel extraction kit. cDNA for the other receptor variants was generated by site-directed mutagenesis via ligation PCR. An upstream fragment was amplified using the CX3CR1 sense primer and a specific antisense primer for the hCX3CR1 variant. Additionally, a downstream fragment was generated with antisense primer for CX3CR1 and sense primers carrying the desired mutations. The upstream and downstream PCR products were phosphorylated separately using polynucleotide kinase and ligated before a PCR with CX3CR1 sense and antisense primers was performed. The cDNA for the different receptor variants was ligated into TOPO cloning vector and positive clones were selected with blue-white screening. Clones were then grown and DNA was purified. The product was subsequently ligated into the expression vector pcDNA3.1+ using *EcoRI* and *XhoI*. All sequences were confirmed by sequencing. All plasmids were amplified in large scale and frozen for immediate use. Protocols for the different steps are given below.

Human CXCR6 cDNA was previously generated by Alexander Schulte from human PBMC using the primers indicated in section 4.1.2 and cloned into pcDNA3.1+ using *XhoI* and *EcoRI* as restriction sites generating hCXCR6-pcDNA3.1+ [Ludwig et al., 2005]. Based on this plasmid, the variants of hCXCR6 were generated by the same strategy used for the CX3CR1 variants.

PCR. For the variants of human CXCR6 and CX3CR1, ligation-PCRs were performed. Alteration of the DRY and NPX2-3Y motifs required two PCRs leading to an upstream and a downstream fragment. DNA polymerase of *Pyrococcus furiosus* (*Pfu* polymerase) was used due to its integrated proof reading function and the generation of blunt end fragments. The following protocol was used:

1 µl forward primer				
1 µl reverse primer		10'	95°C	initial denaturation
0.5 µl <i>pfu</i> polymerase	35 cycles	2'	95°C	denaturation
5 µl <i>pfu</i> buffer		30"	60°C	primer annealing
2 µl dNTP		2'	72°C	elongation
1 µl plasmid		10'	72°C	final elongation
39.5 µl A.dest.				

Agarose gel electrophoresis. After PCR was performed, products were separated using agarose gel electrophoresis. Therefore, samples were mixed with 2x loading dye, loaded onto 1% or 2% agarose gels including ethidiumbromide in TAE buffer and separated using 100 V. Afterwards, bands of the desired size were cut on an UV-light table. As standard, 5 µl of GeneRuler kb DNA Ladder was used.

TAE buffer (50x)

242 g Tris

57.1 ml acetic acid

100 ml 0.5 M EDTA, pH 8.0

ad 1000 ml A.dest.

Gel extraction. For DNA gel-extraction, the NucleoSpin extract II kit was used according to manufacturer's instructions. Briefly, gel fragment was mixed with buffer at 0.5 mg/µl and bound onto a column. After washing off salt and impurities, DNA was eluted in 50 µl H₂O.

Phosphorylation of PCR fragments. PCR fragments had to be phosphorylated for ligation. The following mixture was prepared for each fragment:

10 μ l 10 x ligation buffer

1 μ l PCR product

→ 5' 70°C

2 μ l T4 polynucleotide kinase

→ 30' 37°C

Ligation of PCR fragments. Subsequently, both phosphorylated fragments were ligated using T4 ligase in the following mixture:

5 μ l phosphorylated upstream fragment

5 μ l phosphorylated downstream fragment

1 μ l T4 DNA ligase

→ 60' RT

PCR of ligation product. Ligation products were then amplified using PCR technique. In this case, high fidelity *Taq* polymerase was used due to its integrated proof reading function and the generated A-overhang in products. This PCR protocol was also used for the truncation mutant of the receptor.

1 μ l forward primer

1 μ l reverse primer

0.5 μ l high fidelity *Taq* polymerase

5 μ l high fid. *Taq* (incl Mg^{2+}) buffer 35 cycles

2 μ l dNTP

1 μ l ligation or plasmid

39.5 μ l A.dest.

10' 95°C initial denaturation

2' 95°C denaturation

30" 60°C primer annealing

2' 72°C elongation

10' 72°C final elongation

Subsequently, PCR products were separated using agarose gel electrophoresis and the fragment at about 1 kb was cut and extracted.

TOPO TA cloning. For further amplification PCR products were cloned into TOPO vector using the TOPO TA cloning kit according to manufacturer's instructions. Therefore, the following mixture was prepared:

4 μ l PCR product

1 μ l salt solution

1 μ l vector

→ 10' RT

This mixture was then used for heat-shock transformation.

Heat-shock transformation. To transfer the plasmid containing the desired sequence into bacteria, heat-shock transformation was used. *E.coli* TOP10 bacteria were incubated with 1.5 μ l of plasmid for 30 minutes on ice. For heat-shock, cells were incubated for 40 seconds at 42°C and then incubated for 5 minutes on ice. Cells were then mixed with 450 μ l SOC medium (SOB medium supplemented with 20 mM glucose) and incubated for 1 hour at 37°C while shaking. 100 μ l of cell suspension were spread on agar plates containing ampicillin and X-gal for TOPO cloning and only ampicillin for pcDNA3.1+ cloning. Plates were incubated over night at 37°C.

Clone selection. For TOPO cloning, colonies were selected via blue-white-screening. White colonies represent positive clones that integrated the plasmid, whereas blue colonies did not include the plasmid. For pcDNA3.1+ cloning, colonies were picked randomly with a pipette tip and tested for transformation via colony PCR technique. Picked clones were transferred into 5 ml LB medium and grown over night at 37°C.

Colony PCR. Successful transformation was tested via PCR technique. As template the pipette tip with the picked colony was dipped into the reaction mix. Following protocol was used:

0.5 µl forward primer					
0.5 µl reverse primer		10'	95°C	initial denaturation	
0.5 µl <i>Taq</i> polymerase	30 cycles		1'	95°C	denaturation
3 µl <i>Taq</i> (excl. Mg ²⁺) buffer			30"	63°C	primer annealing
5 µl Mg ²⁺			1'	72°C	elongation
1 µl dNTP			10'	72°C	final elongation
39.5 µl A.dest.					

Subsequently, the products were visualized using agarose gel electrophoresis.

MiniPrep. Amplified plasmids were purified using a plasmid DNA purification kit according to manufacturer's instruction. Briefly, cells were sedimented, lysed and DNA and proteins were precipitated. DNA was then bound onto a silica column. After washing off contaminants, plasmids were eluted in A.dest.

Restriction. In order to express the gene product in mammalian cells, the cDNA was transferred from the TOPO vector into the eukaryotic expression vector pcDNA3.1+. Therefore, the desired sequence was cut out of the TOPO vector, and the pcDNA3.1+ vector was cut for linearization using the following mixture:

- 1 µl *Eco*RI
- 1 µl *Xho*I
- 6 µl Tango Buffer
- 1 µl plasmid (TOPO and pcDNA3.1+)
- 21 µl A.dest.
- 3 h 37°C

Subsequently, products were separated using agarose gel electrophoresis, and the fragment at about 1 kb and the linearized pcDNA3.1+ vector were cut and extracted.

Ligation into pcDNA3.1+. For ligation of the DNA into pcDNA3.1+ with T4 ligase the following protocol was used:

- 10 µl insert
- 1 µl plasmid
- 1 µl T4 DNA ligase
- 3 µl T4 DNA ligase buffer
- 15 µl A.dest.
- over night 16°C

The ligated plasmid was then transferred into *E.coli* using heat-shock transformation as described above.

4.2.2.2 Fractalkine-Fc fusion protein

An expression vector for the fusion protein of human CX3CL1 and human IgG1-Fc-fragment (hFc) was generated previously by Matthias Voss. cDNA coding for hFc was inserted into pcDNA3.1 using *EcoRI* and *XhoI*. Subsequently, a cDNA fragment for the ectodomain of human CX3CL1 was generated by PCR using sense and antisense primers as indicated in table 4.1.2, and then inserted into pcDNA3.1-Fc using *HindIII* and *EcoRI*. All sequences were confirmed by sequencing.

4.2.3 Molecular biology and proteinbiochemistry

4.2.3.1 Analysis of surface expression

Cells were analyzed for surface expression of chemokine receptors or transmembrane chemokines by staining with appropriate antibodies (see table 4.1.4). Cells were

harvested, washed with PBS, and resuspended to 1×10^6 cells/ml in PBS with 0.2% BSA. Cells were then incubated with antibody solution at the indicated final concentration and in a final volume of 25 μ l. For directly fluorescently labeled antibodies, cells were stained for 30 minutes on ice in the dark, washed twice with 250 μ l PBS with 0.2% BSA to remove excess antibody, and resuspended in 100 μ l PBS with 0.2% BSA. For unlabeled antibodies, cells were incubated with first antibody on ice for 30 minutes, after washing they were incubated with the fluorescently labeled detection antibody against the first antibody on ice in the dark for another 30 minutes and washed afterwards. For immediate measurements, no fixation was used, and cells were resuspended in PBS with 0.2% BSA, otherwise cells were resuspended in 4% PFA in PBS with 0.2% BSA and kept cold in the dark. The fluorescence signal was then analyzed by flow cytometry.

PBS (phosphate buffered saline)

137 mM NaCl

2.7 mM KCl

10 mM Na₂HPO₄

2 mM KH₂PO₄

in A.dest.

4.2.3.2 ELISA

For ELISA (enzyme-linked immunosorbent assay) detection of soluble CX3CL1, MaxiSorp flat-bottom 96-well plates were coated over night with coating antibody at a final concentration of 4 μ g/ml in PBS at room temperature. Plates were then washed 3 times with washing buffer (PBS with 0.05% Tween) and blocked for 2 hours with blocking buffer (PBS with 0.05% Tween and 2% BSA) at room temperature. Samples and standard were added after washing and incubated for 1 hour at room temperature. After washing 3 times with washing buffer, anti-CX3CL1-biotin antibody in a final

concentration of 0.3 $\mu\text{g/ml}$ in blocking buffer was added and incubated for 1 hour at room temperature. After washing with washing buffer, Streptavidin-POD was added in a 1:5000 dilution in blocking buffer, and incubated for 1 hour at room temperature. After washing 4 times with washing buffer, substrate solution was added, incubated for 10-20 minutes and the reaction was stopped using 100 μl 1M H_2SO_4 . The signal was then measured in a plate reader at a wavelength of 450 nm with a reference wavelength of 550 nm.

4.2.4 Functional assays

4.2.4.1 Ligand binding

For CX3CL1 binding experiments, cells were harvested, washed with PBS and resuspended to 2×10^6 cells/ml in PBS with 0.2% BSA. Cells were then incubated for 1 hour on ice with a 1:10 dilution of the supernatant of HEK293 cells transfected to express soluble CX3CL1 that was fused to the Fc-part of human IgG1. After washing off excess CX3CL1-Fc twice with 250 μl PBS with 0.2% BSA, the Fc-part was detected using a fluorescently labeled α -Fc-antibody in a final volume of 25 μl . Cells were incubated with the antibody for 30 minutes on ice in the dark. After washing off excess antibody twice with 250 μl PBS with 0.2% BSA, cells were resuspended in 100 μl PBS with 0.2% BSA and the fluorescence signal was measured by flow cytometry.

For CXCL16 binding experiments, cells were harvested, washed with PBS and resuspended to 2×10^6 cells/ml in PBS with 0.2% BSA. Cells were then incubated for 1 hour on ice with 100 ng/ml recombinant 6xHis-tagged CXCL16 in the absence or presence of 1 $\mu\text{g/ml}$ recombinant untagged CXCL16. After washing off excess CXCL16 twice with 250 μl PBS with 0.2% BSA, the 6xHis-tag was detected with a mouse anti-6xHis-antibody for 30 minutes on ice in a final volume of 25 μl . After two washing steps with 250 μl PBS with 0.2% BSA, cells were incubated with a goat anti-mouse PE-

labeled antibody for 30 minutes on ice in the dark. After washing off excess antibody twice with 250 μ l PBS with 0.2% BSA, cells were resuspended in 100 μ l PBS with 0.2% BSA and the fluorescence signal was measured by flow cytometry.

4.2.4.2 Ligand uptake

For ligand uptake experiments, cells were harvested and resuspended to 2×10^6 cells/ml in PBS with 0.2% BSA. Prior to CX3CL1-treatment, cells were left on ice for 30 minutes with or without 0.2% NaN₃. Cells were then incubated with 10 nM AlexaFluor647-labeled CX3CL1 chemokine domain at 4°C or 37°C for 30 minutes in a final volume of 25 μ l. Cells were washed twice with 250 μ l ice-cold PBS with 0.2% BSA or PBS with 0.2% BSA containing 0.2% NaN₃, resuspended with ice-cold PBS with 0.2% BSA or PBS with 0.2% BSA containing 0.2% NaN₃ and kept on ice to avoid further ligand uptake. The fluorescence signal was measured by flow cytometry.

4.2.4.3 Intracellular calcium transients

Cells were harvested, resuspended in PBS to 2×10^6 cells/ml, and loaded with 4 μ g/ml of the calcium-indicator Fluo-3-AM for 30 minutes at 37°C. After two-fold washing with calcium assay buffer, cells were resuspended and kept in calcium assay buffer supplemented with 1% FCS. Before measurement, 2.5×10^6 cells were resuspended in 1.5 ml assay buffer containing no calcium, but 0.3 mM EDTA. Cells were incubated in a plastic cuvette at 37°C under constant stirring and Fluo-3 fluorescence was continuously monitored at excitation and emission wavelengths of 490 and 526 nm, respectively, using a fluorescence spectrophotometer. After 100 seconds, cells were stimulated with 10 nM CX3CL1 or CXCL16 chemokine domain, and the fluorescence signal was recorded for 200 seconds. Finally, loading of cells with fluorescent dye was controlled by addition of calcium (1.6 mM) and digitonin (125 μ g/ml), leading to maximal signal by complex formation of Fluo-3 with calcium, and finally by addition of EGTA (15 mM) for

dissolving the complex.

Calcium Assay Buffer

138 mM NaCl

6 mM KCl

1 mM MgCl₂

5.5 mM D-Glucose

20 mM HEPES

1.6 mM CaCl₂

in A.dest.

pH 7.4

4.2.4.4 Adhesion under static conditions

For adhesion under static conditions, cells expressing the ligand (HUVEC or ECV304) were seeded onto 24-well-plates and were cultured to full confluency as confirmed by microscopy. HUVEC were pretreated with 10 ng/ml TNF α and 10 ng/ml IFN γ 16 hours prior to the experiment to stimulate chemokine expression. L1.2 cells or PBMC were harvested and stained with 10 μ M CalceinAM in PBS for 15 minutes at 37°C in the dark, and after washing off excess dye, 5x10⁵ cells in PBS were centrifuged with 300xg for 3 minutes onto the chemokine expressing HUVEC or ECV304 cell layer. The fluorescence signal of adherent cells was measured in a fluorescence plate reader after each of 12 washing steps with PBS at an excitation wavelength of 480 nm and an emission wavelength of 550 nm.

The number of adherent cells is given as adhesion index (AI) that was determined by dividing the number of adherent cells on ligand-expressing cells by random adhesion of

cells on a cell layer that does not express the ligand.

4.2.4.5 Adhesion under flow conditions

For adhesion under flow conditions, ECV304 cells or HUVEC were seeded onto a flow adhesion chamber and were cultured to full confluency. HUVEC were stimulated with 10 ng/ml IFN γ and TNF α 16 hours prior to assay to induce CX3CL1 expression. HEK293 cells or PBMC were stained with 10 μ M CalceinAM for 15 minutes at 37°C in the dark, washed to remove of excess dye and resuspended in flow adhesion buffer to 5x10⁵ cells/ml. The flow adhesion chamber containing the ECV304 or HUVEC cell layer was then connected to a syringe pump and inserted into a temperature controlled incubation chamber culture on the stage of an inverted microscope. After washing the cell layer with warm flow adhesion buffer for 3 minutes, it was perfused by a suspension of calcein-labeled cells with a shear stress rate of 2 dyne for 1 minute. Thereafter, 8 subsequent pictures were taken, and the number of adherent cells was determined.

Flow Adhesion Assay Buffer

10% HBSS

1% HEPES

1% BSA

in A.dest.

The number of adherent cells is given as adhesion index (AI) that was determined by dividing the number of adherent cells on ligand-expressing cells by random adhesion of cells on a cell layer that does not express the ligand.

4.2.4.6 Chemotaxis

Stably transfected L1.2 cells or PBMC were harvested, washed twice with RPMI1640

with 0.2% BSA, and resuspended at 2×10^6 cells/ml in RPMI1640 with 0.2% BSA. The lower wells of a modified 48-well Boyden chamber were filled with 29.5 μ l RPMI1640 with 0.2% BSA with or without the indicated concentrations of CX3CL1 or CXCL16 chemokine domain, covered with a polycarbonate membrane with 8 μ m pores, and 30 μ l of cell suspension was added to the upper wells. After incubation of 2 hours at 37°C, migrated cells were counted using a hemacytometer.

The number of migrated cells is given as migration index (MI) that was determined by dividing the number of migrated cells treated with a stimulus by random migration of unstimulated cells.

4.2.4.7 Transmigration

ECV304 cells or HUVEC were seeded on transwell filters with 8 μ m pores and grown to confluency. L1.2 cells or PBMC were harvested, washed twice with 0.2% BSA, and resuspended to 2×10^6 cells/ml in RPMI1640 with 0.2% BSA. 24-well culture plates were filled with 600 μ l/well RPMI1640 with 0.2% BSA with or without the indicated concentrations of CX3CL1 or CXCL16 chemokine domain. Transwell inserts containing the HUVEC or ECV304 cell layer were then placed into the wells and filled with 100 μ l of L1.2 or PBMC cell suspension. After incubation for 2 hours at 37°C, transmigrated cells were counted using a hemacytometer.

The number of transmigrated cells is given as transmigration index (TI) that was determined by dividing the number of transmigrated cells treated with a stimulus by random transmigration of unstimulated cells.

4.2.4.8 Pseudopod formation

Wt- or CX3CL1-ECV304 cells were seeded on glass bottom dishes and grown to confluency. L1.2 cells were harvested, washed twice with RPMI1640 with 0.2% BSA,

resuspended to 2×10^5 cells/ml in RPMI1640 with 0.2% BSA and placed on the ECV304-cell layer in the prewarmed chamber at 37°C. Time-lapse videos were captured using a LSM 7 Duo Microscope for 5 minutes, and 100 cells per condition were analyzed for pseudopod formation. Evaluation for pseudopod formation defined as temporal protrusions from the cell body with a minimal length of 0.5 μm was done in a blinded fashion.

4.2.5 Statistical analysis

Data were statistically analyzed by using the one-way ANOVA with posthoc Bonferroni's Multiple Comparison t-tests using GraphPadPrism software (GraphPad Prism 5.01, GraphPad Software, San Diego, CA). In case of heteroscedasticity (Bartlett test), data were log transformed prior to analysis. The data in Figures 23 and 25 were analyzed by the Mixed Model procedure in SAS 9.1 (SAS Institute, Cary, NC). Multiple comparisons were corrected by the Bonferroni-Holm procedure. In the figures only those comparisons with interest to the main hypotheses are indicated.

5 Results

5.1 CX3CR1-CX3CL1 interaction

In order to characterize the interaction between CX3CR1 and CX3CL1, I started by determining whether the interaction of fractalkine and CX3CR1 results in firm adhesion and (trans-)migration of PBMC. Since CX3CR1 is described to be constitutively expressed on monocytes and T-cell populations, peripheral blood mononuclear cells from blood of healthy donors were isolated, and tested for the expression of CX3CR1 using a PE-labeled antibody in flow cytometry. I found that the level of expression varied depending on donor and cell type. As expected, the highest expression of CX3CR1 could be seen on monocytes, and lower expression was found on a subpopulation of T-cells (Figure 7). For further experiments PBMC from donors with a strong expression of CX3CR1 were used.

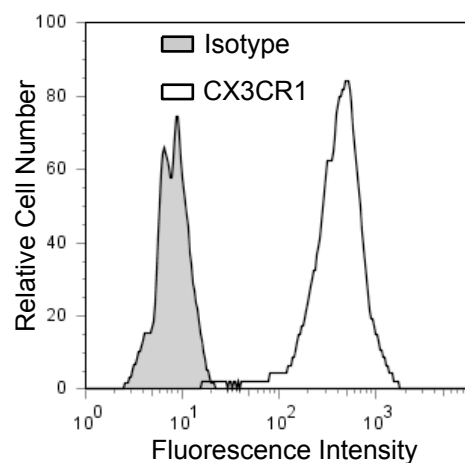


Figure 7: CX3CR1 is expressed on PBMC. Freshly isolated blood mononuclear cells of healthy donors were probed for their expression of CX3CR1 using a PE-labeled anti-hCX3CR1 antibody. Cells were gated for monocytes by sideward and forward scatter dotplot. The grey shaded curve represents the isotype control, the black unshaded curve represents hCX3CR1 expression. Data are shown as a representative histogram.

A fundamental step in leukocyte recruitment is the firm adhesion on the endothelium lining the blood vessel. Therefore, freshly isolated PBMC were tested for their ability to mediate adhesion under flow conditions. For this purpose, wt-ECV304 or CX3CL1-ECV304 were grown to confluency to form a stable cell layer to which PBMC could adhere. Using a syringe pump, freshly isolated PBMC were directed over this cell layer for 1 minute with a shear force stress similar to that of the post-capillary system (2 dyne/cm²), and the adherent PBMC were counted. 8.3 times more PBMC adhered on a CX3CL1-expressing ECV304 cell layer compared to a wt-ECV304 cell layer (Figure 8), indicating that CX3CL1 may function as adhesion molecule as was shown earlier.

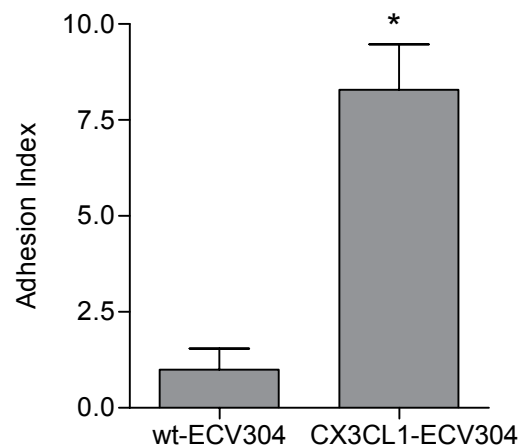


Figure 8: PBMC adhere to a CX3CL1 expressing cell layer under flow conditions. Freshly prepared PBMC were assayed for adhesion under flow conditions on a wt-ECV304 or a CX3CL1-ECV304 cell layer. PBMC were stained with CalceinAM for 15 minutes. Excess dye was removed by washing, and cells were suspended to a concentration of 5×10^5 cells/ml in warmed flow adhesion buffer. The ECV304 cell layer was washed with warmed flow adhesion buffer, and then PBMC were directed onto the layer under a steady shear stress rate of 2 dyne/cm² under a fluorescence microscope. Adherent cells were counted after 1 minute. Data are shown as mean \pm SD of three independent experiments. *, $p < 0.05$ versus the untransfected control.

Since leukocyte adhesion is usually followed by transmigration through endothelial cells, I tested PBMC for their ability to migrate towards CX3CL1. Freshly prepared

PBMC were assayed for chemotaxis in response to soluble CX3CL1 chemokine domain (1 - 100 nM) in a modified 48-well Boyden chamber setting. 2.2 times more PBMC migrated into the lower well when 10 nM CX3CL1 was present in the lower well. Chemotaxis towards CX3CL1 was dose-dependent and showed the characteristic bell shaped curve reported for chemokines, peaking at 10 nM soluble CX3CL1 chemokine domain (Figure 9). Based on this curve, all further experiments were performed with 10 nM soluble CX3CL1 chemokine domain.

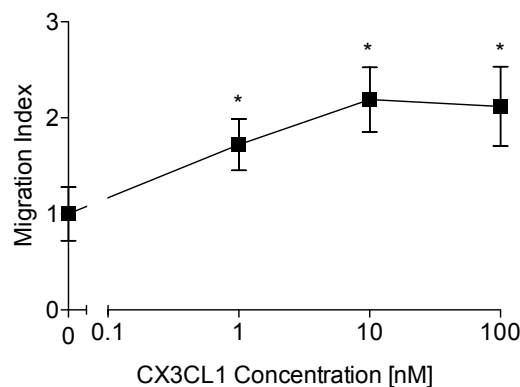


Figure 9: PBMC chemotactically migrate towards CX3CL1. PBMC were seeded onto a polycarbonate membrane with 8 μm pores in a modified Boyden chamber setting. 1 - 100 nM soluble CX3CL1 chemokine domain were used to excite chemotaxis for 2 hours at 37°C. Subsequently, migrated cells were counted. Data are shown as mean \pm SD of three independent experiments. *, $p < 0.05$ versus random migration without stimulus.

Chemotaxis describes the process of cell movement through a membrane instead of the interaction of different cell types with each other and subsequent movement through a confluent cell layer (transmigration). To study the latter process, the capability of freshly isolated PBMC to transmigrate through a cell layer expressing CX3CL1 was tested. Transmigration was studied in the absence or presence of soluble CX3CL1 that was added to the lower compartment of a transwell insert. As expected, transmigration of

PBMC was 1.9 fold increased when soluble CX3CL1 was used as a chemoattractant. Transmigration was also increased (Transmigration Index (TI) = 1.7) when transmembrane CX3CL1 was expressed on the ECV304 cell layer. However, simultaneous presence of transmembrane and soluble CX3CL1 did not further enhance transmigration (TI = 1.8) (Figure 10).

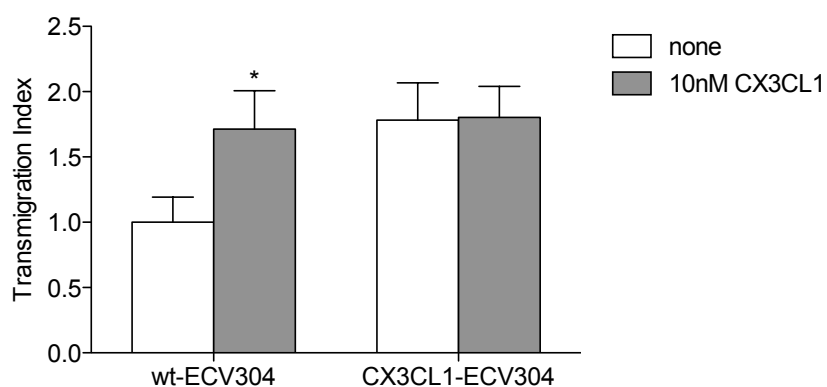


Figure 10: PBMC chemotactically transmigrate in response to CX3CL1. Freshly prepared PBMC were assayed for transmigration through wt- or CX3CL1-ECV304 cell layers cultured in transwell inserts. After washing, 2×10^5 PBMC were seeded onto the confluent cell layer for 2 hours at 37°C. Subsequently, transmigrated cells were counted. Data are shown as mean \pm SD of three independent experiments. *, $p < 0.05$ versus the migration without the addition of stimulus.

In order to use primary endothelial cells as cell layers in transmigration assays, HUVEC were isolated from human umbilical veins. Under normal cell culture conditions, they do not express CX3CL1 endogenously. When these cells were stimulated with IFN γ and TNF α for 16 hours, they expressed CX3CL1 in considerable amounts, as was shown earlier and by FACS analysis (Figure 11) [Ludwig et al., 2002].

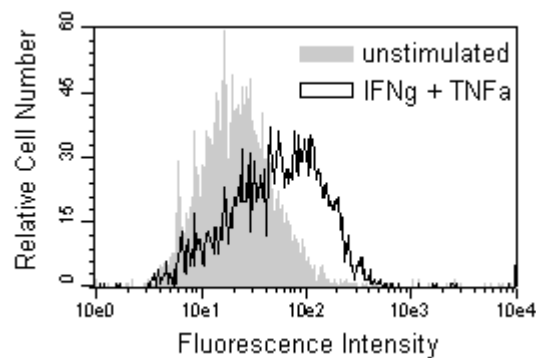


Figure 11: Stimulated HUVEC express CX3CL1. Primary human umbilical vein endothelial cells were stimulated with IFN γ and TNF α (both 10 ng/ml) for 16 hours or left untreated, and were subsequently stained for CX3CL1 surface expression using an anti-CX3CL1 antibody. The grey shaded curve represents the unstimulated control, the black unshaded curve represents hCX3CL1 expression after IFN γ and TNF α treatment. Data are shown as a representative histogram.

To analyze transmigration in a more physiologic setting, I next used HUVEC as a cell layer for transmigration. Transmigration of PBMC was considerably increased (TI = 3) (Figure 12) when these cells were stimulated with IFN γ and TNF α to express endogenous CX3CL1. This transmigration was almost completely suppressed by pretreatment of the HUVEC layer with a neutralizing antibody to CX3CL1. Since firm adhesion occurs prior to the transmigration process, adhesion molecules like ICAM-1 or VCAM-1 might also play an important role in transmigration of PBMC towards CX3CL1. Additionally, treatment of HUVEC with IFN γ and TNF α might not only increase CX3CL1 expression, but also that of adhesion molecules. To find out whether CX3CL1 is sufficient to promote the transmigration process, neutralizing antibodies to ICAM-1 and VCAM-1 were used. The inhibition of VCAM-1 and ICAM-1 was as efficient as that obtained with neutralizing antibodies to CX3CL1 (TI = VCAM-1: 1.4; ICAM-1: 1.3; CX3CL1: 0.9), indicating that CX3CL1 is necessary but not sufficient to induce transmigration.

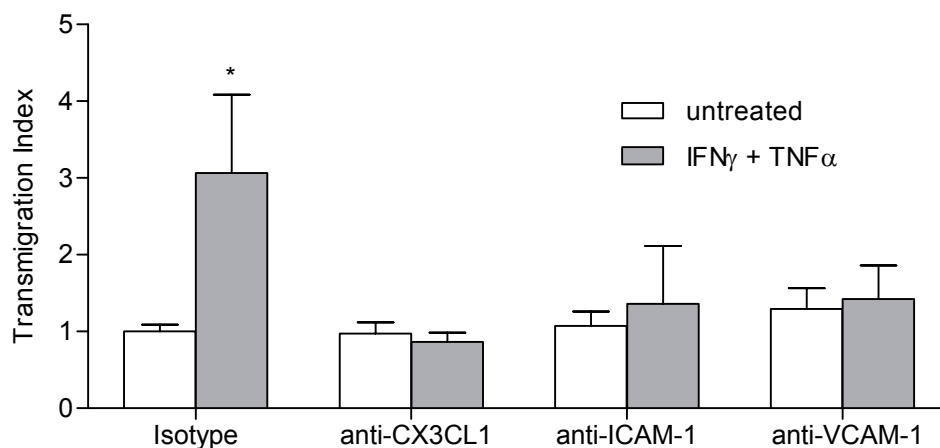


Figure 12: Neutralizing of CX3CL1, ICAM-1 and VCAM-1 prevents PBMC transmigration. HUVEC were left unstimulated or were stimulated with IFN γ and TNF α (both 10 ng/ml) for 16 hours and subsequently treated with neutralizing antibodies against CX3CL1, ICAM-1 and VCAM-1 or isotype control for 1 hour. After washing, 2×10^5 PBMC were seeded onto the cell layer for 2 hours at 37°C. Subsequently, transmigrated cells were counted. Data are shown as mean \pm SD of three independent experiments. *, $p < 0.05$ versus the untreated control.

It is known that chemokines are internalized upon binding to their receptor. This process is mediated by β -arrestin and involves the formation of clathrin-coated vesicles (reviewed in [Moore et al., 2007]). Dynamins are essential for their formation since they are needed in the transition from a fully formed pit to a pinched-off vesicle. Dynasore is a small molecule GTPase inhibitor that targets dynamins and therefore blocks dynamin-dependent endocytosis [Macia et al., 2006]. To address the question, whether internalization of the ligand-receptor complex also plays a critical role in the extravasation process, transmigration of PBMC after pretreatment with dynasore was analyzed. When PBMC were pretreated with dynasore, they did not transmigrate through a wt-ECV304 cell layer towards soluble CX3CL1 chemokine domain or due to the interaction with transmembrane CX3CL1 on ECV304 cells (TI = 1.06, TI = 0.95, control = 1.01) (Figure 13).

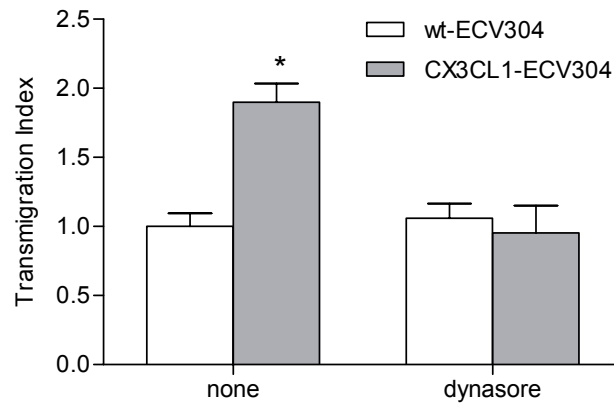


Figure 13: Dynasore prevents transmigration of PBMC. PBMC were pretreated for 30 minutes with 100 μ M dynasore or left untreated. After washing, cells were assayed for transmigration through wt- or CX3CL1- ECV304 cell layers cultured in transwell inserts. 2×10^5 PBMC were seeded onto the confluent cell layer for 2 hours at 37°C. Subsequently, transmigrated cells were counted. Data are shown as mean \pm SD of three independent experiments. *, $p < 0.05$ versus the untransfected control.

The data demonstrate that transmembrane CX3CL1 that is expressed on the cell surface of endothelial cells not only functions as an adhesion molecule for CX3CR1-expressing blood mononuclear cells, but can also mediate transmigration through an endothelial cell layer.

5.2 Model system for CX3CR1-CX3CL1 function

In order to establish a model system for a more detailed molecular analysis of the CX3CR1-CX3CL1 system in adhesion and transmigration, two different cell lines were used that were transfected to express CX3CR1. HEK293 cells were originally derived from human embryonic kidney cells grown in tissue culture and have an epithelial morphology. They were already used in a vast variety of receptor studies. Since HEK293 cells did not migrate in our setting, the murine pre-B-cell line L1.2 (also named 300-19) was used for chemotaxis experiments. Both cell lines do not express CX3CR1 endogenously.

Initial chemotaxis experiments confirmed that CX3CL1 promotes migration of CX3CR1-transfected L1.2 cells towards soluble CX3CL1 chemokine domain as was already shown for PBMC (Figure 14). The migration efficiency was comparable to that obtained for PBMC (Migration Index (MI) = 2.2), with a 2.7 fold increase of migrated cells. Moreover, HEK293 cells were transfected to express CX3CR1 and assayed for their ability to adhere to a CX3CL1-expressing ECV304 cell layer, to show that CX3CR1 mediated adhesion to CX3CL1 under static conditions (Adhesion Index (AI) = 7.4) (Figure 14).

Next, CX3CR1-expressing L1.2 cells were assayed for transmigration through a wt- or CX3CL1-ECV304 cell layer in the absence or presence of soluble CX3CL1 in the lower compartment of the transwell chamber. Both soluble and transmembrane CX3CL1 induced transmigration of CX3CR1-L1.2 cells (TI = 1.7 and 1.9, respectively), but not of wt-L1.2 cells (Figure 15). Simultaneous presence of transmembrane and soluble CX3CL1 did not further enhance transmigration (TI = 1.9), as was previously seen for PBMC.

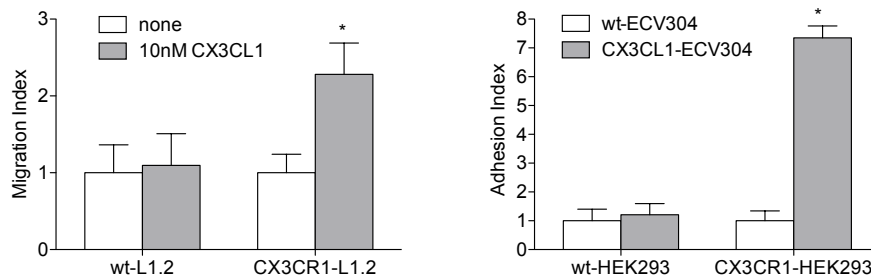


Figure 14: L1.2 cells migrate towards CX3CL1 and HEK293 cells adhere to CX3CL1. (left) L1.2 cells were seeded onto a polycarbonate membrane with 8 μm pores in a modified Boyden chamber setting. 10 nM soluble fractalkine chemokine domain were used to excite chemotaxis for 2 hours at 37°C. Subsequently, migrated cells were counted. (right) Fluorescently labeled wild type or CX3CR1-expressing HEK293 cells were seeded onto wild type ECV304 cells or ECV304 cells expressing transmembrane CX3CL1, and the fluorescence signal of the adherent HEK293 cells was determined after washing. Data are shown as mean \pm SD of three independent experiments. *, $p < 0.05$ versus the controls (random migration of untransfected cells and adhesion of untransfected cells, respectively).

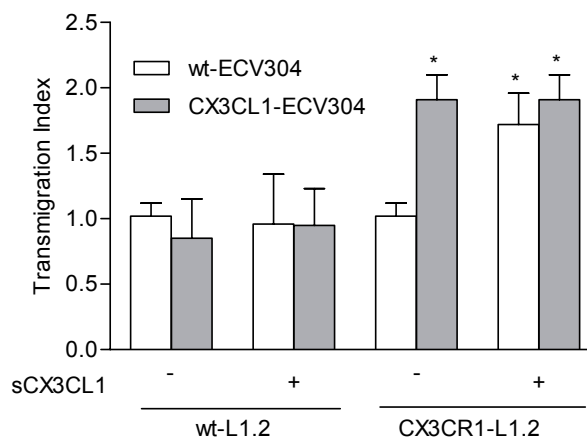


Figure 15: L1.2 cells transmigrate through an ECV304 cell layer. Wt- and CX3CR1-L1.2 were investigated for transmigration across wt- or CX3CL1-ECV304 cells cultured in trans-well inserts. After washing, 2×10^5 L1.2 cells were seeded onto the confluent cell layer for 2 hours at 37°C in the absence or presence of additional 10 nM CX3CL1 chemokine domain in the lower compartment. Subsequently, transmigrated cells were counted. Data are shown as mean \pm SD of three independent experiments. *, $p < 0.05$ versus the random transmigration of untransfected cells without addition of stimulus control.

These studies are well in line with the observations made with primary PBMC and suggest that the transfected cell lines may be used to investigate chemokine-mediated cell recruitment. In the next step, the transmigration process was further analyzed with regard to CX3CL1 expression, signaling and internalization.

I then used HUVEC as a cell layer for transmigration of L1.2 cells. When these cells were stimulated with IFN γ and TNF α to express endogenous CX3CL1, CX3CR1-L1.2 cells but not wt-L1.2 cells transmigrated through the HUVEC layer (TI = 3.1) (Figure 16).

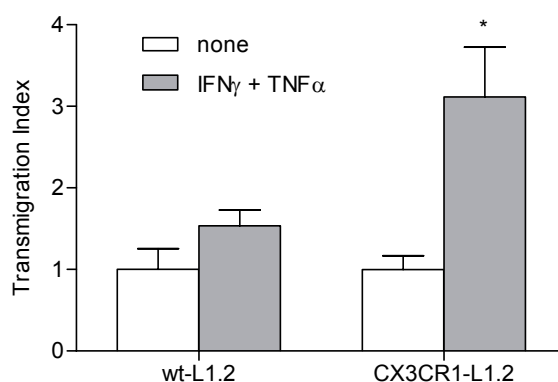


Figure 16: L1.2 cells transmigrate through a HUVEC cell layer. HUVEC were stimulated with IFN γ and TNF α (both 10 ng/ml) for 16 hours or left untreated. Subsequently, wt- and CX3CR1-L1.2 cells were assayed for transmigration across the HUVEC layer. After washing, 2×10^5 L1.2 cells were seeded onto the confluent cell layer for 2 hours at 37°C. Subsequently, transmigrated cells were counted. Data are shown as mean \pm SD of three independent experiments. *, $p < 0.05$ versus the unstimulated, untransfected control.

In the previously shown transmigration assay, HUVEC were stimulated to express CX3CL1 and washed before the assay was performed. To find out whether sufficient amounts of soluble CX3CL1 to induce transmigration were produced during the assay, the medium in both compartments of the transwell system was tested in an ELISA for soluble CX3CL1. As shown in Figure 17, after incubation with pro-inflammatory

cytokines over night soluble CX3CL1 was produced by HUVEC in an amount that was shown to promote chemotaxis of PBMC and CX3CR1-L1.2 cells (Figures 9 and 14). In contrast, 2 hours were not sufficient to produce enough soluble CX3CL1 to mediate efficient chemotaxis, as there were no detectable differences between stimulated and unstimulated cells.

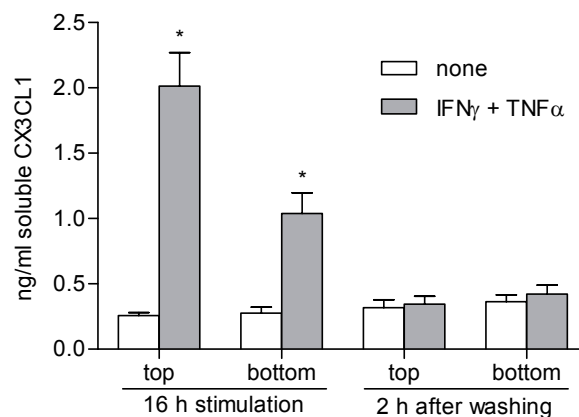


Figure 17: HUVEC produce CX3CL1 after stimulation with cytokines. HUVEC were stimulated with IFN γ and TNF α (both 10 ng/ml) for 16 hours or left untreated. Medium was collected, cells were washed three times and new medium was given. Cells were left untreated for 2 hours at 37°C and afterwards medium was collected and subjected to an ELISA for CX3CL1. Data are shown as mean \pm SD of three independent experiments. *, $p < 0.05$ versus the unstimulated control.

Since CX3CL1 is expressed as transmembrane as well as soluble form by endothelial cells, it is not clear, which form is most important for the transmigration process. The previous experiment provides an indication that transmembrane CX3CL1 is sufficient to promote transmigration of CX3CR1-expressing cells. To elucidate the role of transmembrane CX3CL1, CX3CL1-ECV304 cells were pretreated with a neutralizing antibody against CX3CL1 for 15 minutes prior to the transmigration assay. Pretreatment of CX3CL1-ECV304 cells with a neutralizing antibody against CX3CL1 that was added to the upper compartment of the transwell system (apical site of ECV304 cells) clearly reduced cell transmigration (TI = 3.3 to TI = 1.5), whereas addition of the antibody to the

lower compartment (basolateral site) did not suppress cell transmigration (TI = 3.1 to TI = 2.4) (Figure 18). Simultaneous application of the neutralizing antibody to the upper and lower compartment did not further decrease transmigration (TI = 3.2 to TI = 1.8). These data indicate that transmembrane CX3CL1 is crucial for CX3CL1-dependent transmigration.

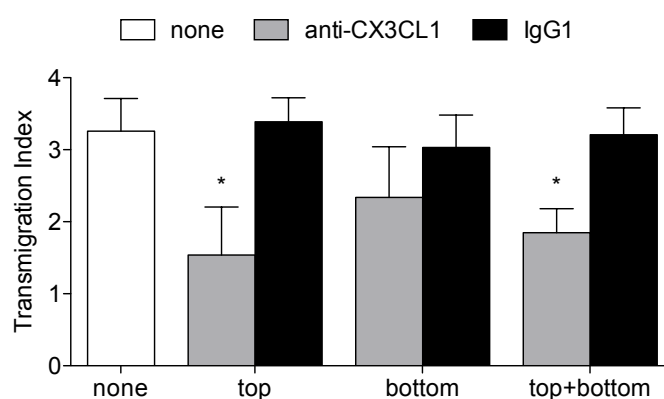


Figure 18: CX3CL1 inhibition influences transmigration. The neutralizing monoclonal antibody to CX3CL1 or isotype control (10 $\mu\text{g/ml}$) was added to the lower or the upper compartment of transwell inserts containing wt- or CX3CL1-ECV304 cells. After 15 minutes, the antibody was removed and the cells were investigated for transmigration of CX3CR1-L1.2 cells. Data are shown as mean \pm SD of three independent experiments. *, $p < 0.05$ versus the untreated, transfected control.

It has been previously demonstrated that pretreatment with soluble CX3CL1 blocks chemotaxis as well as cell adhesion via CX3CL1, whereas pretreatment with the G-protein inhibitor pertussis toxin (PTX) selectively blocks chemotaxis, but not adhesion [Fong et al., 1998; Lucas et al., 2003]. Pertussis toxin is an exotoxin with six subunits released by *Bordetella pertussis*. Once active, it catalyzes the ADP-ribosylation of the α -subunit of the G α -protein and therefore prevents the G-proteins from interacting with G-protein coupled receptors on the cell membrane. To characterize CX3CL1-mediated transmigration, CX3CR1-L1.2 cells were pretreated with soluble CX3CL1 or with PTX, before transmigration through a ECV304 cell layer was assayed. In the transmigration

assays using CX3CL1-ECV304 cells as substrate, pretreatment with soluble CX3CL1 or with PTX efficiently suppressed transmigration of CX3CR1-L1.2 cells (TI = 0.85 and 1.14, respectively; control = 2.2) (Figure 19).

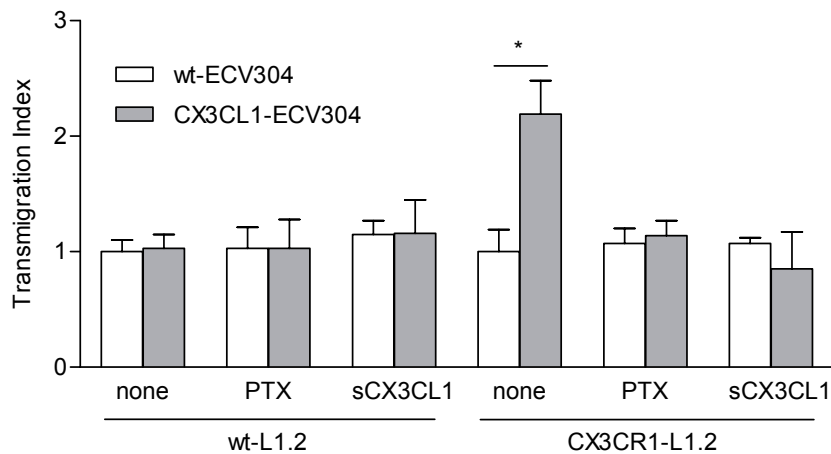


Figure 19: PTX treatment influences transmigration. Wt- and CX3CR1-L1.2 cells were pretreated for 30 minutes with soluble CX3CL1 (10 nM) or 2 hours with PTX (100 ng/ml) and subsequently assayed for transmigration across wt- or CX3CL1-ECV304 cells. After washing, 2×10^5 L1.2 cells were seeded onto the confluent cell layer for 2 hours at 37°C. Subsequently, transmigrated cells were counted. Data are shown as mean \pm SD of three independent experiments. *, $p < 0.05$ versus the transfected, untreated control.

To address the question, whether internalization of the ligand-receptor complex also plays a critical role in the extravasation process of L1.2 cells, chemotaxis of L1.2 cells after pretreatment with dynasore was analyzed. When L1.2 cells were pretreated with dynasore they did not migrate towards soluble CX3CL1 chemokine domain (MI = 1.2, control = 2.8) (Figure 20).

Taken together, the data indicate that HEK293 cells as well as L1.2 cells transfected with CX3CR1 are an appropriate model system for the analysis of molecular determinants of CX3CR1 function with regard to CX3CR1-CX3CL1 interaction.

Furthermore, transmembrane fractalkine seems to be crucial for CX3CL1-mediated transmigration, whereas pretreatment of CX3CR1 expressing cells with soluble CX3CL1 inhibits transmigration. Both, the inhibition of G-protein/GPCR interaction and inhibition of clathrin-coated vesicle formation led to a dramatically reduced chemotaxis of CX3CR1-L1.2 cells towards CX3CL1. This data indicate that signaling as well as internalization are essential for transmigration.

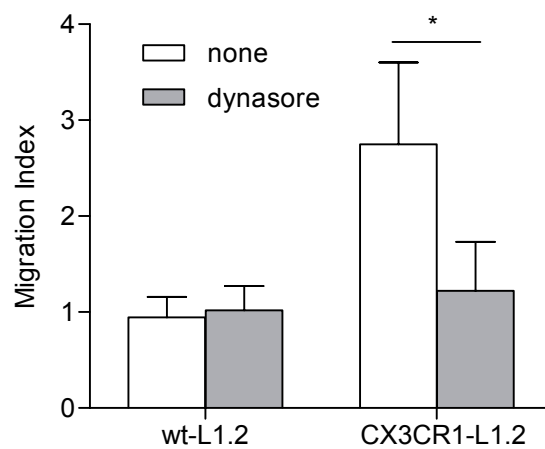


Figure 20: Pretreatment with dynasore prevents L1.2 cell chemotaxis. Wt- and CX3CR1-L1.2 cells were pretreated for 30 minutes with 100 μM dynasore or left untreated. After washing, cells were assayed for chemotaxis towards 100 ng/ml CX3CL1 chemokine domain in a modified Boyden chamber setting for 2 hours at 37°C. Subsequently, migrated cells were counted. Data are shown as mean ± SD of three independent experiments. *, $p < 0.05$ versus the untreated, transfected control.

5.3 Molecular analysis of CX3CR1-CX3CL1 function

To analyze the molecular prerequisites for CX3CL1-mediated adhesion and transmigration, the subsequent experiments concentrated on the receptor and addressed conserved structures in the GPCR superfamily. Analysis showed that there are several highly conserved motifs known to be important for GPCR signaling (Figure 21). The aspartate-arginine-tyrosine (DRY) sequence in the second intracellular loop is required for activation of Gi-proteins, whereas the NPX2-3Y motif located in the seventh transmembrane region of most GPCR contributes to ligand binding, activation and internalization of the receptor.

Rhodopsin	ALWSLVVLAI	ERY	VVCKPMSNF	...	AFFAKSAAIY	NPVIY	IMMNKQFRNC
CX3CR1	SIFFITVISI	DRY	LAIVLAANSM	...	ETVAFSHCCL	NPLIY	AFAGEKFRRY
CXCR1	GILLACISV	DRY	LAIVHATRTL	...	EILGILHSCL	NPLIY	AFIGQKFRHG
CCR5	GIFFIILLTI	DRY	LAVVHAVFAL	...	ETLGMTHCCI	NPIIY	AFVGEKFRNY
GnRHR	PAFMMVVISL	DRS	LAITRPLALK	...	FLFAFLNPCF	DPLIY	GYFSL
CHRM1	SVMNLLIISF	DRY	FSVTRPLSYR				
ADRB1	SIETLCVIAL	DRY	LAITSPFRYQ	...	NWLGYANSFAF	NPIIY	CRSPDFRKAF
CXCR6	SMLILTCITV	DRF	IVVVKATKAY	...	EAIAYLRACL	NPVLY	AFVSLKFRKN

Figure 21: Alignment of conserved motifs in GPCR superfamily. Different members of class A or rhodopsin-like GPCR were aligned to show two important conserved motifs in the GPCR superfamily. The DRY motif is located in the second intracellular loop and always shows the characteristic arginine-residue, whereas the aspartate-residue is sometimes changed to be glutamic acid. The tyrosine residue is unfrequently altered to either serine or phenylalanine. The NPX2-3Y motif is located in the seventh transmembrane domain. The proline and the tyrosine residues are seldom found to be changed, whereas the asparagine residue sometimes is altered to aspartate. The two or three unspecified amino acids are in most cases leucine, isoleucine or valine. Abbreviations and Uniprot.org Accession numbers: Rhodopsin: P30968, CX3CR1: P49238, CXCR1: P25024, CCR5: P51681, GnRHR: Gonadotropin-releasing hormone receptor, P30968, CHRM1: Muscarinic acetylcholine receptor M1, P11229, ADRB1: Beta-1 adrenergic receptor, P08588, CXCR6: O00574.

Additionally, GPCR typically carry several serine residues within the intracellular C-terminal region, which can become phosphorylated by G-protein-coupled receptor

kinases and mediate interaction with β -arrestins, internalization via clathrin-coated vesicles and subsequent desensitization of the receptor towards its ligand. The typical DRY sequence, the NPX2-3Y motif and several C-terminal Ser-residues are also found within CX3CR1 and very likely play a role in CX3CR1 signaling and function. To analyze CX3CR1 function on molecular basis, CX3CR1 variants with altered conserved motifs were constructed. I changed the DRY motif into DNY (R127N), the NPX2-3Y motif into APX2-3Y (N289A) and NPX2-3A (Y293A), and truncated the intracellular stalk at S319 (S319X) to remove all intracellular serine-residues. In Figure 22 all locations for changes are shown.

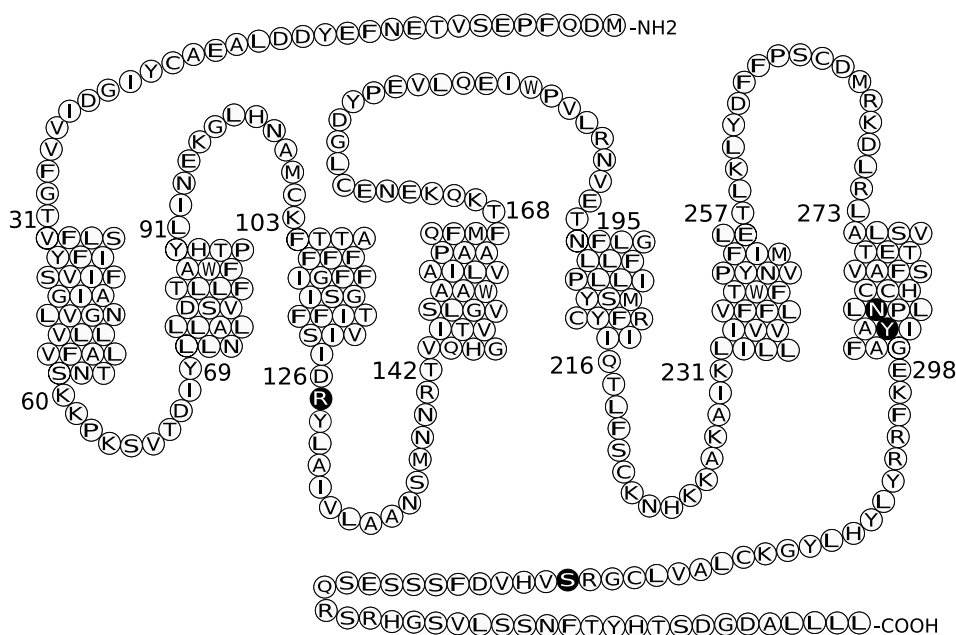


Figure 22: Overview of introduced changes in CX3CR1. CX3CR1 carries a number of conserved sequences, which can be found throughout GPCR superfamily, including a DRY motif in the second intracellular loop, a NPX2-3Y motif in the seventh transmembrane domain and several serine residues at the C-terminus. To alter these motifs, CX3CR1 was mutated at the indicated sites. R127 in the second intracellular loop was mutated to asparagine (R127N), N289 and Y293 in the seventh transmembrane domain were changed into alanine (N289A and Y293A, respectively), and the intracellular C-terminus was truncated before S319 (S319X). Locations for changes are indicated with filled circles.

The cDNA for CX3CR1 variants was constructed using two-fragment ligation (for R127N, N289A and Y293A) or a simple PCR strategy (for S319X) and cloned into pcDNA3.1+ expression vector. All constructs were successfully cloned and confirmed by sequencing. To determine whether the CX3CR1 variants could be expressed, HEK293 cells were transiently transfected and tested for expression of CX3CR1 using flow cytometry. As shown in Figure 23, all constructed variants could be readily detected on the cell surface of HEK293 cells 2 days after transfection, all expressed with similar intensity. To examine whether the transfected receptor variants bind CX3CL1, cells were incubated with CX3CL1 that was fused to the Fc-part of human IgG1. This construct was then detected by flow cytometry using an anti-Fc-antibody (Figure 23). Ligand binding was still detectable for the R127N and S319X variants, but absent in the N289A and Y293A variants. Since ligand binding is the crucial step for mediation of function, I decided to concentrate further functional characterization on the R127N and S319X mutations.

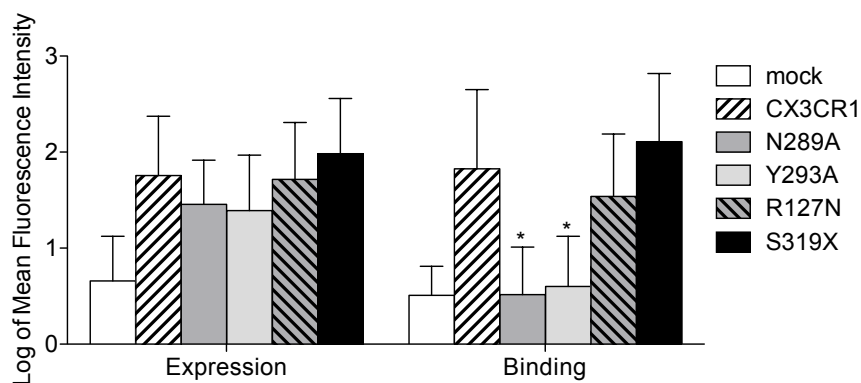


Figure 23: Expression and binding of CX3CR1 variants. Expression of the receptor variants was controlled by flow cytometry using PE-conjugated rat anti-CX3CR1 antibody. Ligand binding was analyzed by flow cytometry using a recombinant CX3CL1-Fc construct as a ligand. Receptor expression and ligand binding were measured as the mean fluorescence intensity increase compared to control. After logarithmic transformation, the data were summarized as means plus SD from five independent experiments. Expression in mock cells was used as a covariate. *, $p < 0.05$ versus CX3CR1 transfected control.

The R127N and S319X receptor variants were transfected in HEK293 cells using lipofectamine. After 48 hours, cells were selected for receptor expression by G418. Only cells that express the plasmid have the resistance for this antibiotic. After several days of G418 preselection, mixed clones were diluted and seeded on a 96-well-plate at the concentration of 1 cell/well. Single clones were grown and subsequently subcultivated. Receptor expression was controlled using flow cytometry. Clones matching the expression of CX3CR1-transfected HEK293 cells were chosen for further experiments (Figure 24).

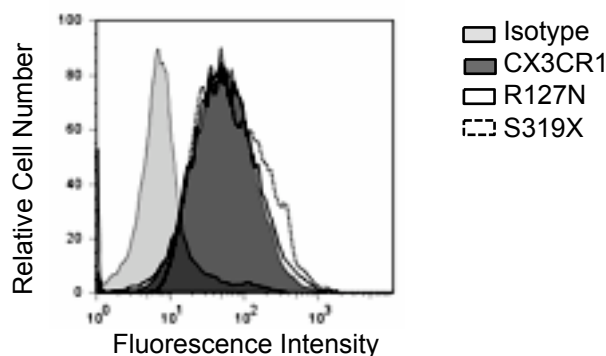


Figure 24: Stably transfected HEK293 cells. CX3CR1 and its R127N and S319X variants were stably expressed in HEK293 cells and selected for comparable surface expression by flow cytometry using PE-conjugated rat anti-CX3CR1. During all further experiments, cells were constantly controlled for stable receptor expression. Data are shown as a representative histogram.

Following ligand binding, most G-protein coupled receptors rapidly become internalized which allows to control desensitization towards the ligand [Ben-Baruch et al., 1995; Kraft et al., 2001]. To further examine the influence of conserved motifs on receptor function, fluorescently labeled CX3CL1 chemokine domain that allows the visualization of internalization processes was used. HEK293 cells expressing the indicated receptor variants were incubated with 10 nM of AlexaFluor647-labeled CX3CL1 chemokine domain for 5 - 30 minutes at 37°C. Immediately after stimulation,

cells were kept on ice to avoid further internalization. As control that the fluorescence increase was due to ligand uptake rather than ligand binding, aliquots of cells were incubated under the same conditions, but in the continuous presence of NaN_3 during the whole experiment in order to prevent ligand uptake.

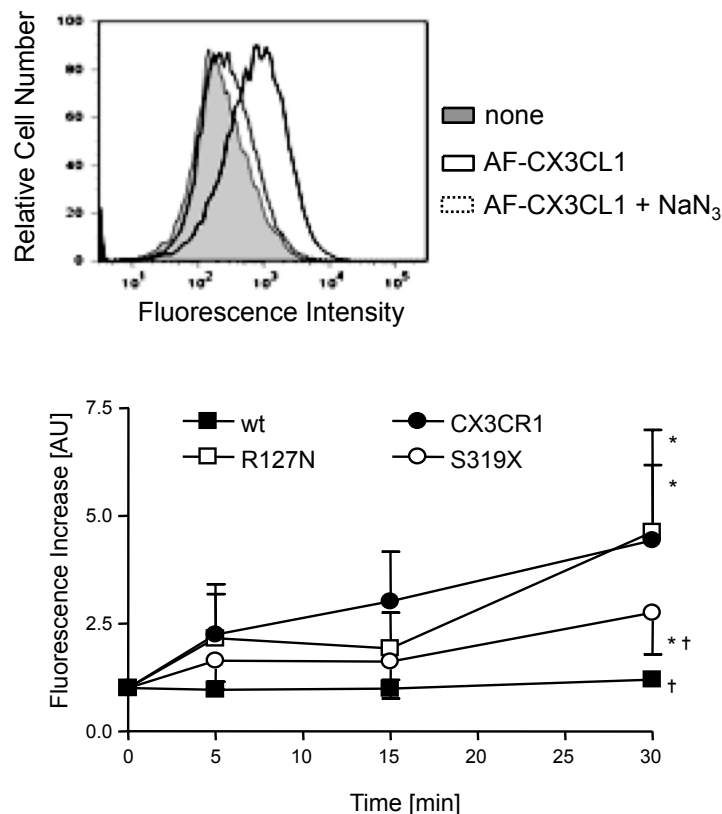


Figure 25: CX3CR1 internalizes upon CX3CL1 treatment and mediates CX3CL1 uptake. (top) HEK293 cells expressing the different receptor variants were incubated with AlexaFluor647-labeled CX3CL1 (AF-CX3CL1) at 37°C in the absence or presence of NaN_3 (0.2%). Subsequently, cells were analyzed for binding and uptake of CX3CL1 by flow cytometric measurement of fluorescence. A representative histogram of the fluorescence signal for CX3CR1-HEK293 cells is shown. (bottom) HEK293 cells expressing the different receptor variants were incubated with AF-CX3CL1 at 37°C for the time periods indicated. The fluorescence intensity for the different HEK293 mutants was expressed in relation to that of the control receiving no AF-CX3CL1, and is presented as mean \pm SD from three independent experiments. *, $p < 0.05$ versus the untransfected control. †, $p < 0.05$ versus CX3CR1-HEK293 cells.

As shown in Figure 25, expression of CX3CR1 or the R127N mutation led to a time-dependent increase in fluorescence, as measured by flow cytometry. This increase was almost completely abolished when cells were continuously treated with NaN_3 . No specific fluorescence uptake was seen with wt-HEK293 cells, and increase in fluorescence was clearly reduced when the S319X variant was expressed, indicating that the receptor's C-terminus contributes to receptor-mediated ligand uptake.

Since the concentration of intracellular free calcium rapidly increases upon activation of most chemokine receptors including CX3CR1 [Imai et al., 1997], I decided to test whether the receptor variants were able to mediate intracellular calcium signals. Therefore, HEK293 cells expressing the indicated receptor variants were loaded with the fluorescent calcium indicator Fluo3-AM. While Fluo3-AM, in contrast to Fluo3, can traverse the cell membrane, the molecule itself does not bind Ca^{2+} . Once the dye is inside the cell, it is hydrolyzed to Fluo3 by endogenous esterases. When bound to calcium Fluo3 absorbs at 506 nm and emits at 526 nm [Kao et al., 1989; Minta et al., 1989]. This signal can be measured in a fluorescence reader to visualize the intracellular calcium flux.

On stimulation with 10 nM CX3CL1 chemokine domain, HEK293 cells expressing CX3CR1 showed a rapid increase of the fluorescence signal of about 0.25 mM Ca^{2+} , peaking at about 5 seconds after stimulation and lasting for about 30 seconds. Wt-HEK293 cells or HEK293 cells expressing the R127N variant, however, did not show any increase in fluorescence signal intensity, whereas the fluorescence signal of HEK293 cells expressing the S319X was slightly lower (about 0.2 mM Ca^{2+}) than that of the wildtype receptor (Figure 26) after treatment with soluble CX3CL1. These data indicate that the induction of intracellular calcium transients by CX3CR1 requires the integrity of the receptor's DRY motif, but is independent of its C-terminus.

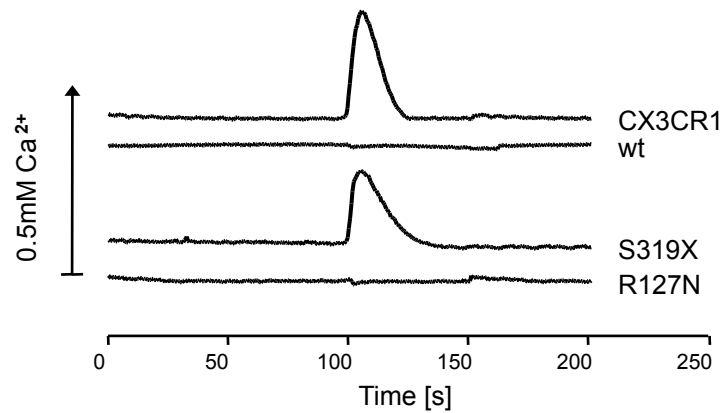


Figure 26: CX3CR1 and S319X, but not R127N mediate intracellular calcium flux. HEK293 cells expressing the indicated receptor variants were loaded with calcium indicator Fluo3-AM and changes in fluorescence intensity upon treatment with soluble CX3CL1 chemokine domain (10 nM at 100 seconds) were recorded. Loading was controlled using digitonin for maximal and EGTA for minimal signal. Length of arrow indicates an increase of 0.5 mM Ca²⁺. Results shown are representative for three independent experiments.

To explore the functional relevance of the R127N and S319X variants of CX3CR1 for cell recruitment, stably transfected HEK293 cells were tested for their ability to adhere to CX3CL1-expressing ECV304 cells and HUVEC under static and flow conditions. Wt-ECV304 or CX3CL1-ECV304 cells were grown to confluency, and fluorescently labeled HEK293 cells expressing the indicated receptor variants were either seeded onto the layer for static adhesion or directed over the cell layer with a constant shear stress rate of 2 dyne/cm² for adhesion under flow conditions. As shown in Figure 27, disruption of conserved motifs in CX3CR1 did neither change its capability to mediate adhesion under static conditions (AI = 7.35; 6.97 and 7.80, respectively) nor under flow conditions (AI = 13.34; 15.49 and 13.12, respectively).

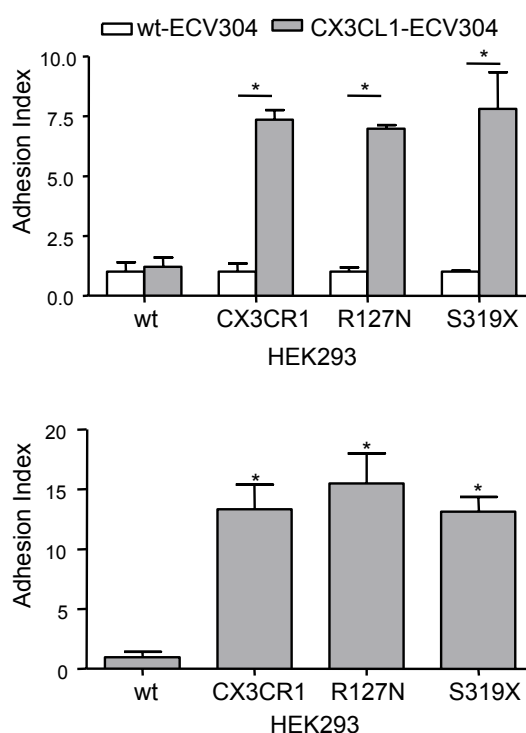


Figure 27: Receptor variants mediate adhesion under static and flow conditions. The ability of receptor variants to mediate adhesion to CX3CL1 was tested under static (top) and flow (bottom) conditions. (top) For static adhesion assays, calcein-labeled HEK293 cells expressing the indicated receptor variants were seeded onto wt- or CX3CL1-ECV304 cells and after washing, the fluorescence signal of the adhering cells was measured. (bottom) For flow adhesion experiments, labeled HEK293 cells expressing the indicated receptor variants were perfused over a layer of cytokine-stimulated HUVEC for 1 minute and adherent cells were counted. Data are shown as mean \pm SD of three independent experiments. *, $p < 0.05$ versus the untransfected control.

Since calcium signals are required for proper migration, I expected that cells expressing the R127N variant of CX3CR1 would not migrate towards CX3CL1. As HEK293 cells did not show migration properties, it was decided to use the murine pre-B-cell line L1.2 that was stably transfected with the indicated receptor variants. L1.2 cells do not express endogenous CX3CR1, but are able to mediate migration towards chemokines when transfected with chemokine receptors, as was previously indicated in

section 5.2. L1.2 cells were transfected using the AMAXA system and selected with G418. L1.2 cell clones expressing the receptor variants were chosen according to their expression level similar to that of L1.2 cells stably expressing CX3CR1.

Chemotaxis experiments were performed to investigate, whether the R127N and S319X variants of CX3CR1 would allow migration in response to soluble CX3CL1. In a modified Boyden chamber chemotaxis assay, only the CX3CR1-expressing cells (MI at 10 nM = 2.46), but not the cells with altered receptors migrated towards increasing concentrations of CX3CL1 (Figure 28) (MI at 10 nM CX3CL1: R127N-CX3CR1 = 1.07 and S319X-CX3CR1 = 1.02). Again, 10 nM CX3CL1 was the optimal concentration for induction of chemotaxis in CX3CR1-L1.2 cells.

I then examined the ability of CX3CR1 variants to induce transmigration through the ECV304 cell layer. When CX3CR1-L1.2 cells were seeded onto CX3CL1-ECV304 cells, transmigration was increased (TI = 2.51). By contrast, transmigration was even below baseline when L1.2 cells expressed the R127N or S319X-mutant (TI = 0.28 and 0.25, respectively) (Figure 28).

To confirm these data in a more physiologic setting, cell layers of cytokine-stimulated HUVEC instead of ECV304 cells were used for transmigration assays. As seen in Figure 29, CX3CR1 expression increased transmigration of L1.2 cells (TI = 3.12), whereas the expression of R127N-CX3CR1 suppressed transmigration (TI = 0.61) (S319X-CX3CR1 was not investigated). These results suggest that receptor function via the DRY motif and the C-terminus are required for transmigration. In the absence of these motifs, however, transmigration is blocked, which could be explained by the retention of leukocytes adhering to transmembrane CX3CL1.

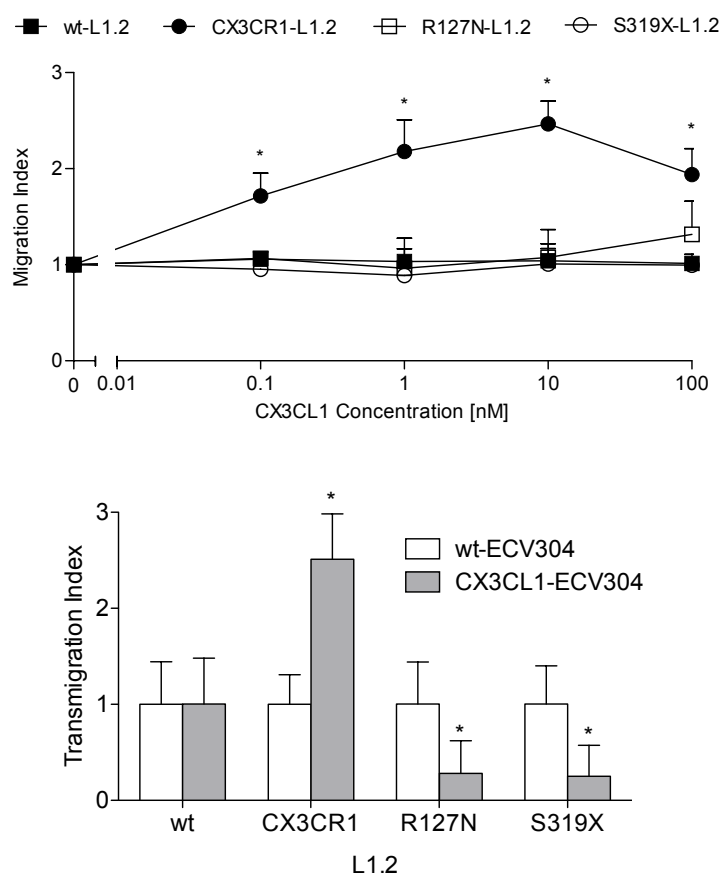


Figure 28: Receptor variants do not mediate (trans-)migration. The ability of receptor variants to mediate migration (top) and transmigration (bottom) towards CX3CL1 was tested. (top) L1.2 cells expressing the indicated receptor variants were tested for their chemotactic response towards increasing concentrations of soluble CX3CL1 (0.1 nM - 100 nM) in a modified Boyden chamber assay. (bottom) L1.2 cells expressing the indicated receptor variants were studied for transmigration through CX3CL1- ECV304 cell layers. Data are shown as mean \pm SD of three independent experiments. *, $p < 0.05$ versus the untransfected controls (unstimulated or untransfected and unstimulated).

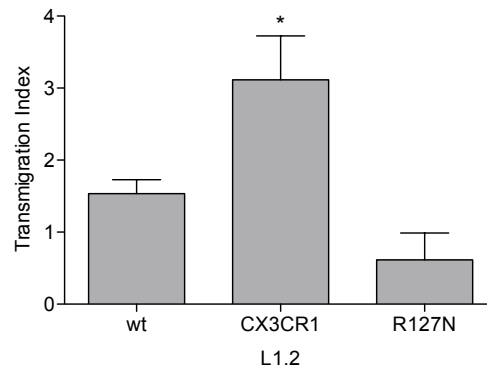


Figure 29: Receptor variant R127N does not mediate transmigration through HUVEC. HUVEC were stimulated with $\text{IFN}\gamma$ and $\text{TNF}\alpha$ (both 10 ng/ml) for 16 hours and subsequently probed for transmigration of L1.2 cells expressing the indicated receptor variants. Data are shown as mean \pm SD of three independent experiments. *, $p < 0.05$ versus the untransfected control.

The extravasation process requires the cell to find an appropriate site for transcellular diapedesis. When L1.2 cells expressing the indicated variants were co-incubated with wt- or CX3CL1-ECV304, L1.2 cells expressing the wildtype receptor crawled on the cell layer expressing CX3CL1 and extended pseudopods (69% of cells). Formation of pseudopods might help the cells to find a site for transmigration and was not present when the ligand was not expressed on the cell layer (13.52 to 14.51% of cells). When L1.2 cells expressing the R127N or S319X-CX3CR1 variants were assayed, the pseudopod formation rate was reduced (24.15% and 12.76% of cells, respectively) (Figure 30).

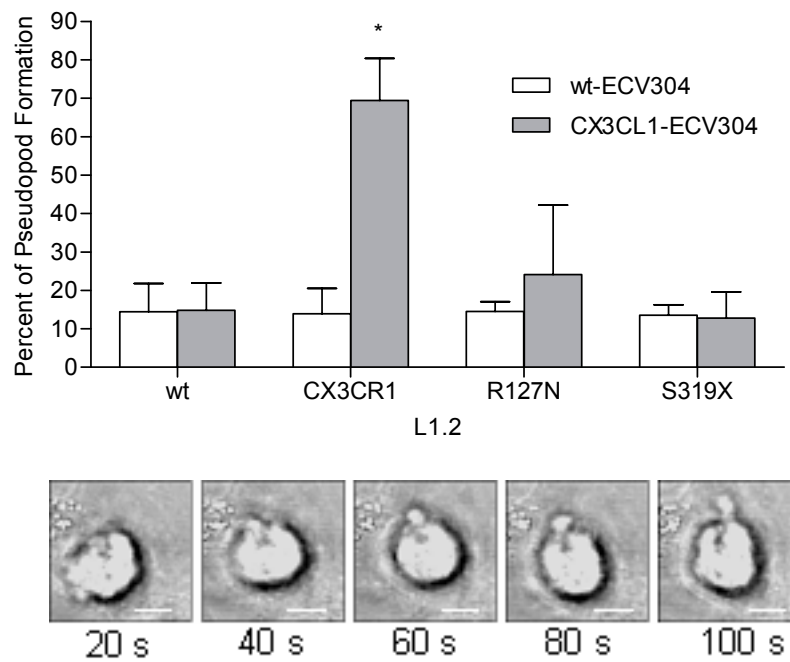


Figure 30: Receptor variants do not mediate pseudopod formation. L1.2 cells expressing the indicated variants were co-incubated with a wt- or CX3CL1-ECV304 cell layer. For 5 minutes every 10 seconds a picture of a randomly chosen field was taken. 100 cells per field were analyzed for pseudopod formation. In the lower panel a representative formation of a pseudopod of a CX3CR1-L1.2 cell on a CX3CL1-ECV304 cell layer is shown (white scale bars represent 3 μ m). Data are shown as mean \pm SD of three independent experiments. The asterisk indicates statistically significant differences versus the untransfected control, $p < 0.05$.

5.4 Involvement of ADAMs in CX3CR1-CX3CL1 function

I then questioned whether the activity of CX3CL1 sheddases on ECV304 cells is required for transmigration towards CX3CL1. To address this issue, the ECV304 cell layer was pretreated with GW280264X, an inhibitor of the metalloproteinases ADAM10 and ADAM17 that shed transmembrane CX3CL1 [Garton et al., 2001; Hundhausen et al., 2003]. To selectively address the role of the proteases on the ECV304 cell layer, the inhibitor was removed prior to starting the transmigration assay with the addition of L1.2 cells. As shown in Figure 31, the inhibitor did not affect L1.2 cell recruitment via soluble CX3CL1 chemokine domain (TI = 1.78; DMSO control: TI = 1.82), but clearly blocked transmigration in response to transmembrane CX3CL1 (TI = 0.97; DMSO control: TI = 1.66). Moreover, this inhibition of transmembrane CX3CL1 activity could not be overcome by addition of soluble CX3CL1 chemokine domain as chemoattractant (TI = 1.21; control: TI = 1.66). Residual transmigration in the absence of CX3CL1 was not affected by GW280264X, indicating that there was no general effect on the integrity of the cell layer. These results indicate that the activity of ADAMs is only required for transmigration in response to transmembrane CX3CL1, but not to soluble CX3CL1.

The following set of experiments was performed to confirm the effect of the inhibitor with PBMC. CX3CL1-ECV304 cells were coincubated in the absence or presence of PBMC to investigate whether PBMC would affect CX3CL1 surface expression on the ECV304 cells. Therefore, PBMC were seeded onto a ECV304 cell layer for 3 hours at 37°C and were then tested for their CX3CR1 surface expression in flow cytometry. To differentiate between PBMC and ECV304 cells, cells were gated for size. The surface expression level was reduced in the presence of PBMC (relative fluorescence intensity = 0.69) (Figure 32). Pretreatment of CX3CL1-ECV304 cells with GW280264X, however, considerably increased CX3CL1 surface expression (relative fluorescence intensity = 3.26), which was not affected when the CX3CL1-ECV304 cell layer was exposed to PBMC (relative fluorescence intensity = 3.40).

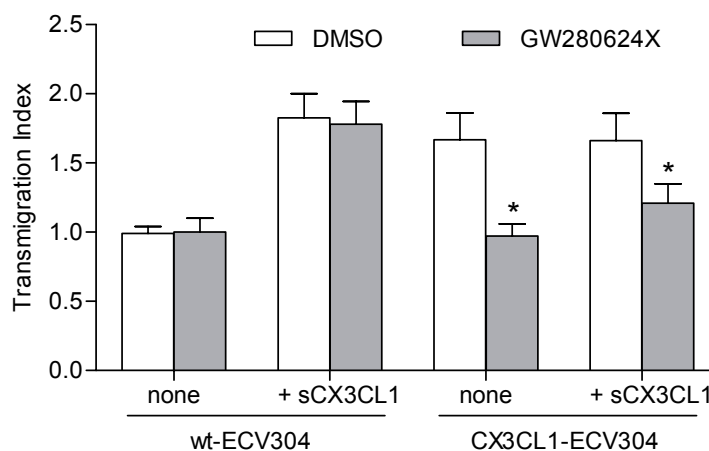


Figure 31: Pharmacologic inhibition of ADAM10/17 abrogates transmembrane CX3CL1-dependent L1.2 cell transmigration. Wt- or CX3CL1-ECV304 cells were grown on transwell inserts and pretreated with GW280264X (10 μ M) or DMSO control for 1 hour. After removal of the inhibitor, the lower compartments of the transwell systems received soluble CX3CL1 chemokine domain (10 nM) or were left without stimulus, and subsequently CX3CR1-L1.2 cells were assayed for transmigration. Data are shown as mean \pm SD of three independent experiments. *, $p < 0.05$ versus the mock-treated control.

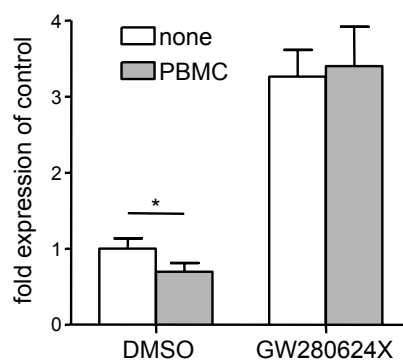


Figure 32: CX3CL1 surface expression is reduced when incubated with PBMC. CX3CL1-ECV304 cells were pretreated with GW280264X (10 μ M) or DMSO for 1 hour, washed and then co-incubated with freshly prepared PBMC for 3 hours. Cells were harvested and analyzed for CX3CL1 surface expression by flow cytometry. The mean fluorescence intensity was expressed in relation to that of CX3CL1-ECV304 cells receiving no inhibitor and no PBMC and data are shown as mean \pm SD of three independent experiments. *, $p < 0.05$ versus the control.

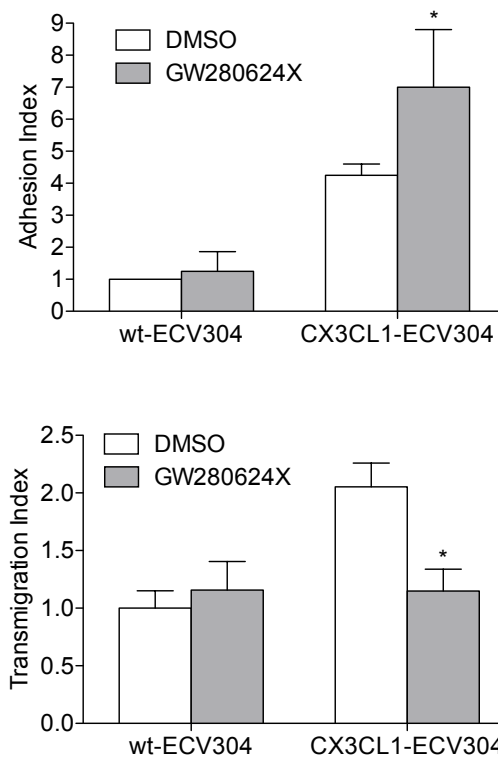


Figure 33: PBMC adhere, but do not transmigrate towards CX3CL1 when ADAM10/17 are inhibited. (top) Wt- or CX3CL1-ECV304 cells were pretreated with DMSO as control or GW280264X (10 μ M) for 1 hour, washed and subsequently analyzed for adhesion of PBMC under flow. (bottom) Wt- or CX3CL1-ECV304 cells were grown on transwell inserts, pretreated with DMSO as control or GW280264X (10 μ M) for 1 hour and subsequently probed for transmigration of PBMC. Data are shown as mean \pm SD of three independent experiments. *, $p < 0.05$ versus the mock-treated controls.

To examine whether the increased CX3CL1 surface expression after treatment with the inhibitor would affect cell recruitment, adhesion assays were performed. CX3CL1-mediated adhesion to ECV304 cells was considerably increased when the cells were pretreated with the ADAM10/17 inhibitor (AI = 7.0; DMSO control: AI = 4.25) (Figure 33). However, despite increased CX3CL1 surface expression and increased CX3CL1-mediated adhesion, CX3CL1-mediated transmigration through the ECV304 cell layer was completely suppressed by the inhibitor (TI = 1.15; DMSO control: TI = 2.05)

(Figure 33). Residual transmigration in the absence of CX3CL1 was not affected by GW280264 (TI = 1.15).

As shown in Figure 34, experiments were repeated with HUVEC, demonstrating that PBMC adhesion to cytokine-stimulated HUVEC is profoundly increased (AI = 3.07; DMSO control: AI = 2.01), whereas transmigration is completely suppressed by the inhibitor (TI = 0.94; DMSO control: TI = 2.02).

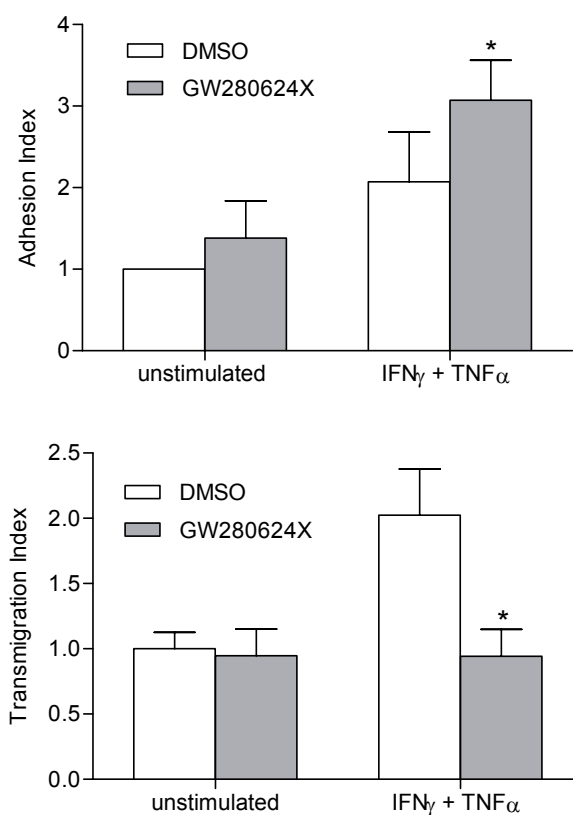


Figure 34: PBMC adhere, but do not transmigrate towards CX3CL1 when ADAM10/17 are inhibited. (top) HUVEC were stimulated with IFN γ and TNF α (both 10 ng/ml) or left unstimulated for 16 hours, and were pretreated with DMSO as control or GW280264X (10 μ M) for 1 hour, washed and subsequently analyzed for adhesion of PBMC under flow. (bottom) HUVEC were grown on transwell inserts, stimulated with IFN γ and TNF α (both 10 ng/ml) or left unstimulated for 16 hours, and were pretreated with DMSO as control or GW280264X (10 μ M) for 1 hour and subsequently probed for transmigration of PBMC. Data are shown as mean \pm SD of three independent experiments. *, $p < 0.05$ versus the mock-treated control.

The importance of ADAM10 and ADAM17 in CX3CL1-dependent transmigration was further investigated by shRNA-mediated silencing of these proteases. Martin Hess of our laboratory generated a lentiviral expression vector for shRNA that was used for efficient and sustained downregulation of ADAM10 and ADAM17 surface expression on ECV304 cells. By ELISA, he confirmed that silencing of ADAM10 led to a reduced release of soluble CX3CL1 and accumulation of CX3CL1 in the cell lysates. Silencing of ADAM17 had no comparable effect on the constitutive release of CX3CL1, which is consistent with the previous observation that this protease is implicated in the PMA-stimulated release of CX3CL1, but not in the constitutive shedding of the chemokine.

CX3CR1-mediated transmigration through CX3CL1-expressing ECV304 cell layers (TI = 1.95) was almost completely suppressed when ADAM10 expression was silenced (TI = 1.02), and moderately reduced when ADAM17 expression was downregulated (TI = 1.34) (Figure 35).

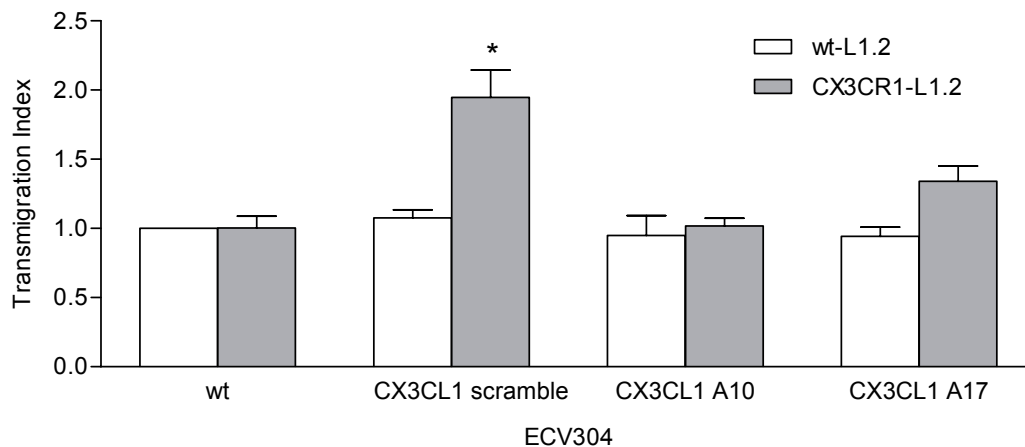


Figure 35: ADAM10, but not ADAM17 silencing leads to an almost complete suppression of CX3CL1-mediated transmigration. Stably transduced CX3CL1-ECV304 cells were investigated for transmigration of wt- and CX3CR1-L1.2 cells. After washing, 2×10^5 L1.2 cells were seeded onto the confluent ECV304 cell layer for 2 hours at 37°C. Subsequently, transmigrated cells were counted. A10 indicates the transduction of CX3CL1-ECV304 cells with shRNA for ADAM10, and A17 indicates the transduction with shRNA for ADAM17. Data are shown as mean \pm SD of three independent experiments. *, $p < 0.05$ versus the untransfected control.

These results indicate that the proteolytic activity of ADAM10, and to a lesser degree of ADAM17, decreases CX3CL1 surface expression and CX3CL1-mediated adhesion and is required for transmigration in response to CX3CL1.

5.5 CXCR6-CXCL16 function

CXCL16 shares a number of structural and functional properties with CX3CL1. It is expressed as transmembrane variant and shed by ADAM10 resulting in a soluble CXCL16 variant that mediates chemotaxis of CXCR6 expressing T-cells [Matloubian et al., 2000; Abel et al., 2004]. When CXCR6 was analyzed for conserved motifs, a DRF motif instead of a DRY motif was found in the second intracellular loop (Figure 21). This alteration was already described for the 5-HT_{2βPan}-receptor of *Panulirus interruptus* (spiny lobster) and implicated in its constitutive activity [Clark et al., 2004]. This raises the question which role the DRY(F) motif would play for the function of CXCR6.

To investigate the function of CXCR6, mononuclear cells from peripheral blood of healthy donors were probed for CXCR6 expression by flow cytometry using a PE-labeled antibody. CXCR6 was previously described to be expressed on CD4+ T-helper 1, CD8+ T-cytotoxic and T-regulatory 1 subsets of T-cells, smooth muscle cells, dendritic cells, B-cells, macrophages and subsets of natural killer cells [Matloubian et al., 2000; Sharron et al., 2000; Kim et al., 2001; Wilbanks et al., 2001; Hofnagel et al., 2002; Sato et al., 2005]. Depending on donor and cell type, the expression level highly varied from nearly absence of detectable CXCR6 expression and high CXCR6 expression. For all donors the strongest expression of CXCR6 could be seen on T-cell subsets (Figure 36).

A fundamental step in leukocyte recruitment is the firm adhesion on the endothelium lining the blood vessel. CXCR6, expressed on T-cells, has been reported to be involved in CXCL16 mediated T-cell recruitment to inflammatory sites [Galkina et al., 2007]. Freshly prepared PBMC from donors expressing high or low levels of CXCR6 were tested for their adhesion to CXCL16-expressing cell layers under static conditions. When PBMC were co-incubated with CXCL16-ECV304 cells and subsequently washed, no adhesion could be observed. This effect was independent from the level of CXCR6 expression (low expression: AI = 0.85, high expression: AI = 0.93, control: AI = 1.0)(Figure 37).

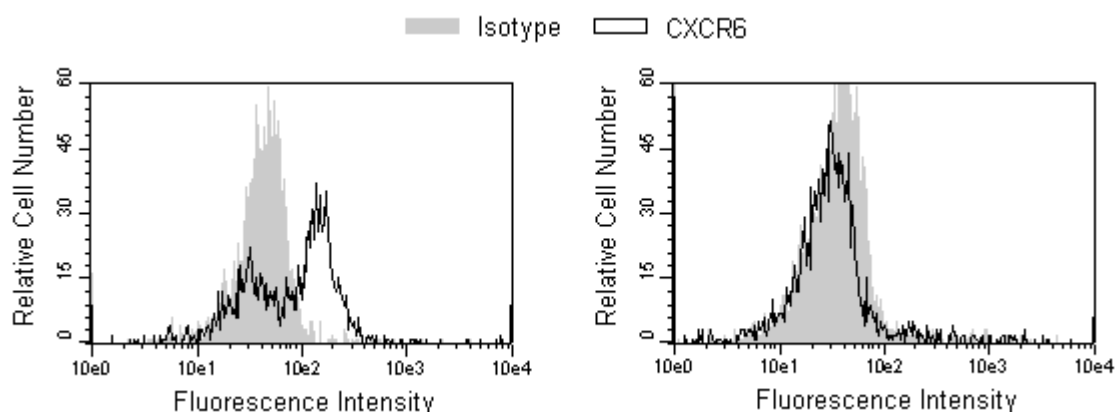


Figure 36: CXCR6 expression varies based on donor. Freshly isolated blood mononuclear cells of healthy donors were probed for their expression of CXCR6 using a PE-labeled anti-hCXCR6 antibody. The grey shaded curve represents the isotype control, the black unshaded curve represents hCXCR6 expression of not gated PBMC. Donor A expresses CXCR6 on PBMC subsets (left), whereas no CXCR6 was detected on PBMC of donor B (right). Data are shown as a representative histogram.

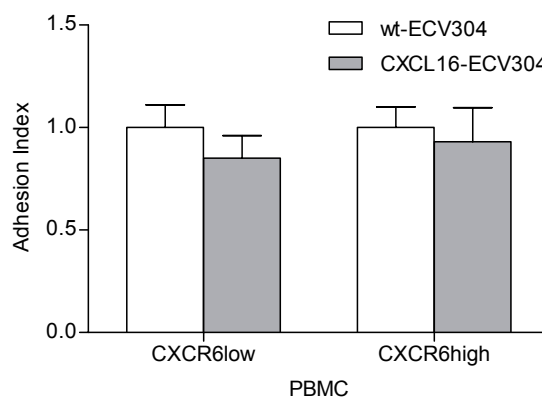


Figure 37: PBMC do not adhere to CXCL16 under static conditions. Freshly isolated PBMC from donors with a high or low expression of CXCR6 were assayed for adhesion under static conditions on wt-ECV304 or CXCL16-ECV304 cell layer. PBMC were stained with CalceinAM for 15 minutes. Excess dye was removed by washing, cells were suspended to a concentration of 5×10^5 cells/ml and seeded onto wt- or CXCL16-ECV304 cells. After washing, the fluorescence signal of the adhering cells was measured. Data are shown as mean \pm SD of three independent experiments.

Due to the high variability of CXCR6 expression on PBMC, I then tested HEK293 cells stably expressing CXCR6 for their ability to adhere to CXCL16 expressing cells under static conditions. Wt-ECV304 or CXCL16-ECV304 cells were grown to confluency, and fluorescently labeled wt-HEK293 and CXCR6-HEK293 were seeded onto the cell layer. As shown in Figure 38, no adhesion of CXCR6 expressing cells to CXCL16 expressing cells could be observed under static conditions (AI = 1.7; control: AI = 1.0).

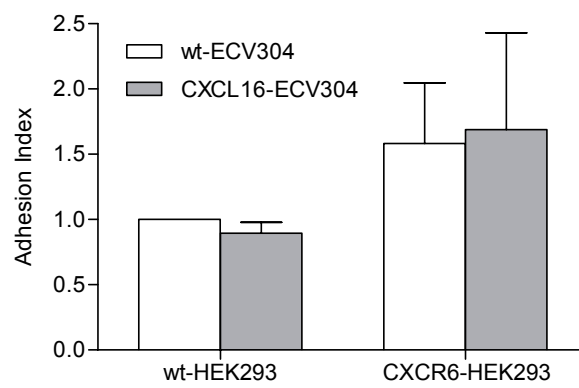


Figure 38: CXCR6-expressing cells do not adhere to CXCL16 under static conditions. Wt-HEK293 and CXCR6-HEK293 cells were assayed for adhesion under static conditions on wt-ECV304 or CXCL16-ECV304 cell layer. HEK293 cells were stained with CalceinAM for 15 minutes. Excess dye was removed by washing, and cells were suspended to a concentration of 5×10^5 cells/ml and seeded onto wt- or CXCL16-ECV304 cells. After washing, the fluorescence signal of the adhering cells was measured. Data are shown as mean \pm SD of three independent experiments.

As CXCL16 is described to bind to CXCR6, I performed a binding assay with 6xHis-tagged recombinant CXCL16 chemokine domain. Cells were incubated with CXCL16-6xHis in the absence or presence of a 10 fold excess of CXCL16 chemokine domain. Bound CXCL16-6xHis was then detected with an anti-6xHis-tag-antibody. When PBMC of a donor with high expression of CXCR6 were analyzed, binding was found that could be diminished by competition with untagged CXCL16 chemokine domain. In contrast, PBMC from donors with a low expression of CXCR6 did not bind

CXCL16-6xHis (Figure 39).

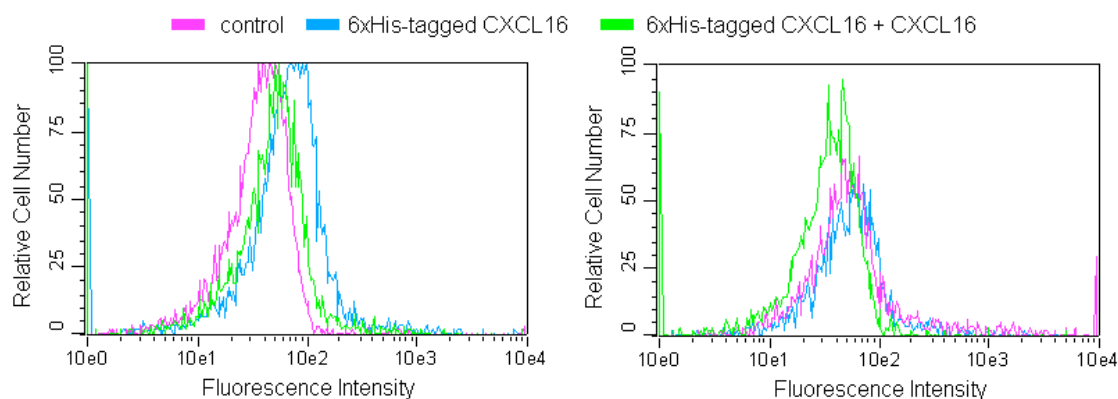


Figure 39: CXCR6 binds CXCL16-6xHis. CXCL16 binding to PBMC was analyzed by flow cytometry using recombinant 6xHis-tagged CXCL16 chemokine domain as ligand in the absence or presence of a 10-fold excess of untagged CXCL16 chemokine domain. The binding was detected using a murine anti-6xHis-tag-antibody and an anti-mouse-PE antibody. The pink curve represents the untreated control, the blue curve represents detected binding of 6xHis-tagged CXCL16 on PBMC and the green curve represents 6xHis-tagged CXCL16 binding when untagged CXCL16 is present for competition. Donor A expresses CXCR6 on PBMC subsets (left), whereas no CXCR6 was detected on PBMC of donor B (right). Results shown are representative for three independent experiments.

Albeit its inability to mediate adhesion, there remains the possibility that the binding of CXCL16 to CXCR6 would mediate chemotaxis. Freshly prepared PBMC were assayed for chemotaxis in response to soluble CXCL16 chemokine domain (1 - 100 nM) in a modified 48-well Boyden chamber setting. When PBMC highly expressing CXCR6 were used, increased migration could be observed (MI = 1.85 at 10 nM CXCL16). Chemotaxis towards CXCL16 chemokine domain was dose-dependent and showed the characteristic bell shaped curve reported for chemokines peaking at 10 nM soluble CXCL16 chemokine domain (Figure 40). Based on this curve, all further experiments were performed with 10 nM soluble CXCL16 chemokine domain. In contrast, when CXCR6 expression could not be detected on PBMC, no migration towards CXCL16 chemokine domain was observed (MI = 0.98 at 10 nM CXCL16). These data indicate

that CXCR6-mediated signaling of chemotaxis occurs despite of the alteration of the conserved DRY motif into DRF.

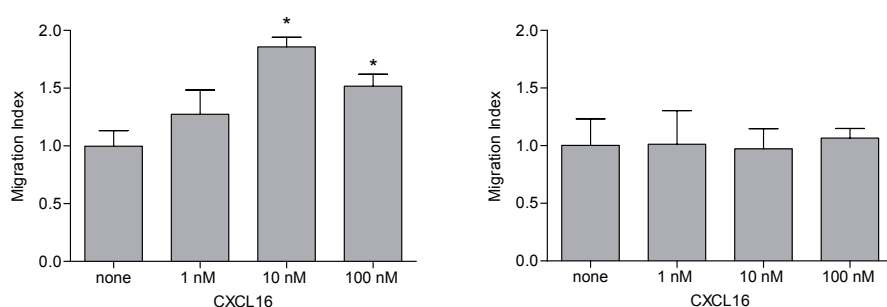


Figure 40: PBMC expressing CXCR6 chemotactically migrate towards CXCL16. PBMC were seeded onto a polycarbonate membrane with 8 μm pores in a modified Boyden Chamber setting. 1-100 nM soluble CXCL16 chemokine domain were used to excite chemotaxis for 2 hours at 37°C. Subsequently, migrated cells were counted. (left) Donor A expressed CXCR6 on PBMC subsets, whereas no CXCR6 was detected on PBMC of donor B (right). Data are shown as mean \pm SD of three independent experiments. *, $p < 0.05$ versus the unstimulated control.

For a better understanding of the DRF motif in CXCR6 function, different receptor variants were created: the DRF motif was changed into DNF (R127N) consistent with the CX3CR1 experiments, and the DRY motif (F128Y) was reconstituted. The cDNA for CXCR6 variants was constructed using two-fragment ligation and cloned into pcDNA3.1+ expression vector. All constructs were successfully cloned and confirmed by sequencing.

To determine whether the mutated CXCR6 variants would be expressed, HEK293 cells were transiently transfected and tested for expression of CXCR6 using flow cytometry. As shown in Figure 41, all constructed variants could be readily detected on the cell surface of HEK293 cells 2 days after transfection. The expression level of CXCR6 seemed not to be influenced by the alteration.

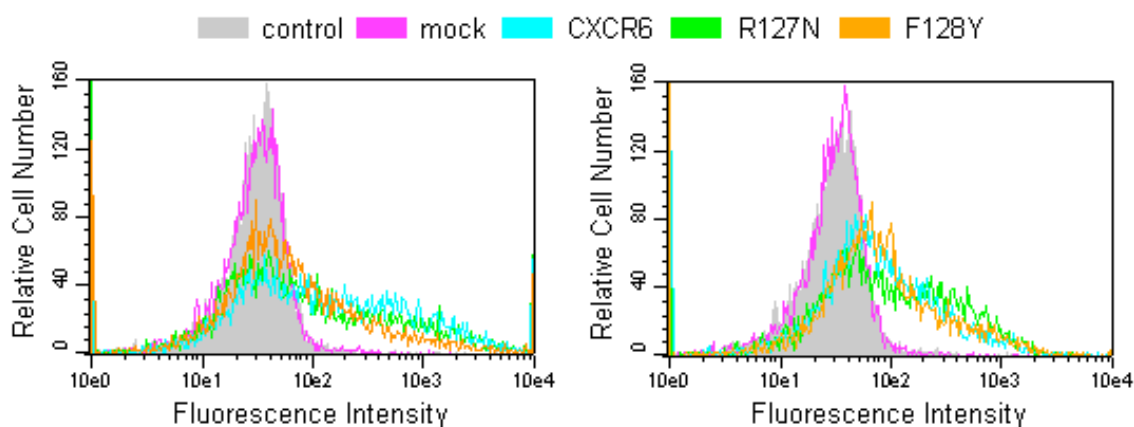


Figure 41: Surface expression and ligand binding of CXCR6 variants. (left) Expression of the receptor variants was controlled by flow cytometry using a PE-conjugated anti-CXCR6 antibody. (right) Ligand binding was analyzed by flow cytometry using a recombinant CXCL16-6xHis construct as a ligand. The binding was detected using a murine anti-6xHis-tag-antibody and an anti-mouse-PE antibody. The grey shaded curve represents unstained wildtype HEK293 cells, the pink curve represents the stained mock transfected control, the blue curve represents stained CXCR6 transfected cells, the green curve represents stained R127N variant transfected cells, and the orange curve represents stained F128Y variant transfected cells. Data are shown as a representative histogram.

Since ligand binding can be affected by mutating CXCR6, transiently CXCR6-transfected HEK293 cells were tested for binding of a recombinant CXCL16-6xHis construct. No differences in ligand binding could be observed between the wildtype receptor and its variants (Figure 41).

To test whether the variants of CXCR6 are still able to mediate intracellular calcium transients, HEK293 cells expressing the indicated receptor variants were loaded with the fluorescent calcium indicator Fluo3-AM. On stimulation with 10 nM CXCL16, HEK293 cells expressing CXCR6 showed a calcium signal of about 0.05 mM Ca^{2+} , peaking at about 10 seconds after stimulation and lasting for about 45 seconds. Wt-HEK293 cells or HEK293 cells expressing the R127N variant, however, did not show any signal. Interestingly, the calcium signal of HEK293 cells expressing the F128Y variant was

slightly decreased (about 0.04 mM Ca^{2+}) compared to the response of cells expressing the wildtype receptor (Figure 42). These data indicate that the induction of intracellular calcium transients by CXCR6 requires the arginine residue of the receptor's DRF motif, but the phenylalanine residue is less critical.

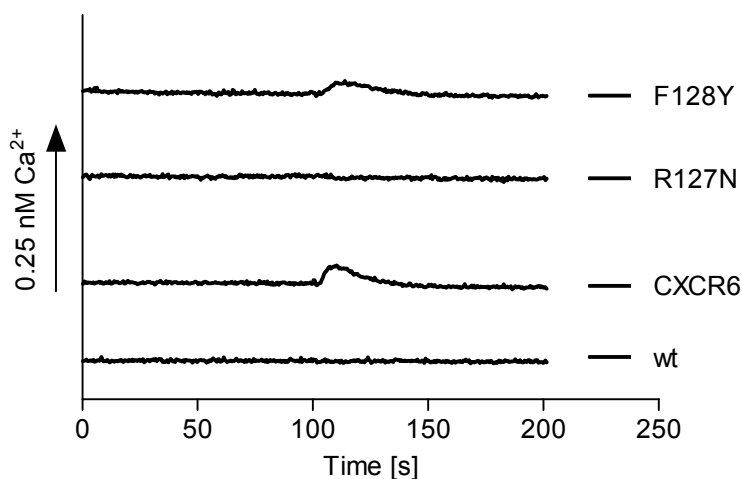


Figure 42: CXCR6 and F128Y, but not R127N mediate intracellular calcium flux. HEK293 cells expressing the indicated receptor variants were loaded with calcium indicator Fluo3-AM and changes in fluorescence intensity upon treatment with soluble CXCL16 chemokine domain (10 nM at 100 seconds) were recorded. Loading was controlled using digitonin for maximal and EGTA for minimal signal. The length of the arrow indicates an increase of 0.25 mM Ca^{2+} . Results shown are representative for three independent experiments.

To explore the functional relevance of the R127N and F128Y mutations for cell recruitment, stably transfected HEK293 cells were tested for their ability to adhere to CXCL16-expressing ECV304 cells under static conditions. As shown in Figure 43, changing the DRF motif in CXCR6 did not enable the receptor to mediate adhesion under static conditions (AI = 0.93; 0.75 and 0.85, respectively).

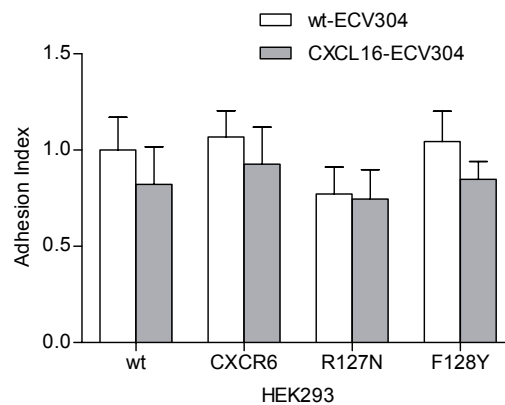


Figure 43: R127N and F128Y do not adhere to CXCL16-ECV304 cells. HEK293 cells expressing the indicated receptor variants were assayed for adhesion under static conditions to wt-ECV304 or CXCL16-ECV304 cell layer. HEK293 cells were stained with CalceinAM for 15 minutes. Excess dye was removed by washing and cells were suspended to a concentration of 5×10^5 cells/ml and seeded onto wt- or CXCL16-ECV304 cells and after washing, the fluorescence signal of the adhering cells was measured. Data are shown as mean \pm SD of three independent experiments.

6 Discussion

The multi-step process of leukocyte extravasation starts with the rolling of leukocytes on the activated endothelium, leading to flow-resistant adhesion to transmembrane adhesion molecules. Subsequently, leukocytes transmigrate through the endothelium towards a gradient of chemotactic molecules, such as formyl peptides, complement factors and especially chemokines that belong to the class of cytokines. CX3CL1 and CXCL16 are exceptional chemokines that are expressed as transmembrane molecules on the surface of physiologic interfaces such as endothelial or epithelial cells. Both chemokines can be shed by members of the ADAM family of metalloproteinases, resulting in a soluble form and are implicated in several pathophysiological situations such as HIV-infection, renal diseases and atherosclerosis [Tong et al., 2000; Furuichi et al., 2001; Greaves et al., 2001; Galkina et al., 2007].

Transmembrane CX3CL1 is known to promote flow resistant adhesion of leukocytes to endothelial or epithelial cells, which is mediated by physical interaction with its receptor CX3CR1 independently from signaling via Gi-proteins [Fong et al., 1998]. Furthermore, CX3CL1 mediates chemotaxis of CX3CR1-expressing cells, like monocytes, via Gi-protein activation and CX3CR1 signaling [Imai et al., 1997]. The present study extends these findings by the detailed analysis of the influence of the CX3CR1-CX3CL1-interaction during transmigration, internalization, signaling and cleavage. It could be shown that transmembrane CX3CL1 that is expressed by endothelial cells is sufficient to promote adhesion and transmigration. Analysis of receptor mutants indicated that transmigration requires the internalization of the ligand-receptor-complex as well as signaling of the receptor. Additionally, activity of ADAM10/17 that shed transmembrane CX3CL1 was needed for efficient transmigration. Based on the results a model of CX3CL1-mediated leukocyte extravasation is proposed.

This thesis expands previous findings by showing that leukocytes not only employ the

receptor CX3CR1 to bind and adhere to endothelial CX3CL1, but also for transmigration of adherent leukocytes. This transmigration could be induced by the presence of transmembrane or soluble CX3CL1, but not further enhanced by the presence of both forms. Pretreatment of the endothelial cell layer with a neutralizing antibody to CX3CL1 abrogated CX3CL1-induced transmigration of peripheral blood mononuclear cells (PBMC). Thus, CX3CR1/CX3CL1 interaction was necessary for leukocyte transmigration. Application of inhibitory antibodies to ICAM-1 and VCAM-1, two major adhesion molecules involved in leukocyte adhesion, led to a reduced level of CX3CL1-mediated transmigration. It has been previously reported that inhibition of VCAM-1 on activated endothelial cells reduced C5a-induced transmigration of monocytes, while inhibition of ICAM-1 does not [Chuluyan and Issekutz, 1993]. However, CX3CR1 expression on stably transfected L1.2 cells did not activate integrin-mediated adhesion to VCAM-1 [Haskell et al., 1999], whereas soluble CX3CL1 induced ICAM-1 expression in endothelial cells [Yang et al., 2007]. The adhesion of CX3CR1 positive cells to endothelial cells was previously shown to be ICAM-1-dependent [Yang et al., 2007]. Since the pretreatment of endothelial cells with inhibitory antibodies to VCAM-1 and ICAM-1 abolished CX3CL1-mediated transmigration to a similar extent, not only ICAM-1 but also VCAM-1 appear to contribute to CX3CL1-induced transmigration.

As in a transmigration assay with stimulated (and thoroughly washed) HUVEC as cell layer, the transmigration of responsive cells was comparable to that obtained with ECV304 cells, I asked if sufficient soluble CX3CL1 is produced to mediate transmigration within the duration of the assay. As was shown by ELISA, the amount of soluble CX3CL1 after 2 hours in both compartments of the transwell system was comparable to that produced by unstimulated HUVEC. Since this quantity is not sufficient to induce chemotaxis of PBMC or L1.2 cells it is unlikely that transmigration is mediated by soluble CX3CL1. This data indicates a crucial role for transmembrane CX3CL1 in the transmigration process.

In a transmigration assay with an inhibitory antibody against CX3CL1 that was

applied basolaterally and/or apically, it could be shown that transmigration was predominantly mediated by apically expressed transmembrane CX3CL1, whereas the inhibition of basal transmembrane CX3CL1 did not affect transmigration. This result is consistent with the fact that immobilized chemokines can induce haptotactic migration of responsive leukocytes, and that a concentration gradient of soluble chemokine is not required for this activity [Rot and von Andrian, 2004].

Furthermore, the pretreatment of CX3CR1-expressing cells with soluble CX3CL1 abolished CX3CL1-mediated transmigration. This effect was either due to internalization, and therefore desensitization of the receptor towards CX3CL1, or due to binding site occupancy.

Endocytosis of ligand-receptor complexes plays a vital role in signal termination and receptor resensitization, and is mediated by intracellular phosphorylation of the receptor, and β -arrestin-binding with subsequent uncoupling of G-proteins. Internalization by clathrin-coated vesicles eventually leads to the dissociation of the ligand and dephosphorylation of the receptor. It is still under discussion whether internalized receptor-ligand-pairs still signal or receptor resensitization enhances ligand-induced signaling. Once the receptor is recycled back to the cell surface, it is resensitized and competent to signal again [Wolfe and Trejo, 2007]. Dynasore is a small molecule inhibitor of dynamin, which is essential for the formation of clathrin-coated vesicles. Just recently it has been shown that dynasore prevents the CCL2-mediated endocytosis of CCR2 [García Lopez et al., 2009]. Since pretreatment with dynasore inhibited transmigration towards CX3CL1, it is very likely that internalization of the receptor plays a crucial role in CX3CR1/CX3CL1-mediated transmigration.

As internalization seemed to be important for transendothelial migration, I next established receptor variants to analyze the molecular determinants for this receptor function. Therefore, a highly conserved region in G-protein coupled receptor superfamily

implicated in internalization of the receptor, namely NPX2-3Y in the seventh transmembrane region, was changed into APLIY and NPLIA. Additionally, a truncation mutant was constructed that lacked all C-terminal serine residues that can become phosphorylated and interact with β -arrestins [Barak et al., 1994]. These receptor variants were then stably transfected into HEK293 and L1.2 cells. Both cell lines did not express CX3CR1 endogenously. Although HEK293 cells were previously described to migrate [Dijkstra et al., 2004], no migration of CX3CR1-transfected cells towards CX3CL1 could be observed, but CX3CR1-expressing HEK293 cells adhered as efficiently as PBMC to CX3CL1-expressing cells. Consistently, CX3CR1-transfected L1.2 cells showed similar migration properties towards CX3CL1 compared to PBMC. These results justify the use of both cell lines as a model system for CX3CR1-CX3CL1-interaction.

The mutational analysis of the regions revealed that they are not required for surface expression, but for ligand binding and trafficking of the receptor, respectively. The NPX2-3Y motif of CX3CR1 is needed for ligand binding, as it has been reported for some G-protein coupled receptors, like type 1 angiotensin II receptor [Hunyady et al., 1995]. In contrast, in other G-protein coupled receptors, like β 2-adrenergic receptor, the NPX2-3Y motif is implicated in internalization, but not ligand binding [Barak et al., 1995]. Ligand binding takes place at the receptor's N-terminus that ends in the first transmembrane domain, and also on extracellular loops [Harrison et al., 2001]. Since the NPX-3Y motif is located in the seventh transmembrane domain, which does not bind the ligand directly, the loss of ligand binding is most likely due to sterical changes, as the seventh transmembrane domain is located adjacent to the first [Palczewski et al., 2000].

Most chemoattractant receptors including CXCR2 and CCR5 carry a number of serine residues that become phosphorylated upon ligand engagement and may trigger the interaction with β -arrestin which in turn mediates receptor desensitization and internalization [Ben-Baruch et al., 1995; Kraft et al., 2001]. Accordingly, deletion of the serine-rich C-terminal part of CX3CR1 attenuated ligand uptake by internalization, but not calcium signaling. In line with the observation that internalization plays an important

role in the transmigration process, CX3CL1-mediated (trans-)migration of L1.2 cells expressing the truncation variant of CX3CR1 was impaired. Thus, the C-terminus contributes to trafficking, but not to induction of intracellular calcium transients.

Lucas and coworkers previously showed that Gi-protein inhibition abrogates CX3CL1-mediated chemotaxis [Lucas et al., 2003]. Accordingly, pretreatment of CX3CR1-L1.2 cells with the Gi-protein inhibitor pertussis toxin resulted in the suppression of transmigration. These findings indicate that CX3CL1-induced transmigration critically depends on Gi-protein signaling. From previous studies it is known that the calcium response of G-protein coupled receptors depends on the DRY motif and its interaction with Gi-proteins [Lagane et al., 2005; Berchiche et al., 2007]. Additionally, the arginine residue of this region has been shown to have effects on receptor expression, internalization, and binding of the gonadotropin-releasing hormone receptor [Arora et al., 1997; Ballesteros et al., 1998]. A CX3CR1 variant with a DNY instead of the DRY motif was constructed, stably expressed in HEK293 and L1.2 cells, and analyzed. As expected, the induction of intracellular calcium transients upon treatment with soluble CX3CL1 was abolished in cells expressing the receptor variant. As (trans-)migration of CX3CR1-R127N expressing cells is impaired, calcium-signaling is essential for CX3CR1-mediated (trans-)migration. Apparently, this rapid calcium response occurs independently of slower processes such as receptor internalization. Taken together, the DRY motif of CX3CR1 is critical for the activation of calcium signals, but contrary to other reports for different class A GPCR not for receptor trafficking, as assessed by studying ligand uptake.

Probing of the cell substrate in order to find an appropriate site for transmigration is a crucial part in the extravasation process of leukocytes and was previously described for neutrophils in response to the chemoattractant N-formyl-methionyl-leucyl-phenylalanine [Alteraifi and Zhelev, 1997]. When L1.2 cells were co-incubated with wt- or CX3CL1-ECV304 cells, L1.2 cells expressing the wildtype receptor extended pseudopods on the

CX3CL1-expressing cell layer. This behavior could not be seen on wt-ECV304 cell layers or by L1.2 cells expressing no CX3CR1 or the R127N and S319X variants. Both, intracellular calcium signaling and F-actin network rearrangement are required for efficient migration, although different signaling pathways seem to be involved. It has been described that clathrin-deficient cells show an increase in turning and roundness, and a decrease in polarity, velocity and chemotaxis-efficiency suggesting a role for the suppression of pseudopod formation and stability [Wessels et al., 2000]. Thus, CX3CR1/CX3CL1 interaction and the distinct coupled signaling processes are necessary for pseudopod formation as an initial step of transmigration.

Although the DRY sequence as well as the C-terminus of CX3CR1 differentially contribute to signaling and trafficking, they are both required for the induction of chemotaxis and transmigration. The importance of the DRY motif may be explained by the fact that it represents a critical motif for Gi-protein activation, which triggers phospholipase C activation followed by diacylglycerol formation and calcium mobilization. This signaling pathway is involved in the control of actin polymerization, which is important for cell migration [Murdoch and Finn, 2000; Samstag et al., 2003]. In murine CX3CR1, the DRY motif may have a similar function, as indicated by the finding that its mutation into DNY blocks chemotaxis towards soluble CX3CL1 [Haskell et al., 1999]. The integrity of the receptor's C-terminus is required for receptor desensitization via endocytosis, as shown for other chemokine receptors such as CXCR2 [Ludwig et al., 1997] and clathrin-mediated signaling. This may explain why both Gi-protein activation by the DRY motif as well as receptor regulation at the C-terminus are critical for induction of chemotaxis by soluble CX3CL1. The data furthermore demonstrate that both motifs are required for transmigration in response to transmembrane CX3CL1 suggesting that they may fulfill very similar functions in chemotaxis and transmigration. Consistent with previous publications showing that adhesion does not require signaling, adhesion is neither affected by mutating the DRY motif nor by truncation of the C-

terminus [Fong et al., 1998; Haskell et al., 1999].

Transmembrane CX3CL1 can be cleaved proximal to the cell membrane resulting in the release of its soluble ectodomain and the downregulation of CX3CL1 from the cell surface [Garton et al., 2001; Hundhausen et al., 2003]. This effect on the one hand leads to reduced adhesiveness for CX3CR1-expressing leukocytes via transmembrane CX3CL1. On the other hand, leukocytes bound to transmembrane CX3CL1 may become released upon cleavage of the transmembrane chemokine [Hundhausen et al., 2007]. Such a process could be relevant for transmigration when adherent leukocytes move from the apical site of the endothelium towards the lateral junction for transmigration between two substrate cells and would require the detachment from the apical side including the interruption of the initial contacts between leukocytes and endothelial cells. Since the binding of CX3CL1 to its receptor is extremely tight due to a low dissociation rate from the receptor and a rather high average bond strength, cleavage of CX3CL1 might be the only way to disrupt the cell-cell contact and thereby allow transmigration [Haskell et al., 2000; Lee et al., 2004].

In the present work, it was demonstrated that activity of ADAM10 and ADAM17 was required for CX3CL1-induced transmigration. For this purpose, ADAM10 and ADAM17 were inhibited by using pharmacologic inhibitors and shRNA. It could be shown that the application of the inhibitor led to an increased surface expression and a reduced shedding of CX3CL1. While the blockade of shedding resulted in an enhanced adhesive activity of CX3CL1, transmigration of CX3CR1-expressing L1.2 cells towards CX3CL1 was dramatically reduced, as was shown for ECV304 cells as well as cytokine-stimulated HUVEC. This data support the model that not only signaling and internalization of the receptor are crucial for facilitating transmigration, but also the cleaving activity of ADAM10 and ADAM17. It has been shown earlier that the inhibition of shedding of cell adhesion molecules, like L-selectin (ADAM17) and VE-Cadherin (ADAM10), decreases transmigration of T-cells [Faveeuw et al., 2001; Schulz et al., 2008]. Metalloproteinase activation and activity could be one step in a cascade of events required for lymphocytes

to extravasate the blood vessel. Thereby, ADAMs might not only regulate the degradation of apical adhesion complexes, but also the loosening of adherens junctions, as was shown for the VE-cadherin/ α -catenin/ β -catenin/plakoglobin complex that was lost from adherens junctions at sites of monocyte penetration of the endothelial layer and rapidly regained after transmigration [Allport et al., 2000].

Extravasation of leukocytes out of the bloodstream is thought to take place in a multi-step process that starts with rolling onto endothelial cells via selectins, turns into chemokine-mediated firm adhesion to adhesion molecules such as integrins, and ends with the migration of leukocytes towards chemotactic factors through the endothelial barrier [Springer, 1994]. These events can be mediated by coordinated activity of selectins, chemokines and integrins. Unlike other chemokines, CX3CL1 has the capacity to mediate capture under flow, tight adhesion and directional transmigration. Therefore, it could contribute to all steps of the recruitment process. From this study, I would like to propose that the process of CX3CL1-mediated cell recruitment involves a sequence of events starting with physical binding of the receptor, activation of the receptor initiating the transmigration process, and ending with the cleavage of CX3CL1 by ADAM10 and ADAM17 allowing the cells to proceed in diapedesis. The last step of transmigration may involve the cleavage of several surface molecules that contribute to the transmigration process such as VCAM-1, JAM-A and VE-cadherin, and very likely also the shedding of transmembrane CX3CL1 [Pruessmeyer and Ludwig, 2008].

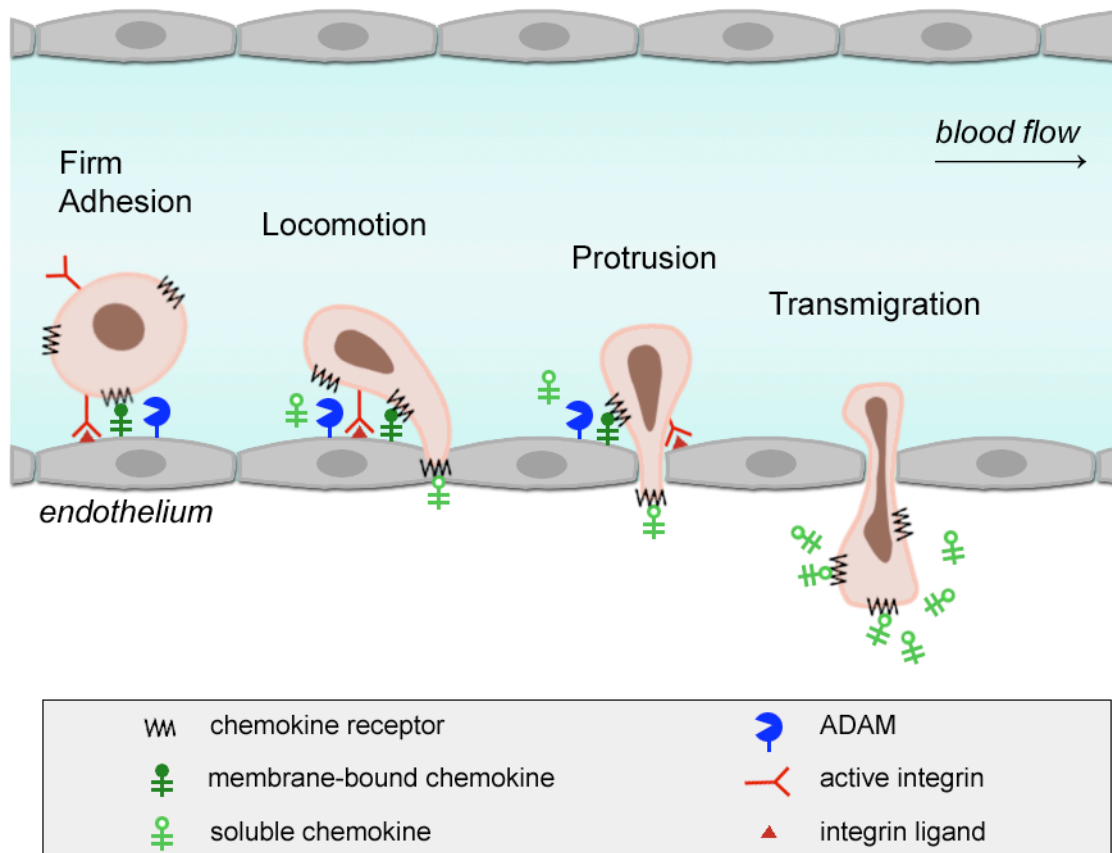


Figure 44: Proposed model. Based on the findings presented in this thesis, a model concerning the involvement of CX3CR1/CX3CL1 interaction in the extravasation process can be proposed. Expression of transmembrane CX3CL1 is induced by the activation of the blood vessel lining endothelium on the luminal as well as the abluminal membrane. While PBMC (and especially monocytes) roll on the endothelium due to interactions with selectins, they can be captured not only by classical adhesion molecules, like ICAM-1 and VCAM-1, but also by transmembrane CX3CL1. Acting as a signaling receptor, CX3CR1 might mediate important signals for the transmigration process. In order to find an appropriate site to extravasate, PBMC have to probe the tissue they are adhering to. Therefore, bonds have to be dissolved and others closed. Important molecules in dissolving the bond between endothelial cell and leukocyte formed by CX3CR1 and CX3CL1 are the metalloproteases ADAM10 and ADAM17. Additionally, they cleave unoccupied CX3CL1 forming a gradient of soluble chemokines and dissolving complexes between endothelial cells facilitating leukocyte transmigration.

The data provide a molecular explanation for the proinflammatory activity of the

CX3CR1/CX3CL1 axis in vascular diseases such as atherosclerosis, which is well documented by a number of recent studies using CX3CR1- or CX3CL1-deficient mice [Combadière et al., 2003; Lesnik et al., 2003; Teupser et al., 2004]. Finally, when considering the CX3CR1/CX3CL1 axis as a therapeutic target in order to block leukocyte recruitment in atherosclerosis, it seems preferable to interfere with the initial step of adhesion using a receptor antagonist rather than blocking CX3CR1 signaling or CX3CL1 shedding, which would both lead to the accumulation of adherent leukocytes at the vascular surface.

In the future a set of further experiments should be conducted to elucidate the role of CX3CR1/CX3CL1 in the extravasation process. It is known that β -arrestins are important for the internalization of G-protein coupled receptors and subsequent signaling and interact with the intracellular part of the receptor [Kraft et al., 2001]. Additionally, some reports show that CX3CL1 and CX3CR1 are involved in survival and proliferation signals in microglia, epithelial cells and smooth muscle cells in a NF- κ b-dependent manner [Boehme et al., 2000; Brand et al., 2002; Chandrasekar et al., 2003]. Since both, the DRY sequence as well as the C-terminus of CX3CR1 are required for transmigration, the analysis of other pathways would possibly lead to a better understanding of signaling pathways, other than intracellular calcium flux, involved in CX3CR1/CX3CL1 function.

There are two possibilities to analyze the involvement of CX3CR1/CX3CL1-mediated adhesion and transmigration: first, the construction of a signaling-deficient receptor variant and second the construction of a non-cleavable ligand variant. As it is known that ADAMs are able to employ a vast number of different cleavage sites, the construction of a non-cleavable ligand variant seemed to be more difficult than that of receptor variants. Still, it would be a great help to have a CX3CL1 variant that can not be cleaved, and this project should be pursued with different approaches.

As was shown earlier, the CX3CR1/CX3CL1 axis is involved in the progression of

inflammatory diseases like atherosclerosis [McDermott et al., 2001; Moatti et al., 2001] and nephropathies [Furuichi et al., 2001; Cockwell et al., 2002]. In further experiments the CX3CR1 variants should be analyzed in inflammatory models *in vivo*. Therefore, the receptor has to be reconstituted in CX3CR1-deficient mice by either knock-in technique or by lentiviral transfer. This will help to evaluate the magnitude and manner of contribution of CX3CR1/CX3CL1 in the extravasation process of leukocytes during inflammation.

CXCL16 and its receptor CXCR6 are implicated in a multitude of pathophysiological situations as atherosclerosis and HIV infection [Deng et al., 1997; Matloubian et al., 2000; Galkina et al., 2007]. Recent data from studies using mice deficient in either CXCR6 or CXCL16 support a role for both ligand and receptor in atherogenesis [Aslanian and Charo, 2006; Galkina et al., 2007].

When peripheral blood mononuclear cells (PBMC) of healthy donors were tested for expression of CXCR6, it was surprising that the expression of CXCR6 strongly varied depending on the donor and cell type. Consequently, PBMC from CXCR6^{low}-expressing donors did not migrate in response to CXCL16 whereas PBMC from donors showing an expression of CXCR6 migrated towards CXCL16. Surprisingly, unlike published earlier [Shimaoka et al., 2004], CXCR6-expressing cells did not adhere to CXCL16-expressing cells. Just recently it was shown that stimulated macrophages do not adhere to coronary artery smooth muscle cells in a CXCL16-dependent manner under static conditions [Barlic et al., 2009]. The differential receptor expression and the non-adherence of CXCR6-positive cells raised the question whether the adhesion of CXCR6-expressing cells to CXCL16-expressing cells is relevant under physiological conditions. For other adhesion molecules, shear stress on endothelial cells is important for the mediation of firm adhesion. Shear stress has been shown to modulate the adhesive capacity of endothelial cells by adjusting the expression of adhesion molecules as for example ICAM-1 [McKinney et al., 2006]. Therefore, flow assays are needed to

elucidate the possibility that CXCL16 only induces adhesion under flow conditions. Furthermore, a network of interactions might be necessary for the CXCR6-CXCL16 interaction to become relevant under physiological conditions.

Instead of the highly conserved DRY motif found in many chemokine receptors, CXCR6 bears a DRF motif within the second intracellular loop. This DRF motif is also found in the 5-HT_{2βPan}-receptor of *Panulirus interruptus* (spiny lobster) and implicated in its constitutive activity [Clark et al., 2004]. The DRF motif in the Gonadotropin releasing hormone receptor (GnRH-R) of *Callithrix jacchus* (common marmoset) mediates a slightly faster internalization rate than the DRS motif found in GnRH-R of most mammals [Byrne et al., 1999]. When the DRF motif of CXCR6 was changed into the conventional DRY, only slight changes in calcium signaling could be observed, whereas the mutation into DNF abolished the calcium signal. As seen for CX3CR1, the arginine residue seems to play the crucial role in the mediation of calcium signals, whereas the tyrosine residue does not contribute. The tyrosine residue is believed to be a potential phosphorylation site, acting as a substrate for a G-protein receptor kinase, and thus is important for receptor desensitization and internalization [Palczewski, 1997]. This suggestion was supported by the findings of a study carried out by Arora and colleagues, which demonstrated that mutating the serine to a tyrosine in the mouse GnRH-R increased the rate of receptor internalization and agonist binding affinity, although no effect was observed on G-protein coupling [Arora et al., 1995]. However, it has also been shown that generating a mouse GnRH-R DRS to DRA mutation had no significant effects on ligand binding, receptor coupling or internalization [Arora et al., 1997]. Therefore, for functional analysis the next step should be the investigation of internalization rates after binding of CXCL16 to CXCR6, similar to the experiments done for CX3CR1 variants.

Additionally, knock-down of CXCR6 led to the formation of medullablastoma, suggesting a role in cancer development [Sasai et al., 2007]. The interaction of CXCR6 and CXCL16 is also thought to mediate cell recruitment in rheumatoid arthritis, and CXCR6 acts as secondary co-receptor for all HIV-strains [Liao et al., 1997; Ruth et al., 2006]. In upcoming experiments the interaction of CXCR6 and CXCL16 should be further characterized. Therefore, L1.2 cell expressing CXCR6 and its variants, consistent with the experiments for CX3CR1 in this thesis, should be generated and analyzed in (trans)-migration and other functional assays, like phosphorylation of signaling molecules or mediation of proliferation/survival.

While CXCR6 is thought to be a pro-atherogenic chemokine receptor, as its knock-down resulted in a decrease of susceptibility to atherosclerosis, CXCL16 might be atheroprotective due to the fact that its knock-down resulted in accelerated atherosclerosis, which has been associated with the additional scavenger receptor function of the chemokine. CXCL16 not only binds to CXCR6 to mediate cell recruitment, but also acts as scavenger receptor for oxidized low density lipoproteins. This function of CXCL16 is not influenced by CXCR6. The uptake of low density lipoproteins eventually leads to an upregulation of atheroprotective genes, such as ATP-binding cassette transporter-1 and apolipoprotein E [Liao et al., 2002; Barlic et al., 2009]. This supports the hypothesis that CXCL16 mediates atheroprotection not through the interaction of CXCR6 and CXCL16, but through its scavenger function. Antagonism of the CXCR6-CXCL16 interaction without affecting the scavenger receptor activity may be of therapeutic potential.

Although both chemokines exist as soluble as well as transmembrane forms, the functions they mediate on binding to their receptors seem to differ. While CX3CR1 mediates adhesion as well as migration, CXCR6 only mediates migration. The

experiments showed that transmembrane CX3CL1 contributes to the extravasation of leukocytes, while there is no contribution of transmembrane CXCL16. To obtain a better understanding of the underlying mechanisms receptor variants were generated. Although the CX3CR1 (and to a lesser degree the CXCR6) variants were extensively characterized, some questions remain open and should be addressed in a future set of experiments. The importance of the C-terminal part of CX3CR1 was shown in the context of receptor desensitization but it is still unclear what pathways and functions exactly are affected. Therefore, experiments targeting the receptor phosphorylation at intracellular serine-residues, receptor recycling or F-actin network rearrangement should be performed. Additionally, the unusual DRF motif in CXCR6 might influence the receptor's activity turning it into a constitutively active receptor in contrast to receptors bearing the conserved DRY motif. The consequence of such a potential constitutive activity in the context of chemotaxis should be investigated. Furthermore, the impact of CX3CL1 and CXCL16 shedding still remains unclear even though it was shown that the activity of the sheddases is required for efficient CX3CL1-mediated transmigration. With the variety of mediated functions, the CX3CR1-CX3CL1 axis, and possibly also CXCR6-CXCL16, may constitute important regulators involved in leukocyte extravasation.

As all the presented data were generated *in vitro*, these results should be confirmed by *in vivo* experiments. Despite their different structural characteristics and activity, CX3CR1 and CXCR6 show a pro-atherogenic potential as confirmed by usage of knock-out mice for CX3CR1 and CXCR6 [Combadière et al., 2003; Galkina et al., 2007]. These mice can now be reconstituted with the mutated murine receptors by knock-in technique or lentiviral genetransfer as is currently established in our laboratory. The impact of the alteration of conserved motifs in CX3CR1 and CXCR6 should be investigated in the context of inflammatory animal models, such as the ApoE^{-/-} diet-induced atherosclerosis or wire-induced injury model. In the latter model, CX3CL1 is upregulated in intimal smooth muscle cells and endothelial cells. Furthermore, CX3CR1 deficiency is

associated with a decreased infiltration of monocytes [Liu et al., 2006]. The relevance of CX3CR1-CX3CL1 axis in humans is underlined by the fact that the CX3CR1 polymorphism V249I is associated with increased monocyte adhesiveness increasing the risk for restenosis after coronary stent implantation [Daoudi et al., 2004; Niessner et al., 2005]. Accordingly, the alteration of the DRF motif of CX3CR1 or truncation of the C-terminal serine-residues can have the following impact in a murine model of inflammation: cells expressing the CX3CR1 variants, that both block transmigration, should accumulate on the arterial wall and the infiltration into the lesion should be reduced.

Similarly, in a model of ApoE^{-/-} diet-induced atherosclerosis, mice deficient in CXCR6 display reduced atherosclerosis associated with a lower content of CXCR6⁺ T cells and macrophages in the aorta [Galkina et al., 2007]. Since CXCR6-dependent chemotaxis requires signaling, less cells expressing the receptor variants should be recruited into the lesion, when the DRF motif is abolished. In contrast to CX3CL1, CXCL16 does not mediate adhesion. Therefore, as indicated by the *in vitro* experiments, cells expressing the mutated DRF motif of CXCR6 should not accumulate at the vascular wall. Thus, mutating either receptor should result in a less severe inflammatory response. This may be complicated by the fact that mutated CX3CR1 still functions as adhesion molecule leading to an accumulation of CX3CR1-variant expressing cells at the arterial wall. A pharmacological interference with transmembrane CX3CL1 should block both, the accumulation of leukocytes at the site of inflammation and their infiltration into the lesion.

7 Literature

1. Abel, S. et al. The transmembrane CXC-chemokine ligand 16 is induced by IFN-gamma and TNF-alpha and shed by the activity of the disintegrin-like metalloproteinase ADAM10. *J Immunol* **172**, 6362-6372 (2004).
2. Acharya, S. & Karnik, S. S. Modulation of GDP release from transducin by the conserved Glu134-Arg135 sequence in rhodopsin. *J Biol Chem* **271**, 25406-25411 (1996).
3. Alewijnse, A. E. et al. The effect of mutations in the DRY motif on the constitutive activity and structural instability of the histamine H(2) receptor. *Mol Pharmacol* **57**, 890-898 (2000).
4. Allen, S. J., Crown, S. E. & Handel, T. M. Chemokine: receptor structure, interactions, and antagonism. *Annu Rev Immunol* **25**, 787-820 (2007).
5. Allport, J. R., Muller, W. A. & Luscinskas, F. W. Monocytes induce reversible focal changes in vascular endothelial cadherin complex during transendothelial migration under flow. *J Cell Biol* **148**, 203-216 (2000).
6. Alteraifi, A. M. & Zhelev, D. V. Transient increase of free cytosolic calcium during neutrophil motility responses. *J Cell Sci* **110**, 1967-1977 (1997).
7. Arora, K. K., Cheng, Z. & Catt, K. J. Mutations of the conserved DRS motif in the second intracellular loop of the gonadotropin-releasing hormone receptor affect expression, activation, and internalization. *Mol Endocrinol* **11**, 1203-1212 (1997).
8. Arora, K. K., Sakai, A. & Catt, K. J. Effects of second intracellular loop mutations on signal transduction and internalization of the gonadotropin-releasing hormone receptor. *J Biol Chem* **270**, 22820-22826 (1995).
9. Aslanian, A. M. & Charo, I. F. Targeted disruption of the scavenger receptor and chemokine CXCL16 accelerates atherosclerosis. *Circulation* **114**, 583-590 (2006).
10. Ballesteros, J. et al. Functional microdomains in G-protein-coupled receptors. The conserved arginine-cage motif in the gonadotropin-releasing hormone receptor. *J Biol Chem* **273**, 10445-10453 (1998).

11. Barak, L. S., Ménard, L., Ferguson, S. S., Colapietro, A. M. & Caron, M. G. The conserved seven-transmembrane sequence NP(X)₂,3Y of the G-protein-coupled receptor superfamily regulates multiple properties of the beta 2-adrenergic receptor. *Biochemistry* **34**, 15407-15414 (1995).
12. Barak, L. S., Oakley, R. H., Laporte, S. A. & Caron, M. G. Constitutive arrestin-mediated desensitization of a human vasopressin receptor mutant associated with nephrogenic diabetes insipidus. *Proc Natl Acad Sci USA* **98**, 93-98 (2001).
13. Barak, L. S. et al. A highly conserved tyrosine residue in G protein-coupled receptors is required for agonist-mediated beta 2-adrenergic receptor sequestration. *J Biol Chem* **269**, 2790-2795 (1994).
14. Barlic, J., Zhu, W. & Murphy, P. M. Atherogenic lipids induce high-density lipoprotein uptake and cholesterol efflux in human macrophages by up-regulating transmembrane chemokine CXCL16 without engaging CXCL16-dependent cell adhesion. *J Immunol* **182**, 7928-7936 (2009).
15. Barreiro, O., Vicente-Manzanares, M., Urzainqui, A., Yanez-Mo, M. & Sanchez-Madrid, F. Interactive protrusive structures during leukocyte adhesion and transendothelial migration. *Front Biosci* **9**, 1849-1863 (2004).
16. Bazan, J. F. et al. A new class of membrane-bound chemokine with a CX3C motif. *Nature* **385**, 640-644 (1997).
17. Beglova, N., Blacklow, S. C., Takagi, J. & Springer, T. A. Cysteine-rich module structure reveals a fulcrum for integrin rearrangement upon activation. *Nat Struct Biol* **9**, 282-287 (2002).
18. Ben-Baruch, A. et al. Interleukin-8 receptor beta. The role of the carboxyl terminus in signal transduction. *J Biol Chem* **270**, 9121-9128 (1995).
19. Berchiche, Y. A. et al. Direct assessment of CXCR4 mutant conformations reveals complex link between receptor structure and G(alpha)(i) activation. *J Biol Chem* **282**, 5111-5115 (2007).
20. Boehme, S. A., Lio, F. M., Maciejewski-Lenoir, D., Bacon, K. B. & Conlon, P. J. The chemokine fractalkine inhibits Fas-mediated cell death of brain microglia. *J Immunol* **165**, 397-403 (2000).
21. Bokoch, G. M. Chemoattractant signaling and leukocyte activation. *Blood* **86**, 1649-1660 (1995).

22. Boulday, G., Coupel, S., Coulon, F., Soulillou, J. P. & Charreau, B. Antigrft antibody-mediated expression of metalloproteinases on endothelial cells. Differential expression of TIMP-1 and ADAM-10 depends on antibody specificity and isotype. *Circ Res* **88**, 430-437 (2001).
23. Brand, S., Sakaguchi, T., Gu, X., Colgan, S. P. & Reinecker, H. C. Fractalkine-mediated signals regulate cell-survival and immune-modulatory responses in intestinal epithelial cells. *Gastroenterology* **122**, 166-177 (2002).
24. Byrne, B. et al. Isolation and characterisation of the marmoset gonadotrophin releasing hormone receptor: Ser(140) of the DRS motif is substituted by Phe. *J Endocrinol* **163**, 447-456 (1999).
25. Campbell, J. J. et al. Chemokines and the arrest of lymphocytes rolling under flow conditions. *Science* **279**, 381-384 (1998).
26. Chandrasekar, B., Bysani, S. & Mummidi, S. CXCL16 signals via Gi, phosphatidylinositol 3-kinase, Akt, I kappa B kinase, and nuclear factor-kappa B and induces cell-cell adhesion and aortic smooth muscle cell proliferation. *J Biol Chem* **279**, 3188-3196 (2004).
27. Chandrasekar, B. et al. Fractalkine (CX3CL1) stimulated by nuclear factor kappaB (NF-kappaB)-dependent inflammatory signals induces aortic smooth muscle cell proliferation through an autocrine pathway. *Biochem J* **373**, 547-558 (2003).
28. Chen, Y., Green, S. R., Almazan, F. & Quehenberger, O. The amino terminus and the third extracellular loop of CX3CR1 contain determinants critical for distinct receptor functions. *Mol Pharmacol* **69**, 857-865 (2006).
29. Chuluyan, H. E. & Issekutz, A. C. VLA-4 integrin can mediate CD11/CD18-independent transendothelial migration of human monocytes. *J Clin Invest* **92**, 2768-2777 (1993).
30. Clark, M. C. et al. Arthropod 5-HT₂ receptors: a neurohormonal receptor in decapod crustaceans that displays agonist independent activity resulting from an evolutionary alteration to the DRY motif. *J Neurosci* **24**, 3421-3435 (2004).
31. Cockwell, P., Chakravorty, S. J., Girdlestone, J. & Savage, C. O. Fractalkine expression in human renal inflammation. *J Pathol* **196**, 85-90 (2002).

32. Combadiere, C., Gao, J., Tiffany, H. L. & Murphy, P. M. Gene cloning, RNA distribution, and functional expression of mCX3CR1, a mouse chemotactic receptor for the CX3C chemokine fractalkine. *Biochem Biophys Res Commun* **253**, 728-732 (1998).
33. Combadière, C. et al. Decreased atherosclerotic lesion formation in CX3CR1/apolipoprotein E double knockout mice. *Circulation* **107**, 1009-1016 (2003).
34. Daoudi, M. et al. Enhanced adhesive capacities of the naturally occurring Ile249-Met280 variant of the chemokine receptor CX3CR1. *J Biol Chem* **279**, 19649-19657 (2004).
35. del Pozo, M. A., Sanchez-Mateos, P., Nieto, M. & Sanchez-Madrid, F. Chemokines regulate cellular polarization and adhesion receptor redistribution during lymphocyte interaction with endothelium and extracellular matrix. Involvement of cAMP signaling pathway. *J Cell Biol* **131**, 495-508 (1995).
36. Deng, H. K., Unutmaz, D., KewalRamani, V. N. & Littman, D. R. Expression cloning of new receptors used by simian and human immunodeficiency viruses. *Nature* **388**, 296-300 (1997).
37. Dichmann, S. et al. Fractalkine induces chemotaxis and actin polymerization in human dendritic cells. *Inflamm Res* **50**, 529-533 (2001).
38. Dijkstra, I. M., Hulshof, S., van der Valk, P., Boddeke, H. W. & Biber, K. Cutting edge: activity of human adult microglia in response to CC chemokine ligand 21. *J Immunol* **172**, 2744-2747 (2004).
39. Fanelli, F., Barbier, P., Zanchetta, D., de Benedetti, P. G. & Chini, B. Activation mechanism of human oxytocin receptor: a combined study of experimental and computer-simulated mutagenesis. *Mol Pharmacol* **56**, 214-225 (1999).
40. Faure, S. et al. Rapid progression to AIDS in HIV+ individuals with a structural variant of the chemokine receptor CX3CR1. *Science* **287**, 2274-2277 (2000).
41. Faveeuw, C., Preece, G. & Ager, A. Transendothelial migration of lymphocytes across high endothelial venules into lymph nodes is affected by metalloproteinases. *Blood* **98**, 688-695 (2001).
42. Feng, L. et al. Prevention of crescentic glomerulonephritis by immunoneutralization of the fractalkine receptor CX3CR1 rapid communication. *Kidney Int* **56**, 612-620 (1999).

43. Fong, A. M. et al. Fractalkine and CX3CR1 mediate a novel mechanism of leukocyte capture, firm adhesion, and activation under physiologic flow. *J Exp Med* **188**, 1413-1419 (1998).
44. Foussat, A. et al. Deregulation of the expression of the fractalkine/fractalkine receptor complex in HIV-1-infected patients. *Blood* **98**, 1678-1686 (2001).
45. Furuichi, K. et al. Upregulation of fractalkine in human crescentic glomerulonephritis. *Nephron* **87**, 314-320 (2001).
46. Galkina, E. et al. CXCR6 Promotes Atherosclerosis by Supporting T-Cell Homing, Interferon- γ Production, and Macrophage Accumulation in the Aortic Wall. *Circulation* (2007).
47. García Lopez, M. A., Aguado Martínez, A., Lamaze, C., Martínez-A, C. & Fischer, T. Inhibition of dynamin prevents CCL2-mediated endocytosis of CCR2 and activation of ERK1/2. *Cell Signal* (2009).
48. Garcia, G. E. et al. NF-kappaB-dependent fractalkine induction in rat aortic endothelial cells stimulated by IL-1beta, TNF-alpha, and LPS. *J Leukoc Biol* **67**, 577-584 (2000).
49. Garin, A., Pellet, P., Deterre, P., Debré, P. & Combadière, C. Cloning and functional characterization of the human fractalkine receptor promoter regions. *Biochem J* **368**, 753-760 (2002).
50. Garton, K. J. et al. Tumor necrosis factor-alpha-converting enzyme (ADAM17) mediates the cleavage and shedding of fractalkine (CX3CL1). *J Biol Chem* **276**, 37993-38001 (2001).
51. Geiger, B. & Bershadsky, A. Exploring the neighborhood: adhesion-coupled cell mechanosensors. *Cell* **110**, 139-142 (2002).
52. Gosling, J. et al. Molecular uncoupling of C-C chemokine receptor 5-induced chemotaxis and signal transduction from HIV-1 coreceptor activity. *Proc Natl Acad Sci USA* **94**, 5061-5066 (1997).
53. Greaves, D. R. et al. Linked chromosome 16q13 chemokines, macrophage-derived chemokine, fractalkine, and thymus- and activation-regulated chemokine, are expressed in human atherosclerotic lesions. *Arterioscler Thromb Vasc Biol* **21**, 923-929 (2001).

54. Harrison, J. K. et al. Mutational analysis of the fractalkine chemokine domain. Basic amino acid residues differentially contribute to CX3CR1 binding, signaling, and cell adhesion. *J Biol Chem* **276**, 21632-21641 (2001).
55. Haskell, C. A., Cleary, M. D. & Charo, I. F. Molecular uncoupling of fractalkine-mediated cell adhesion and signal transduction. Rapid flow arrest of CX3CR1-expressing cells is independent of G-protein activation. *J Biol Chem* **274**, 10053-10058 (1999).
56. Haskell, C. A., Cleary, M. D. & Charo, I. F. Unique role of the chemokine domain of fractalkine in cell capture. Kinetics of receptor dissociation correlate with cell adhesion. *J Biol Chem* **275**, 34183-34189 (2000).
57. Hofnagel, O., Luechtenborg, B., Plenz, G. & Robenek, H. Expression of the novel scavenger receptor SR-PSOX in cultured aortic smooth muscle cells and umbilical endothelial cells. *Arterioscler Thromb Vasc Biol* **22**, 710-711 (2002).
58. Hundhausen, C. et al. The disintegrin-like metalloproteinase ADAM10 is involved in constitutive cleavage of CX3CL1 (fractalkine) and regulates CX3CL1-mediated cell-cell adhesion. *Blood* **102**, 1186-1195 (2003).
59. Hundhausen, C. et al. Regulated shedding of transmembrane chemokines by the disintegrin and metalloproteinase 10 facilitates detachment of adherent leukocytes. *J Immunol* **178**, 8064-8072 (2007).
60. Hunyady, L., Bor, M., Baukal, A. J., Balla, T. & Catt, K. J. A conserved NPLFY sequence contributes to agonist binding and signal transduction but is not an internalization signal for the type 1 angiotensin II receptor. *J Biol Chem* **270**, 16602-16609 (1995).
61. Imai, T. et al. Identification and molecular characterization of fractalkine receptor CX3CR1, which mediates both leukocyte migration and adhesion. *Cell* **91**, 521-530 (1997).
62. Kao, J. P., Harootunian, A. T. & Tsien, R. Y. Photochemically generated cytosolic calcium pulses and their detection by fluo-3. *J Biol Chem* **264**, 8179-8184 (1989).
63. Kim, C. H. et al. Bonzo/CXCR6 expression defines type 1-polarized T-cell subsets with extralymphoid tissue homing potential. *J Clin Invest* **107**, 595-601 (2001).
64. Kim, J. H., Cho, E. Y., Min, C., Park, J. H. & Kim, K. M. Characterization of functional roles of DRY motif in the 2nd intracellular loop of dopamine D2 and D3 receptors. *Arch Pharm Res* **31**, 474-481 (2008).

65. Kim, K. M. & Caron, M. G. Complementary roles of the DRY motif and C-terminus tail of GPCRS for G protein coupling and beta-arrestin interaction. *Biochem Biophys Res Commun* **366**, 42-47 (2008).
66. Kraft, K. et al. Characterization of sequence determinants within the carboxyl-terminal domain of chemokine receptor CCR5 that regulate signaling and receptor internalization. *J Biol Chem* **276**, 34408-34418 (2001).
67. Krueger, K. M., Daaka, Y., Pitcher, J. A. & Lefkowitz, R. J. The role of sequestration in G protein-coupled receptor resensitization. Regulation of beta2-adrenergic receptor dephosphorylation by vesicular acidification. *J Biol Chem* **272**, 5-8 (1997).
68. Lagane, B. et al. Mutation of the DRY motif reveals different structural requirements for the CC chemokine receptor 5-mediated signaling and receptor endocytosis. *Mol Pharmacol* **67**, 1966-1976 (2005).
69. Landsman, L. et al. CX3CR1 is required for monocyte homeostasis and atherogenesis by promoting cell survival. *Blood* **113**, 963-972 (2009).
70. Laporte, S. A. et al. The beta2-adrenergic receptor/betaarrestin complex recruits the clathrin adaptor AP-2 during endocytosis. *Proc Natl Acad Sci U S A* **96**, 3712-3717 (1999).
71. Lee, F. H., Haskell, C., Charo, I. F. & Boettiger, D. Receptor-ligand binding in the cell-substrate contact zone: a quantitative analysis using CX3CR1 and CXCR1 chemokine receptors. *Biochemistry* **43**, 7179-7186 (2004).
72. Lee, S. J. et al. Fractalkine stimulates angiogenesis by activating the Raf-1/MEK/ERK- and PI3K/Akt/eNOS-dependent signal pathways. *Am J Physiol Heart Circ Physiol* **291**, H2836-46 (2006).
73. Lesnik, P., Haskell, C. A. & Charo, I. F. Decreased atherosclerosis in CX3CR1^{-/-} mice reveals a role for fractalkine in atherogenesis. *J Clin Invest* **111**, 333-340 (2003).
74. Liao, F. et al. STRL33, A novel chemokine receptor-like protein, functions as a fusion cofactor for both macrophage-tropic and T cell line-tropic HIV-1. *J Exp Med* **185**, 2015-2023 (1997).
75. Liao, H., Langmann, T., Schmitz, G. & Zhu, Y. Native LDL upregulation of ATP-binding cassette transporter-1 in human vascular endothelial cells. *Arterioscler Thromb Vasc Biol* **22**, 127-132 (2002).

76. Liu, P. et al. CX3CR1 deficiency confers protection from intimal hyperplasia after arterial injury. *Arterioscler Thromb Vasc Biol* **26**, 2056-2062 (2006).
77. Lucas, A. D. et al. Smooth muscle cells in human atherosclerotic plaques express the fractalkine receptor CX3CR1 and undergo chemotaxis to the CX3C chemokine fractalkine (CX3CL1). *Circulation* **108**, 2498-2504 (2003).
78. Ludwig, A. et al. Enhanced expression and shedding of the transmembrane chemokine CXCL16 by reactive astrocytes and glioma cells. *J Neurochem* **93**, 1293-1303 (2005).
79. Ludwig, A., Berkhout, T., Moores, K. E., Groot, P. & Chapman, G. Fractalkine is expressed by smooth muscle cells in response to IFN-gamma and TNF-alpha and is modulated by metalloproteinase activity. *J Immunol* **168**, 604-612 (2002).
80. Ludwig, A. et al. Metalloproteinase inhibitors for the disintegrin-like metalloproteinases ADAM10 and ADAM17 that differentially block constitutive and phorbol ester-inducible shedding of cell surface molecules. *Comb Chem High Throughput Screen* **8**, 161-171 (2005).
81. Ludwig, A. et al. The CXC-chemokine neutrophil-activating peptide-2 induces two distinct optima of neutrophil chemotaxis by differential interaction with interleukin-8 receptors CXCR-1 and CXCR-2. *Blood* **90**, 4588-4597 (1997).
82. Macia, E. et al. Dynasore, a cell-permeable inhibitor of dynamin. *Dev Cell* **10**, 839-850 (2006).
83. Man, S., Ubogu, E. E. & Ransohoff, R. M. Inflammatory cell migration into the central nervous system: a few new twists on an old tale. *Brain Pathol* **17**, 243-250 (2007).
84. Martin-Padura, I. et al. Junctional adhesion molecule, a novel member of the immunoglobulin superfamily that distributes at intercellular junctions and modulates monocyte transmigration. *J Cell Biol* **142**, 117-127 (1998).
85. Matloubian, M., David, A., Engel, S., Ryan, J. E. & Cyster, J. G. A transmembrane CXC chemokine is a ligand for HIV-coreceptor Bonzo. *Nat Immunol* **1**, 298-304 (2000).
86. McDermott, D. H. et al. Chemokine receptor mutant CX3CR1-M280 has impaired adhesive function and correlates with protection from cardiovascular disease in humans. *J Clin Invest* **111**, 1241-1250 (2003).

87. McDermott, D. H. et al. Association between polymorphism in the chemokine receptor CX3CR1 and coronary vascular endothelial dysfunction and atherosclerosis. *Circ Res* **89**, 401-407 (2001).
88. McKinney, V. Z., Rinker, K. D. & Truskey, G. A. Normal and shear stresses influence the spatial distribution of intracellular adhesion molecule-1 expression in human umbilical vein endothelial cells exposed to sudden expansion flow. *J Biomech* **39**, 806-817 (2006).
89. Minta, A., Kao, J. P. & Tsien, R. Y. Fluorescent indicators for cytosolic calcium based on rhodamine and fluorescein chromophores. *J Biol Chem* **264**, 8171-8178 (1989).
90. Mizoue, L. S., Bazan, J. F., Johnson, E. C. & Handel, T. M. Solution structure and dynamics of the CX3C chemokine domain of fractalkine and its interaction with an N-terminal fragment of CX3CR1. *Biochemistry* **38**, 1402-1414 (1999).
91. Moatti, D. et al. Polymorphism in the fractalkine receptor CX3CR1 as a genetic risk factor for coronary artery disease. *Blood* **97**, 1925-1928 (2001).
92. Moore, C. A., Milano, S. K. & Benovic, J. L. Regulation of receptor trafficking by GRKs and arrestins. *Annu Rev Physiol* **69**, 451-482 (2007).
93. Muller, W. A., Weigl, S. A., Deng, X. & Phillips, D. M. PECAM-1 is required for transendothelial migration of leukocytes. *J Exp Med* **178**, 449-460 (1993).
94. Murdoch, C. & Finn, A. Chemokine receptors and their role in inflammation and infectious diseases. *Blood* **95**, 3032-3043 (2000).
95. Nakayama, T. et al. Cutting edge: profile of chemokine receptor expression on human plasma cells accounts for their efficient recruitment to target tissues. *J Immunol* **170**, 1136-1140 (2003).
96. Niessner, A. et al. Fractalkine receptor polymorphisms V249I and T280M as genetic risk factors for restenosis. *Thromb Haemost* **94**, 1251-1256 (2005).
97. Nieto, M. et al. Polarization of chemokine receptors to the leading edge during lymphocyte chemotaxis. *J Exp Med* **186**, 153-158 (1997).
98. Nishida, N. et al. Activation of leukocyte beta2 integrins by conversion from bent to extended conformations. *Immunity* **25**, 583-594 (2006).
99. Onuffer, J. J. & Horuk, R. Chemokines, chemokine receptors and small-molecule antagonists: recent developments. *Trends Pharmacol Sci* **23**, 459-467 (2002).

100. Palczewski, K. et al. Crystal structure of rhodopsin: A G protein-coupled receptor. *Science* **289**, 739-745 (2000).
101. Palczewski, K. GTP-binding-protein-coupled receptor kinases--two mechanistic models. *Eur J Biochem* **248**, 261-269 (1997).
102. Passam, A. M. et al. Polymorphisms of Cx(3)CR1 and CXCR6 Receptors in Relation to HAART Therapy of HIV Type 1 Patients. *AIDS Res Hum Retroviruses* **23**, 1026-1032 (2007).
103. Pruessmeyer, J. & Ludwig, A. The good, the bad and the ugly substrates for ADAM10 and ADAM17 in brain pathology, inflammation and cancer. *Semin Cell Dev Biol* (2008).
104. Rosenthal, W., Antaramian, A., Gilbert, S. & Birnbaumer, M. Nephrogenic diabetes insipidus. A V2 vasopressin receptor unable to stimulate adenylyl cyclase. *J Biol Chem* **268**, 13030-13033 (1993).
105. Ross, R. The pathogenesis of atherosclerosis: a perspective for the 1990s. *Nature* **362**, 801-809 (1993).
106. Rostene, W., Kitabgi, P. & Parsadaniantz, S. M. Chemokines: a new class of neuromodulator? *Nat Rev Neurosci* **8**, 895-903 (2007).
107. Rot, A. et al. RANTES and macrophage inflammatory protein 1 alpha induce the migration and activation of normal human eosinophil granulocytes. *J Exp Med* **176**, 1489-1495 (1992).
108. Rot, A. & von Andrian, U. H. Chemokines in innate and adaptive host defense: basic chemokinese grammar for immune cells. *Annu Rev Immunol* **22**, 891-928 (2004).
109. Ruth, J. H. et al. CXCL16-mediated cell recruitment to rheumatoid arthritis synovial tissue and murine lymph nodes is dependent upon the MAPK pathway. *Arthritis Rheum* **54**, 765-778 (2006).
110. Samstag, Y., Eibert, S. M., Klemke, M. & Wabnitz, G. H. Actin cytoskeletal dynamics in T lymphocyte activation and migration. *J Leukoc Biol* **73**, 30-48 (2003).
111. Sasai, K. et al. Medulloblastomas derived from Cxcr6 mutant mice respond to treatment with a smoothed inhibitor. *Cancer Res* **67**, 3871-3877 (2007).
112. Sato, T. et al. Role for CXCR6 in recruitment of activated CD8+ lymphocytes to inflamed liver. *J Immunol* **174**, 277-283 (2005).

113. Scheer, A. et al. Mutational analysis of the highly conserved arginine within the Glu/Asp-Arg-Tyr motif of the alpha(1b)-adrenergic receptor: effects on receptor isomerization and activation. *Mol Pharmacol* **57**, 219-231 (2000).
114. Schenkel, A. R., Mamdouh, Z., Chen, X., Liebman, R. M. & Muller, W. A. CD99 plays a major role in the migration of monocytes through endothelial junctions. *Nat Immunol* **3**, 143-150 (2002).
115. Schulz, B. et al. ADAM10 regulates endothelial permeability and T-Cell transmigration by proteolysis of vascular endothelial cadherin. *Circ Res* **102**, 1192-1201 (2008).
116. Sharron, M. et al. Expression and coreceptor activity of STRL33/Bonzo on primary peripheral blood lymphocytes. *Blood* **96**, 41-49 (2000).
117. Shimaoka, T. et al. Molecular cloning of a novel scavenger receptor for oxidized low density lipoprotein, SR-PSOX, on macrophages. *J Biol Chem* **275**, 40663-40666 (2000).
118. Shimaoka, T. et al. Cell surface-anchored SR-PSOX/CXC chemokine ligand 16 mediates firm adhesion of CXC chemokine receptor 6-expressing cells. *J Leukoc Biol* **75**, 267-274 (2004).
119. Slice, L. W. et al. The conserved NPXnY motif present in the gastrin-releasing peptide receptor is not a general sequestration sequence. *J Biol Chem* **269**, 21755-21761 (1994).
120. Springer, T. A. Traffic signals for lymphocyte recirculation and leukocyte emigration: the multistep paradigm. *Cell* **76**, 301-314 (1994).
121. Stocker, W. & Bode, W. Structural features of a superfamily of zinc-endopeptidases: the metzincins. *Curr Opin Struct Biol* **5**, 383-390 (1995).
122. Tanaka, Y., Adams, D. H. & Shaw, S. Proteoglycans on endothelial cells present adhesion-inducing cytokines to leukocytes. *Immunol Today* **14**, 111-115 (1993).
123. Teupser, D. et al. Major reduction of atherosclerosis in fractalkine (CX3CL1)-deficient mice is at the brachiocephalic artery, not the aortic root. *Proc Natl Acad Sci USA* **101**, 17795-17800 (2004).
124. Tong, N. et al. Neuronal fractalkine expression in HIV-1 encephalitis: roles for macrophage recruitment and neuroprotection in the central nervous system. *J Immunol* **164**, 1333-1339 (2000).

125. Wessels, D. et al. Clathrin plays a novel role in the regulation of cell polarity, pseudopod formation, uropod stability and motility in Dictyostelium. *J Cell Sci* **113**, 21-36 (2000).
126. Wilbanks, A. et al. Expression cloning of the STRL33/BONZO/TYMSTRligand reveals elements of CC, CXC, and CX3C chemokines. *J Immunol* **166**, 5145-5154 (2001).
127. Wilbanks, A. M., Laporte, S. A., Bohn, L. M., Barak, L. S. & Caron, M. G. Apparent loss-of-function mutant GPCRs revealed as constitutively desensitized receptors. *Biochemistry* **41**, 11981-11989 (2002).
128. Wolfe, B. L. & Trejo, J. Clathrin-dependent mechanisms of G protein-coupled receptor endocytosis. *Traffic* **8**, 462-470 (2007).
129. Wolfsberg, T. G. & White, J. M. ADAMs in fertilization and development. *Dev Biol* **180**, 389-401 (1996).
130. Wong, S. K. G protein selectivity is regulated by multiple intracellular regions of GPCRs. *Neurosignals* **12**, 1-12 (2003).
131. Yang, X. P. et al. Fractalkine Upregulates Intercellular Adhesion Molecule-1 in Endothelial Cells Through CX3CR1 and the Jak Stat5 Pathway. *Circ Res* (2007).
132. Zhu, S. Z., Wang, S. Z., Hu, J. & el-Fakahany, E. E. An arginine residue conserved in most G protein-coupled receptors is essential for the function of the m1 muscarinic receptor. *Mol Pharmacol* **45**, 517-523 (1994).

8 List of figures

Figure 1: Multiple steps are necessary for leukocyte extravasation.....	8
Figure 2: Chemokines are divided into four groups.....	11
Figure 3: Schematic view of CX3CR1.....	17
Figure 4: Schematic view of CX3CR1 signaling.....	19
Figure 5: Structure of GW280264X.....	30
Figure 6: Structure of Dynasore.....	31
Figure 7: CX3CR1 is expressed on PBMC.....	48
Figure 8: PBMC adhere to a CX3CL1 expressing cell layer under flow conditions.....	49
Figure 9: PBMC chemotactically migrate towards CX3CL1.....	50
Figure 10: PBMC chemotactically transmigrate in response to CX3CL1.....	51
Figure 11: Stimulated HUVEC express CX3CL1.....	52
Figure 12: Neutralizing of CX3CL1, ICAM-1 and VCAM-1 prevents transmigration.....	53
Figure 13: Dynasore prevents transmigration of PBMC.....	54
Figure 14: Cells migrate towards CX3CL1 and adhere to CX3CL1.....	56
Figure 15: L1.2 cells transmigrate through an ECV304 cell layer.....	56
Figure 16: L1.2 cells transmigrate through a HUVEC cell layer.....	57
Figure 17: HUVEC produce CX3CL1 after stimulation with cytokines.....	58
Figure 18: CX3CL1 inhibition influences transmigration.....	59
Figure 19: PTX treatment influences transmigration.....	60
Figure 20: Pretreatment with dynasore prevents L1.2 cell chemotaxis.....	61
Figure 21: Alignment of conserved motifs in GPCR superfamily.....	62
Figure 22: Overview of introduced changes in CX3CR1.....	63
Figure 23: Expression and binding of CX3CR1 variants.....	64
Figure 24: Stably transfected HEK293 cells.....	65
Figure 25: CX3CR1 internalizes and mediates CX3CL1 uptake.....	66
Figure 26: CX3CR1 and S319X, but not R127N mediate intracellular calcium flux.....	68
Figure 27: Receptor variants mediate adhesion under static and flow conditions.....	69

Figure 28: Receptor variants do not mediate (trans-)migration.	71
Figure 29: Receptor variant R127N does not mediate transmigration through HUVEC.	72
Figure 30: Receptor variants do not mediate pseudopod formation.....	73
Figure 31: Inhibition of ADAM10/17 abrogates transmigration.	75
Figure 32: CX3CL1 surface expression is reduced when incubated with PBMC.	75
Figure 33: PBMC adhere, but do not transmigrate when ADAM10/17 are inhibited.	76
Figure 34: PBMC adhere, but do not transmigrate when ADAM10/17 are inhibited.	77
Figure 35: ADAM10 silencing leads to suppression of transmigration.	78
Figure 36: CXCR6 expression varies based on donor.....	81
Figure 37: PBMC do not adhere to CXCL16 under static conditions.....	81
Figure 38: CXCR6-expressing cells do not adhere to CXCL16 under static conditions.	82
Figure 39: CXCR6 binds CXCL16-6xHis.	83
Figure 40: PBMC expressing CXCR6 chemotactically migrate towards CXCL16.....	84
Figure 41: Surface expression and ligand binding of CXCR6 variants.	85
Figure 42: CXCR6 and F128Y, but not R127N mediate intracellular calcium flux.	86
Figure 43: R127N and F128Y do not adhere to CXCL16-ECV304 cells.....	87
Figure 44: Proposed model.....	96

9 List of tables

Table 1: Conserved motifs in GPCR class A.....15

10 Abbreviations

A

ADAM	a disintegrin and metalloproteinase
ADP	adenosine diphosphate
AF	AlexaFluor
AI	adhesion index
AIDS	acquired immunodeficiency syndrome
AM	acetoxymethylester
Amp	ampicillin
ANOVA	analysis of variance
apoE	apolipoprotein E
ATP	adenosine-5'-triphosphate

B

Bad	Bcl-2-associated death promoter
Bcl	B-cell leukemia
BSA	bovine serum albumine

C

CAM	cellular adhesion molecule
cAMP	cyclic adenosine monophosphate
CD	chemokine domain
cDNA	complementary DNA
CTAK	cutaneous T-cell-attracting chemokine

D

DAG	diacylglycerol
DNA	desoxyribonucleic acid
DMEM	Dulbecco's modified Eagle's Medium
DMSO	dimethyl sulfoxide
dNTP	desoxy nucleoside triphosphate

E

<i>E.coli</i>	<i>Escherichia coli</i>
EDTA	N,N'-1,2-ethanediylbis(N-(carboxymethyl)glycine)edetic acid
EGTA	(Ethylenebis(oxyethylenenitrilo))tetra-; ethylene glycol bis(2-aminoethyl ether)-N,N,N'N'tetraacetic acid
E-selectin	endothelial selectin

ELISA	enzyme-linked immunosorbent assay
eNOS	endothelial nitric oxide synthase
ERK	extracellular-signal regulated kinase
F	
FACS	fluorescence-activated cell sorter
FCS	fetal calf serum
Fig.	figure
G	
g	standard gravity
G418	geneticin sulfate
GDP	guanosine diphosphate
Gi-protein	inhibitory G-protein
GnRH-R	gonadotropin-releasing hormone receptor
GTP	guanosine-5'-triphosphate
GPCR	G-protein coupled receptor
H	
h	hour
HAART	highly active anti-retroviral therapy
HBSS	Hank's buffered salt solution
HEPES	4-2-hydroxyethyl-1-piperazineethanesulfonic acid
HCl	hydrochloric acid
HIV	human immunodeficiency virus
HRP	horseradish peroxidase
5-HT _{2βPan}	5-hydroxytryptamin receptor 2β Pan
HUVEC	human umbilical vein endothelial cells
I	
ICAM	intercellular adhesion molecule
IC50	half maximal inhibitory concentration
IFN	interferon
IgG	immunglobulin G
I-κB	inhibitors of NF-κB
I-κK	I-κB kinase complex
IL	interleukin
IP3	inositol 1,4,5-trisphosphate

J	
JAM	junctional adhesion molecule
JNK	c-Jun N-terminal kinases
K	
kb	kilo base pairs
kDa	kilo Dalton
L	
LFA	lymphocyte function associated antigen
LPS	lipopolysaccharide
L-selectin	leukocyte selectin
M	
M	molar
mAb	monoclonal antibody
Mac-1	macrophage antigen-1
MAP kinase	mitogen-activated protein kinase
MI	migration index
min	minute
MIP	macrophage inflammatory protein
mRNA	messenger ribonucleic acid
N	
NaCl	sodium chloride
NF- κ B	nuclear factor 'kappa-light-chain-enhancer' of activated B-cells
O	
ORF	open reading frame
ox-LDL	oxidized low density lipoprotein
P	
PBMC	peripheral blood mononuclear cell
PBS	phosphate buffered saline
PCR	polymerase chain reaction
PE	phycoerythrin
PECAM	platelet/endothelial cell adhesion molecule
Pen/Strep	penicillin/streptomycin
PFA	paraformaldehyde
<i>pfu</i>	<i>Pyrococcus furiosus</i>
PI3K	phosphoinositide 3-kinase

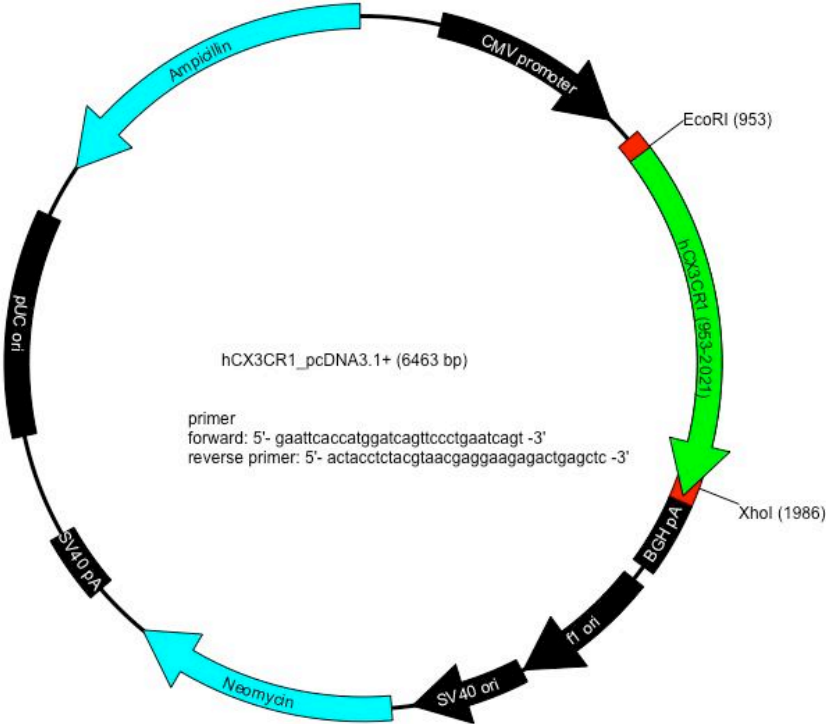
PIP2	phosphatidylinositol 4,5-bisphosphate
PKB	protein kinase B
PKC	protein kinase C
PLC	phospholipase C
PMA	phorbol-12-myristat-13-acetate
POD	peroxidase
P-selectin	platelet selectin
PTX	pertussis toxin
R	
RANTES	regulated upon activation, normal T-cell expressed, and secreted
RNA	ribonucleic acid
rpm	rounds per minute
RPMI	roswell park memorial institute
RT	room temperature
S	
s	second
SAPK	stress-activated phospho-kinases
SD	standard deviation
SDS	sodium dodecyl sulfate
SH3	Src-homology 3
shRNA	short interfering RNA
SIV	simian immunodeficiency viruses
Src	sarcoma
SR-PSOX	scavenger receptor that binds phosphatidylserine and oxidized lipoprotein
SOB	super optimal broth
T	
TACE	tumor necrosis factor alpha converting enzyme
<i>Taq</i>	<i>Thermus aquaticus</i>
TECK	thymus-expressed chemokine
TI	transmigration index
TNF	tumor necrosis factor
U	
U	unit

V	
VCAM	vascular cell adhesion molecule
VE-Cadherin	vascular endothelial cadherin
VLA-4	very late antigen 4
W	
wt	wildtype
X	
X-gal	bromo-chloro-indolyl-galactopyranoside

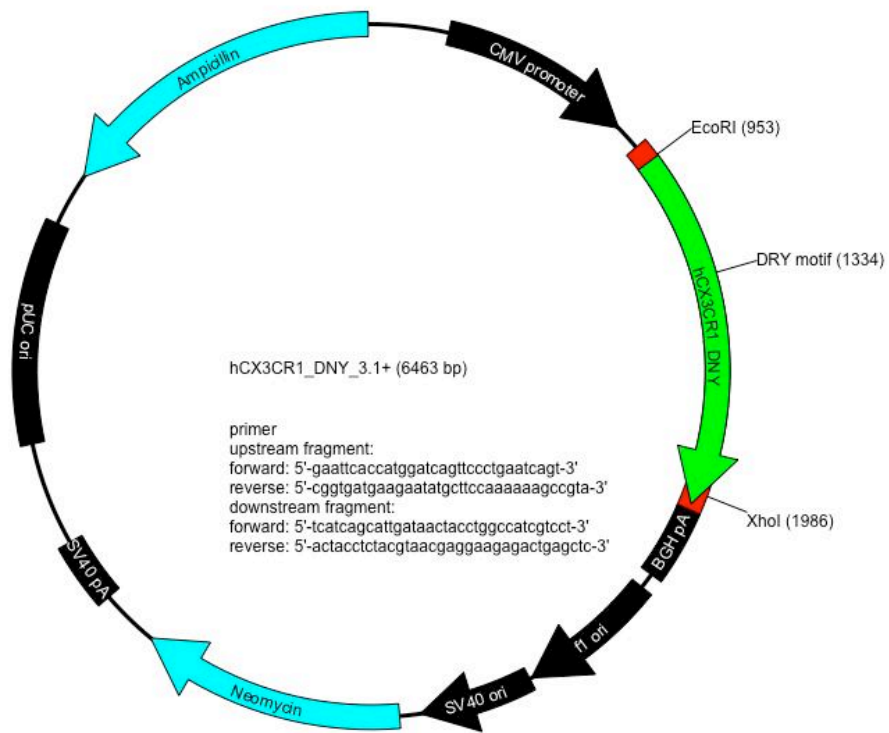
A alanine (Ala)	G glycine (Gly)	M methionine (Met)	S serine (Ser)
C cysteine (Cys)	H histidine (His)	N asparagine (Asn)	T threonine (Thr)
D aspartic acid (Asp)	I isoleucine (Ile)	P proline (Pro)	V valine (Val)
E glutamic acid (Glu)	K lysine (Lys)	Q glutamine (Gln)	W tryptophane (Trp)
F phenylalanine (Phe)	L leucine (Leu)	R arginine (Arg)	Y tyrosine (Tyr)

11 Vectors

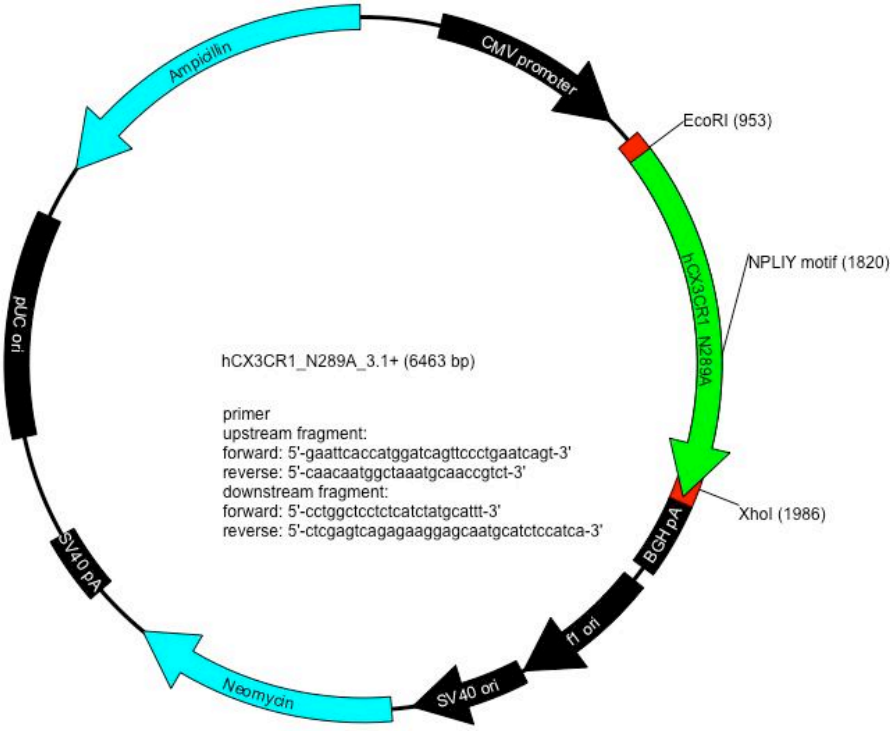
11.1 hCX3CR1 in pcDNA3.1+



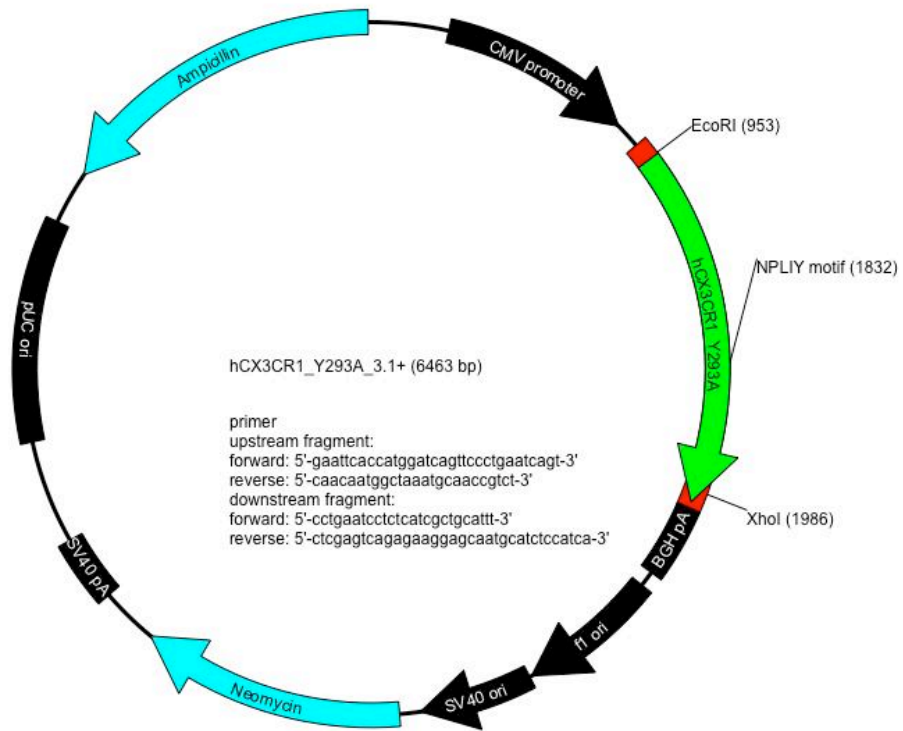
11.2 hCX3CR1 R127N in pcDNA3.1+



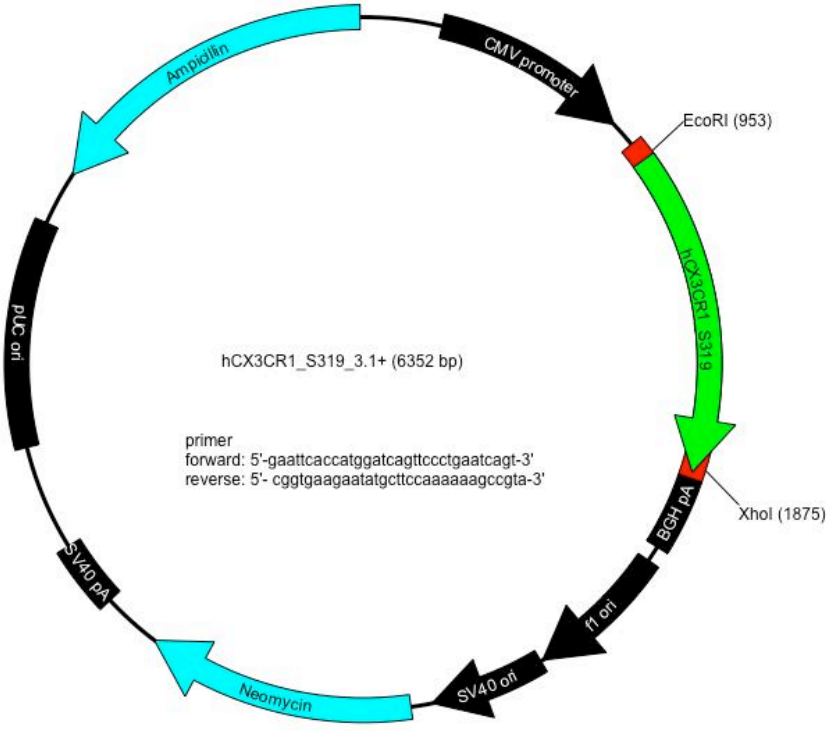
11.3 hCX3CR1 N289A in pcDNA3.1+



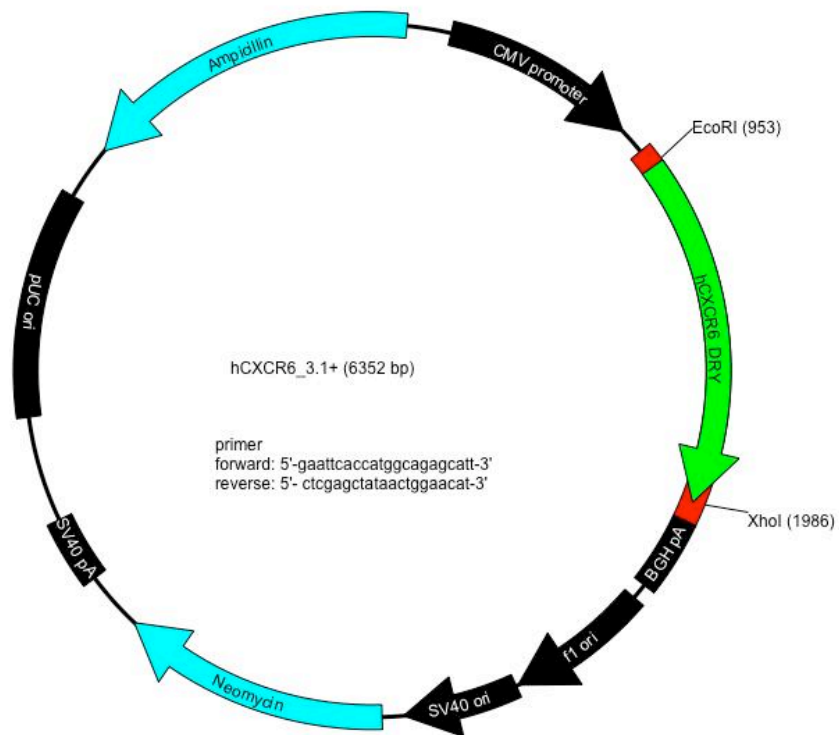
11.4 hCX3CR1 Y293A in pcDNA3.1+



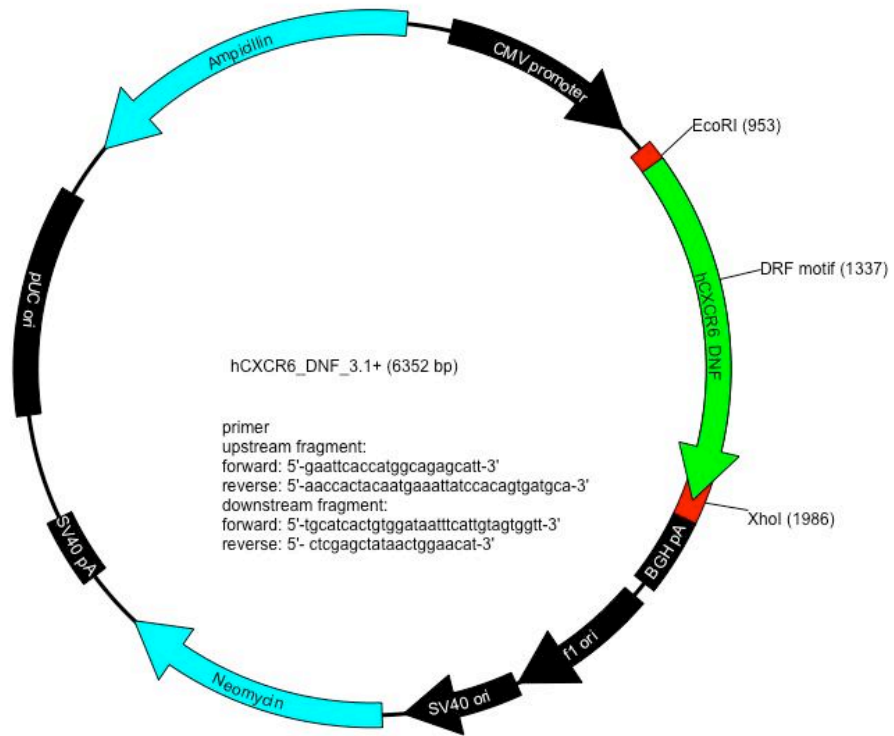
11.5 hCX3CR1 S319X in pcDNA3.1+



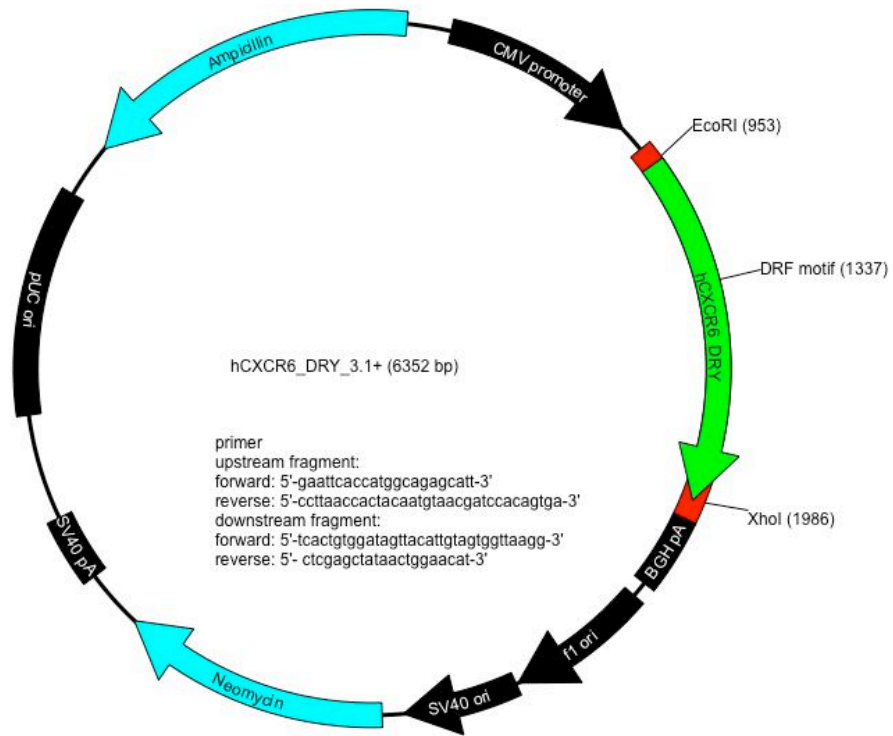
11.6 hCXCR6 in pcDNA3.1+



11.7 hCXCR6 R127N in pcDNA3.1+



11.8 hCXCR6 F128Y in pcDNA3.1+



12 Curriculum Vitae

Personal data

Birth date	29.10.1981
Birth place	Strausberg, Germany
Nationality	german

School education

1994 - 2001	Angelagymnasium Osnabrück
05/2001	Allgemeine Hochschulreife

University education

10/2001 - 07/2004	Bachelor: Molecular Biotechnology, University of Lübeck
04/2004 - 07/2004	Bachelor-Thesis: Etablierung des Modells der beschichteten Kapillare für in vitro Untersuchungen von mononukleären Zellen unter Flussbedingungen
08/2004	Bachelor of Science in Molecular Biotechnology
10/2004 - 06/2006	Master: Biomedical Engineering, Hochschule Anhalt and Martin-Luther-University Halle-Wittenberg
10/2005 - 06/2006	Master-Thesis: Einfluss von Lymphoid Enhancer Factor (Lef-1) auf den Zellzyklus von Kardiomyozyten
06/2006	Master of Engineering in Biomedical Engineering
from 07/2006	PhD-student, RWTH Aachen
from 07/2006	PhD-Thesis: Requirements for leukocyte transendothelial migration via the transmembrane chemokines CX3CL1 and CXCL16

13 Publications

Articles

N. Schwarz, J. Pruessmeyer, F. M. Hess, E. Pantaler, R. Windoffer, M. Voss, A. Sarabi, C. Weber, A. Sechi, S. Uhlig, A. Ludwig

Requirements for leukocyte transendothelial migration via the transmembrane chemokine CX3CL1

submitted

J. Pruessmeyer, C. Martin, F. M. Hess, N. Schwarz, S. Schmidt, T. Kogel, N. Hoettecke, B. Schmidt, A. Sechi, S. Uhlig, A. Ludwig

The disintegrin and metalloproteinase 17 (ADAM17) mediates inflammation-induced shedding of syndecan-1 and -4 by lung epithelial cells

J Biol Chem. 2009 Oct 29. [Epub ahead of print]

R. R. Koenen, J. Pruessmeyer, O. Soehnlein, L. Fraemohs, A. Zerneck, N. Schwarz, K. Reiss, A. Sarabi, L. Lindbom, T. M. Hackeng, C. Weber, A. Ludwig

Regulated release and functional modulation of junctional adhesion molecule A by disintegrin metalloproteinases

Blood. 2009 May 7;113(19):4799-809

C. Hundhausen, A. Schulte, B. Schulz, M.G. Andrzejewski, N.Schwarz, P. von Hundelshausen, U. Winter, K. Paliga, K. Reiss, P. Saftig, C. Weber, A. Ludwig

Regulated Shedding of Transmembrane Chemokines by the Disintegrin and Metalloproteinase 10 Facilitates Detachment of Adherent Leukocytes

J Immunol. 2007 Jun 15;178(12):8064-72

Poster

Regulated Cleavage of transmembrane chemokines by ADAM10 and ADAM17.

M. G. Andrzejewski, N. Schwarz, C. Weber, A. Ludwig

37th Symposium of the Germany Society for Immunology (DGfI), Heidelberg, 2007

Symposium of the Bonner Forum for Biomedicine, Bonn, 2007

Distinct structural determinants are required for CX3CR1-mediated cell adhesion and chemotaxis

N. Schwarz, E. Pantaler, A. Ludwig

Symposium of the Austrian Society for Allergology/Immunology, together with Germany Society for Immunology (DGfI), Wien, Österreich, 2008

Society for Microcirculation and Vascular Biology, Aachen, 2008

Sequential steps of leukocyte recruitment via the transmembrane chemokine CX3CL1

N. Schwarz, J. Pruessmeyer, F.M. Hess, R. Windoffer, M. Voss, A. Sarabi, C. Weber, A. Sechi, S. Uhlig, A. Ludwig

2nd European Congress of Immunology, Berlin, 2009

Signal Transduction and Disease, Aachen, 2009

The proinflammatory cytokines IFN γ and TNF α induce shedding of endothelial and epithelial surface molecules via upregulation of ADAM17 activity

J. Pruessmeyer, N. Schwarz, F.M. Hess, T. Kogel, C. Martin, S. Uhlig, A. Ludwig

2nd European Congress of Immunology, Berlin, 2009

Signal Transduction and Disease, Aachen, 2009

14 Declaration

I hereby declare, that this thesis was carried out at RWTH Aachen University, within the Institute for Pharmacology and Toxicology and the Institute for Molecular and Cardiovascular Research. It was exclusively performed by myself, unless otherwise stated in the text. To my knowledge, it contains no material used in other publications or thesis, except where reference is made in the text.

Aachen, 14. Januar 2010

15 Acknowledgements

Ich möchte mich bei all denjenigen Personen bedanken, die zum Gelingen dieser Dissertation beigetragen und mich unterstützt haben.

An erster Stelle geht mein Dank an PD Dr. Andreas Ludwig. Vielen Dank für die Geduld, die exzellente Betreuung und die Begutachtung der Doktorarbeit. Darüber hinaus, danke für bitter benötigten Kaffee und Tee in allen Lebenslagen, danke für jede Menge offener Ohren bei absurden Gedanken, danke für die investierte Zeit, die ab und an sicher viele Nerven gekostet hat.

Ich danke Prof. Stefan Uhlig für die unkomplizierte Aufnahme in seine Arbeitsgruppe. Ausserdem vielen Dank für die Übernahme des Gutachtens.

Prof. Werner Baumgartner möchte ich für die Übernahme des Gutachtens ohne langes Nachdenken danken. Mir ist ein riesiger Stein vom Herzen gefallen.

Mein Dank geht an Jessica Prüßmeyer für die vielen fruchtbaren Gespräche bei Kännchen oder Schnitzel sowohl auf privater als auch professioneller Ebene.

Besonderer Dank geht an unsere Chef-TA Tanja Kogel und ihre Vize Melanie Esser. Danke für die Geduld, den Spaß und vor allem die Unterstützung. Let's do the dynasore rock!

Danke an Daniela Dreymüller für das Erschlagen der kleinen Fehler-teufelchen. Vergiss unser Date im Sommer nicht. ;)

Ganz besonders möchte ich mich bei meiner Familie bedanken. Ihr wart während all der Jahre immer eine große Unterstützung und habt nie aufgehört, an mich zu glauben.

Und zum Schluss noch ein ganz großes Danke an Patrick Beier für die Hilfe mit den Bildern, das Nutzen teurer Satelliten um Tupperdosen im Wald zu suchen und vorallem die Zeit, die wir miteinander verbracht haben und in Zukunft verbringen werden.

Danke!